SATBAYEV UNIVERSITY

ISSN 2959-2348 (Online)

ENGINEERING JOURNAL of Satbayev University

Volume 147 (Issue 2)
April 2025

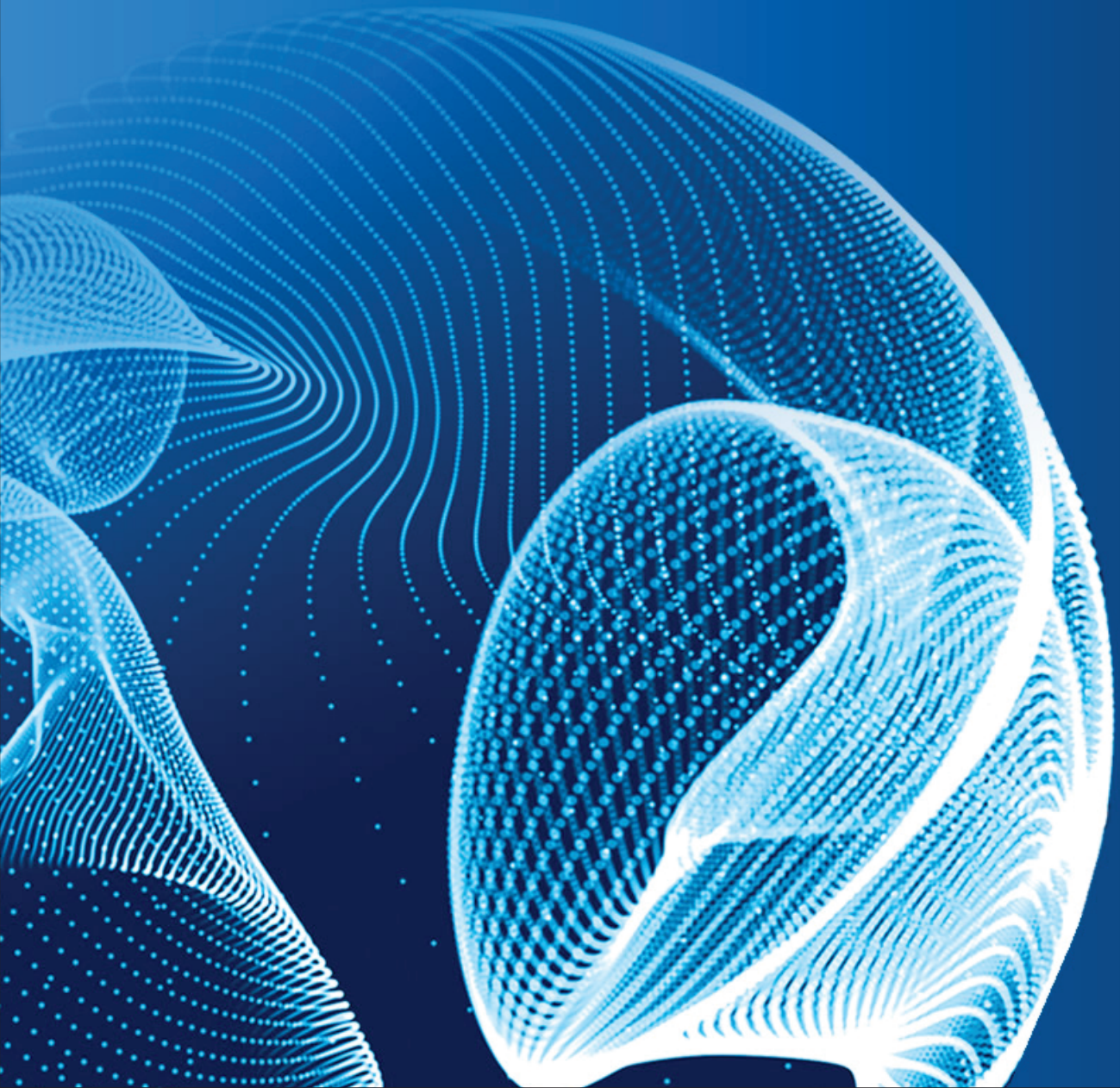

eISSN 2959-2348

eISSN 2959-2348

eISSN 2959-2348

SATBAYEV UNIVERSITY

Engineering Journal of Satbayev University

Volume 147 (2025), Issue 2, 1-9

https://doi.org/10.51301/ejsu.2025.i2.01

The role of zirconium in the formation of structure and properties of titanium alloys during superplastic deformation

A.M. Alimzhanova[1*], A.Zh. Terlikbaeva[1], B.T. Sakhova[1,2], R.A. Shayakhmetova[1], G.M. Koishina[2], A.A. Mukhametzhanova[1], G.K. Maldybaev[3]

[1]*National Center for Integrated Processing of Mineral Raw Materials of the Republic of Kazakhstan, Almaty, Kazakhstan*
[2]*Satbayev University, Almaty, Kazakhstan*
[3]*Kazakh-British Technical University, Almaty, Kazakhstan*

**Corresponding author: aliyuchca@mail.ru*

Abstract. This study investigates the effect of zirconium on the superplastic properties of titanium alloys at various temperatures and strain rates. It has been established that zirconium significantly influences the strain rate sensitivity coefficient (m), mechanical stability, and plasticity. At elevated temperatures, zirconium-containing alloys exhibit a stable m-value within a specific strain rate range, followed by a sharp decline. In contrast, zirconium-free alloys show a gradual decrease in m as the strain rate increases. The optimal temperature-strain rate conditions for superplastic deformation depend on zirconium content. Alloys with lower zirconium concentrations demonstrate high plasticity at moderate temperatures and intermediate strain rates, whereas alloys with higher zirconium content require lower strain rates to achieve uniform deformation. Beyond a certain threshold, an increase in zirconium content results in reduced plasticity and strain localization. Additionally, zirconium increases flow stress, while higher temperatures contribute to its reduction; however, this is accompanied by grain coarsening, which negatively affects mechanical properties. Microstructural analysis using scanning electron microscopy revealed that after superplastic deformation, all investigated alloys develop a fine-grained structure consisting of equiaxed α- and β-grains. The average grain size increases compared to the initial state, indicating dynamic recovery and recrystallization processes. The results confirm the feasibility of using these titanium alloys in superplastic forming technologies. The identified correlations provide a basis for optimizing thermomechanical processing parameters to achieve a balance between high plasticity and mechanical stability, which is crucial for industrial applications.

Keywords: *ultrafine-grained, severe plastic deformation, structure, nanoscale, superplasticity, zirconium.*

Received: 10 January 2025
Accepted: 15 April 2025
Available online: 30 April 2025

1. Introduction

Severe plastic deformation (SPD) is one of the most effective methods for forming an ultrafine-grained (UFG) structure in metals and alloys. This approach significantly improves the mechanical properties of materials by reducing the average grain size and increasing the density of crystal lattice defects. As a result, SPD-processed materials exhibit enhanced strength, fatigue limit, and superplasticity, making them promising for applications in various industries [1-4].

In recent years, various SPD techniques have been developed to refine the structure of titanium alloys efficiently. The most common methods include equal-channel angular pressing (ECAP), high-pressure torsion, high-cycle impact treatment, and multistep forging. Studies have shown that SPD by torsion can produce an ultrafine-grained structure with an average grain size of approximately 80 nm [5-7]. In turn, multistep forging performed within the temperature range of 800–400 °C facilitates the formation of equiaxed grains with an average size of about 200 nm [8-13]. The ECAP method, applied to bulk billets, enables the achievement of a grain size of approximately 260 nm after eight processing cycles [14-17].

However, despite the significant increase in strength, the formation of a UFG structure is often accompanied by a reduction in impact toughness and fracture resistance, which may limit the application of such materials in structural components. To address this issue, specialized UFG structures are being actively developed to achieve an optimal balance between strength and fracture toughness [18-21]. One promising approach involves creating microstructural composites consisting of «hard» and «soft» phases. In two-phase titanium alloys, the α-phase serves as a strengthening component, while the β-phase enhances plasticity due to the presence of multiple slip systems [22, 23].

Controlling the shape, volume ratio, and spatial distribution of these phases plays a key role in regulating the material's mechanical properties. The introduction of alloying elements enables targeted modifications of the phase composition and microstructure, enhancing the material’s performance characteristics. One promising direction for improv-

aliyuchca@mail.ru; alma_terlikbaeva@mail.ru; 4667357@gmail.com; rozozhka@mail.ru; Gulzada.koishina@mail.ru; narike.91@mail.ru; galimjan_87@mail.ru
Engineering Journal of Satbayev University. eISSN 2959-2348. Published by Satbayev University

ing UFG titanium alloys involves microalloying with rare-earth elements such as gadolinium. Studies show that gadolinium promotes β-grain refinement and controls phase transformation rates, leading to improved mechanical properties, especially under severe plastic deformation [24].

UFG titanium alloys are of significant interest for applications under superplastic deformation conditions. Two-phase titanium alloys are at the center of modern research aimed at developing technological processes that utilize their superplastic properties. It is important to note that optimizing the temperature range for superplasticity (150-400°C) is crucial for ensuring the high manufacturability of such materials [25]. The application of superplasticity at lower temperatures significantly reduces energy consumption while maintaining high mechanical properties, making this process particularly attractive for industrial manufacturing. For example, low-temperature superplasticity improves the strength characteristics and enhances the quality of thin-walled components formed in complex geometries [26, 27].

The main mechanisms of superplasticity include grain boundary sliding, intragranular dislocation slip, diffusion creep, and dynamic recrystallization. A key characteristic of superplastic flow is grain size: the finer the grain, the higher the material's strain rate sensitivity, the lower its yield strength, and the greater its deformation capacity. This is why an ultrafine-grained structure significantly enhances superplasticity efficiency [28-46].

Additionally, studies indicate that metallic glasses can exhibit superplastic behavior at relatively high strain rates. This effect opens new prospects for developing materials with high technological plasticity, capable of withstanding significant loads without failure [47].

In prototype studies, the mechanical behavior of materials under superplastic conditions is examined with a focus on uniaxial tension, compression, and torsion under applied pressure, as well as punching and compression in specially designed dies. Based on deformation diagrams and characteristic curves, such as the relationship between true yield stress, strain rate sensitivity, maximum plasticity, and other factors as functions of strain rate, it is assumed that superplastic behavior under certain temperature-strain rate regimes is reasonable [28-47].

Various types of tests are conducted to study the mechanical behavior of materials under superplasticity, including uniaxial tension, compression, torsion under pressure, and material extrusion in dies. Essential aspects of the research include constructing deformation diagrams and characteristic curves, which help characterize the adaptive properties of the material and its superplastic behavior under different temperature and strain rate conditions. In particular, the dependencies of true flow stress $\sigma_y(a)$, strain rate sensitivity coefficient $m(a)$, and maximum elongation at fracture $\delta(a) = \frac{l}{l_0} - 1$ on the strain rate can be described by the following equations:

$$\alpha := \dot{\varepsilon} = \dot{l} / l = V / l, \quad (1)$$

where, $\varepsilon = \ln l / l_o$; V – the crosshead speed of the testing machine. These curves are typically plotted in (semi-) logarithmic coordinates:

$$\lg\sigma - \lg a, m - \lg a, \delta - \lg a, \quad (2)$$

Based on their qualitative appearance, these curves can determine whether a material is in a superplastic state or exhibits conventional deformation behavior. Superplastic materials are characterized by specific deformation curves, where an initial sharp increase in stress is followed by a plateau with constant stress (without strain hardening), and in some cases, even a decrease in stress.

Alloying elements such as zirconium (Zr), chromium (Cr), and manganese (Mn) play a crucial role in achieving superplasticity. They influence plastic deformation mechanisms, enhancing structural stability and increasing plasticity. Studies have shown that aluminum-magnesium alloys with zirconium additions exhibit significant improvements in superplasticity due to the stabilization of the microstructure by dispersed Al_3Zr particles. These particles prevent grain growth at high temperatures, ensuring stable superplasticity up to 525°C [48]. For example, a modified Al-Mg-Zr alloy at 500°C demonstrates a maximum elongation of 1013% at a strain rate of $5 \cdot 10^{-2}$ s^{-1}, making it a promising material for applications requiring high plasticity [48].

The introduction of zirconium into titanium and aluminum alloys significantly lowers the temperature for superplastic deformation and increases the strain rate at which high plasticity is maintained. This improves the material's processability, reduces energy consumption during processing, and enhances the efficiency of forming processes.

Studying the dependence of the strain rate sensitivity coefficient on strain rate and temperature is an important aspect of research, as it helps determine optimal temperature-strain rate conditions that maximize superplasticity. This, in turn, plays a key role in improving manufacturing efficiency and expanding the use of materials with enhanced properties in industrial applications.

2. Materials and methods

The study examined alloys with varying zirconium content: 0Zr, 0.5Zr, 1Zr, and 1.5Zr. Samples with the geometry shown in Figure 1 were cut from 1 mm-thick titanium sheets along the rolling direction.

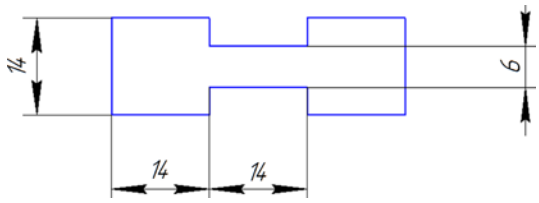

Figure 1. Sample geometry for superplasticity testing

The samples were tested using a ZWICK 250 universal testing machine.

To determine the deformation conditions (strain rate and temperature) for superplasticity testing, step strain rate tests were conducted at temperatures of 700, 725, and 750°C. The strain rate varied within the range of $5 \cdot 10^{-5}$ s^{-1} to $2 \cdot 10^{-2}$ s^{-1}, with a step increment of $2.5 \cdot 10^{-5}$ s^{-1} every 2% strain.

Based on the results of the step strain rate tests, the strain rate sensitivity coefficient (m) was determined.

$$m = \partial Ln\sigma / \partial Ln\varepsilon, \quad (3)$$

The microstructure of the obtained samples was analyzed using a TESCAN VEGA 3 scanning electron microscope.

3. Results and discussion

The study of the superplasticity of the alloys was conducted at constant strain rates, where both strain rate and temperature were set based on preliminary step strain rate tests. These tests allowed for determining the limit values of the strain rate sensitivity coefficient (m), which plays a key role in evaluating a material's superplasticity. The m coefficient characterizes the degree of dependence of flow stress on strain rate and, accordingly, indicates the dominant plastic deformation mechanism.

Figure 2 presents the dependence of the strain rate sensitivity coefficient of the studied alloys on strain rate at 700, 725, and 750°C.

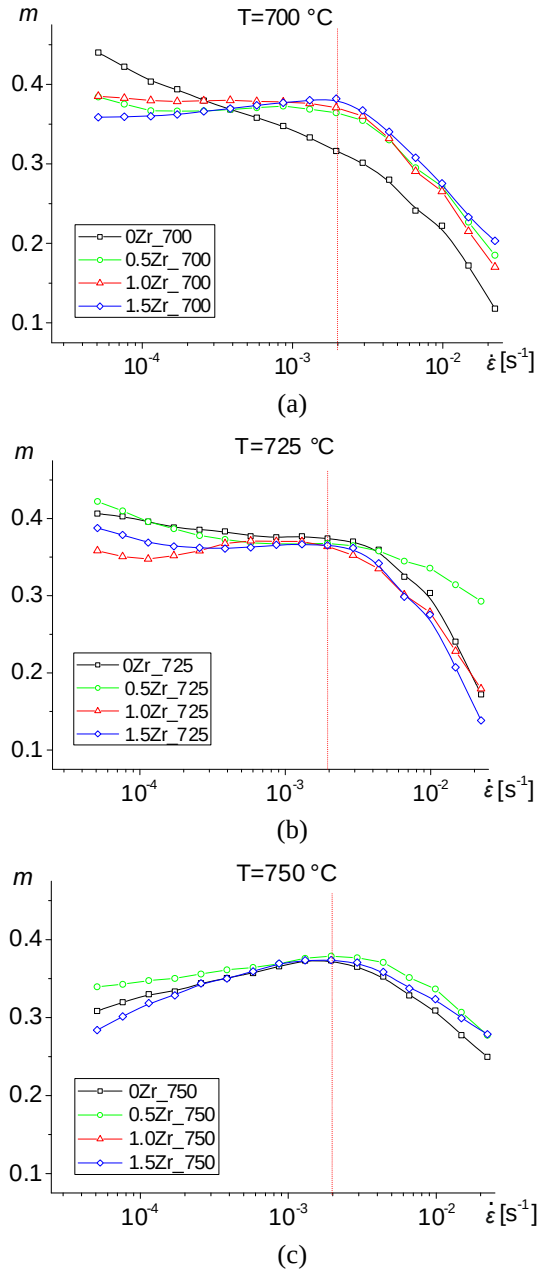

Figure 2. Dependence of the strain rate sensitivity coefficient of the alloys on strain rate at different temperatures (°C): (a) – 700; (b) – 725; (c) – 750

At 700°C, alloys containing zirconium (0.5Zr, 1Zr, 1.5Zr) show a similar dependence of the m coefficient on strain rate. In the strain rate range up to $2 \cdot 10^{-3}$ s^{-1}, the m coefficient remains nearly constant, indicating stability of the superplastic state under these conditions. This suggests that within this strain rate range, the dominant plastic deformation mechanism is grain boundary sliding (GBS), which is active at high grain boundary diffusion mobility.

However, when the strain rate exceeds $2 \cdot 10^{-3}$ s^{-1}, a sharp decrease in the m coefficient is observed. This indicates a transition from a superplastic regime to a conventional plastic deformation regime, associated with the activation of dislocation slip and subsequent material hardening. It is likely that at high strain rates, grain boundary sliding can no longer accommodate plastic deformation, leading to a decrease in m.

At the same time, the zirconium-free alloy exhibits a monotonic decrease in the m coefficient with increasing strain rate. This may be due to the lower superplasticity capability of this alloy, possibly related to limited grain boundary mobility and a more pronounced dislocation-based deformation mechanism.

At 700°C, alloys containing zirconium (0.5Zr, 1Zr, 1.5Zr) exhibit similar values of the strain rate sensitivity coefficient m as a function of strain rate. In the strain rate range below $2 \cdot 10^{-3}$ s^{-1}, the coefficient m remains nearly constant, indicating the stability of the superplastic state under these conditions. This behavior is associated with the dominant grain boundary sliding (GBS) mechanism, which, at moderate strain rates, ensures uniform redistribution of plastic deformation without significant material hardening. However, as the strain rate increases beyond $2 \cdot 10^{-3}$ s^{-1}, the m value begins to decrease significantly, signaling a gradual transition of the material from a superplastic state to conventional deformation behavior, characteristic of dislocation slips mechanisms. This phenomenon occurs because, at high strain rates, grain boundary sliding does not have sufficient time to accommodate localized plastic deformation, leading to the activation of hardening processes.

At 725°C, all studied alloys exhibit high m values exceeding the required superplasticity threshold (0.3). The dependencies of m on strain rate are similar to those observed at 700°C, but with a wider strain rate range ensuring stable superplastic behavior. For alloys containing 0.5-1.5% Zr, the maximum m values are reached at strain rates around $2 \cdot 10^{-3}$ s^{-1}, which corresponds to an optimal balance between grain boundary sliding and dislocation processes.

The highest efficiency of zirconium in promoting superplastic deformation is observed at 750°C. In this temperature range, all studied alloys exhibit similar m dependencies on strain rate. The greatest increase in m is noted at a strain rate of $2 \cdot 10^{-3}$ s^{-1}, where the maximum value reaches approximately 0.35.

The addition of zirconium significantly influences the mechanical properties of titanium alloys by stabilizing the fine-grained structure.

Superplasticity studies enabled the determination of elongation values for different alloys under various temperature-strain rate conditions, where the strain rate sensitivity coefficient m approaches its maximum values.

Figure 3 presents the tensile curves for the alloys at different temperatures and strain rates. All investigated alloys demonstrate superplastic behavior, with elongation exceeding 200% under the selected deformation conditions, confirming a significant potential for superplastic deformation.

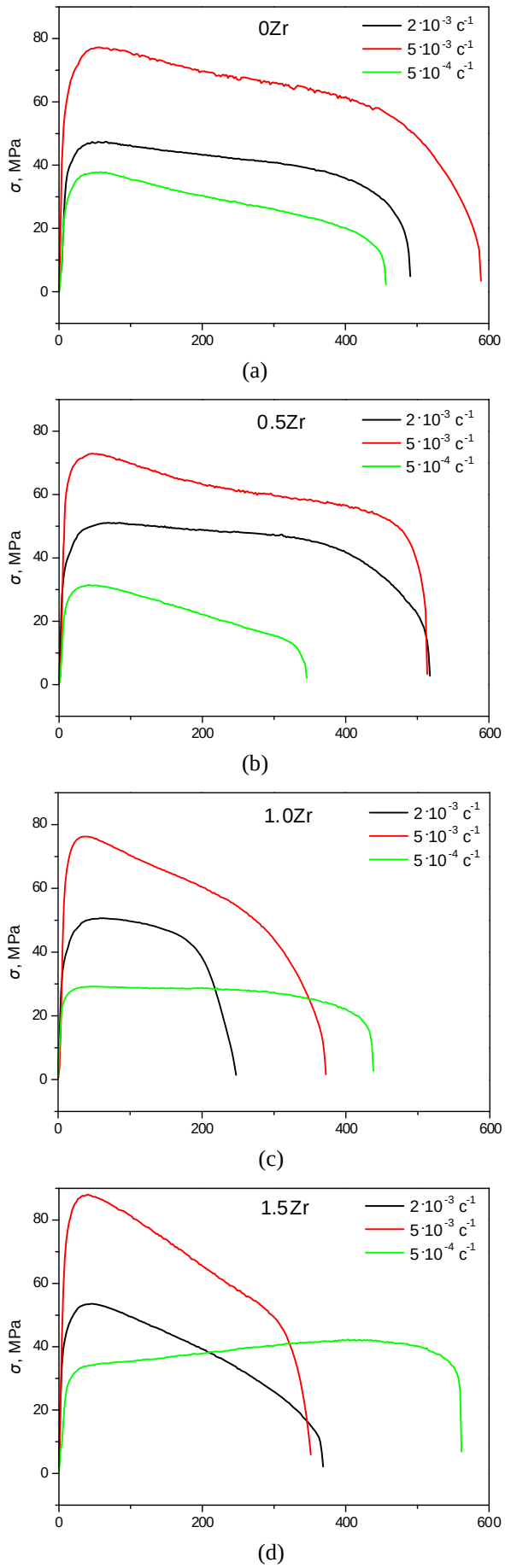

Figure 3. Tensile curves of alloys: a) 0Zr, b) 0.5Zr, c) 1Zr, and d) 1.5Zr at a temperature of 725 °C

However, as the specific zirconium content in the alloy exceeds 0.5%, elongation increases, but deformation becomes less uniform, and the flow stress rises. Alloys with a lower zirconium content exhibit a weaker dependence on strain rate and temperature, indicating better superplasticity in these compositions.

In contrast, when the zirconium content increases to 1% or more, a sharp decrease in elongation is observed with increasing strain rate, indicating a deterioration in superplastic behavior at high deformation rates.

A decrease in deformation temperature leads to reduced elongation and non-uniform deformation, highlighting the inadvisability of lowering the deformation temperature below 725°C.

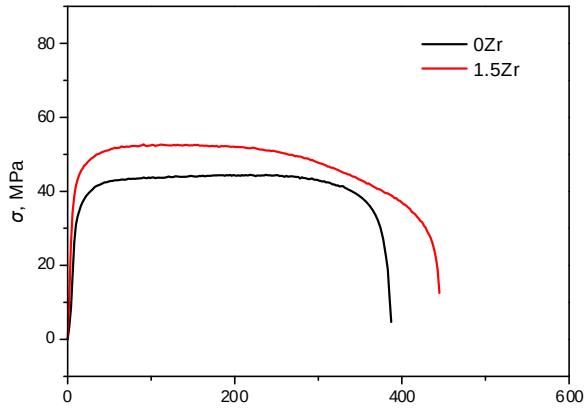

Figure 4. Tensile curves of alloys at a temperature of 750 °C and a strain rate of 2·10⁻³ s⁻¹

Increasing the deformation temperature to 750°C leads to a significant decrease in the flow stress of the investigated alloys, which is explained by increased dislocation mobility and enhanced diffusion processes. However, along with this, a decrease in deformation uniformity is observed, which may be associated with uneven grain growth and the localization of plastic deformation in certain zones.

Nevertheless, the increase in temperature is also accompanied by a reduction in elongation, which is likely due to the intensive grain growth during deformation. At 750°C, grain boundaries become less stable, leading to grain coarsening, reduced grain boundary sliding, and deteriorated conditions for superplasticity. This effect is associated with a diminished ability of the material to maintain superplastic behavior at high temperatures, where dynamic recrystallization and grain coalescence begin to dominate. As a result, plasticity decreases, and the material becomes more prone to unstable flow, as confirmed by experimental data (Figure 4).

Table 1 presents the elongation test results of the alloys under various temperature-strain rate conditions.

The analysis of the data in Table 1 shows that the elongation of the alloys significantly depends on the temperature and strain rate. Thus, the optimal temperature-strain rate conditions for the 0Zr and 0.5Zr alloys are a temperature of 725°C and strain rates in the range of 2–5·10⁻³ s⁻¹. For the 1Zr and 1.5Zr alloys, the optimal conditions are a temperature of 725°C and a strain rate of 5·10⁻⁴ s⁻¹.

Table 2 presents data on the grain sizes of the α- and β-phases, as well as the volume fraction of the β-phase in the alloys after superplastic deformation under various temperature-strain rate conditions.

Table 1. Elongation values of alloys at different temperature-strain rate conditions

Alloy	Temperature, °C	Strain rate, c^{-1}	Elongation, %
0Zr	700	$2\cdot10^{-3}$	280
	725	$5\cdot10^{-4}$	450
		$2\cdot10^{-3}$	490
		$5\cdot10^{-3}$	580
	750	$2\cdot10^{-3}$	380
0.5Zr	700	$2\cdot10^{-3}$	380
	725	$5\cdot10^{-4}$	340
		$2\cdot10^{-3}$	515
		$5\cdot10^{-3}$	510
1Zr	700	$2\cdot10^{-3}$	450
	725	$5\cdot10^{-4}$	430
		$2\cdot10^{-3}$	240
		$5\cdot10^{-3}$	360
1.5Zr	700	$2\cdot10^{-3}$	400
	725	$5\cdot10^{-4}$	550
		$2\cdot10^{-3}$	360
		$5\cdot10^{-3}$	350
	750	$2\cdot10^{-3}$	440

Table 2. Grain sizes of phases and volume fraction of β-phase in alloys after superplastic deformation under different conditions

Alloy	Temperature, °C	Strain rate, c^{-1}	Grain size of the α-phase, μm	Grain size of the β-phase, μm	Volume fraction of the β-phase, %
0Zr	725	$2\cdot10^{-3}$	1.7 ± 0.3	2.2 ± 0,3	56
		$5\cdot10^{-3}$	1.6 ± 0.25	1.8 ± 0,15	46
0.5Zr	700	$2\cdot10^{-3}$	1.2 ± 0.1	1.5 ± 0,15	48
	725	$2\cdot10^{-3}$	1.3 ± 0.1	1.75 ± 0.15	47
		$5\cdot10^{-3}$	1.1 ± 0.1	1.6 ± 0.15	52
1Zr	725	$5\cdot10^{-3}$	1.2 ± 0.1	1.5 ± 0.1	45
		$5\cdot10^{-4}$	1.3 ± 0.1	1.9 ± 0.25	47
1.5Zr	725	$5\cdot10^{-3}$	1.0 ± 0.1	1.55 ± 0.15	44
		$5\cdot10^{-4}$	1.8 ± 0.1	2.3 ± 0.2	44
	750	$2\cdot10^{-3}$	1.4 ± 0.1	2.5 ± 0.25	63

As seen from Table 2, an increase in deformation temperature leads to a growth in the volume fraction of the β-phase. Additionally, the grain size of the α-phase remains almost unchanged under different testing conditions, whereas the grain size of the β-phase increases with decreasing strain rate and increasing deformation temperature.

To determine the mechanical properties of the alloys after superplastic deformation, tensile tests were conducted at a temperature of 725°C and a strain rate of $2\cdot10^{-3}$ s^{-1} (Table 3). The samples were stretched to 100%, quenched in water, and then subjected to tensile testing at room temperature with a strain rate of 4 mm/min.

Table 3. Mechanical properties of alloys after 100% elongation at 725 °C and a strain rate of $2\cdot10^{-3}$ s^{-1}

Alloy	Yield strength, MPa	Tensile strength, MPa	Elongation, %
0Zr	600	620	3
0.5Zr	655	695	6
1Zr	535	541	1
1.5Zr	630	650	3

From the table, it is evident that the addition of zirconium enhances the strength characteristics of the alloys in both the initial and superplastic states. The highest yield strength and ultimate tensile strength values are observed in the 0.5Zr alloy, which also exhibits the greatest elongation, indicating an optimal combination of strength and ductility. However, a further increase in zirconium content leads to a decline in mechanical properties, likely due to grain growth and an increase in the volume fraction of the β-phase.

In particular, the 1Zr alloy demonstrates the lowest values of yield strength, tensile strength, and elongation, indicating a significant reduction in ductility. To assess the impact of superplastic deformation on the alloy structure, microstructural studies were conducted using scanning electron microscopy (SEM). Figures 5 and 6 present the microstructures of alloys with different zirconium contents after deformation at 725°C with strain rates ranging from $5\cdot10^{-4}$ s^{-1} to $2\cdot10^{-3}$ s^{-1}.

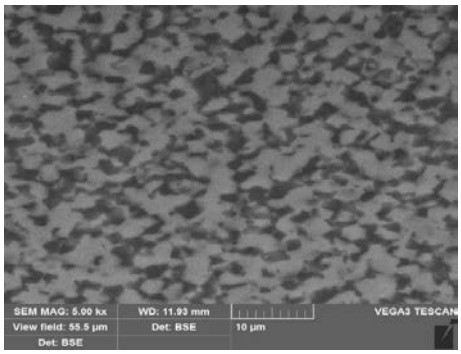

(a)

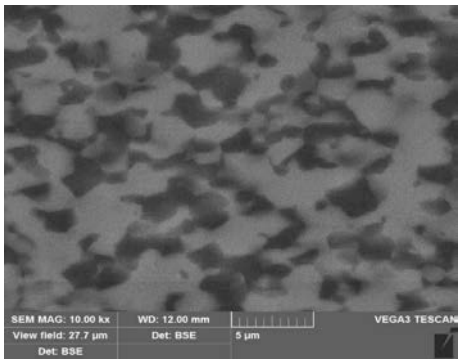

(b)

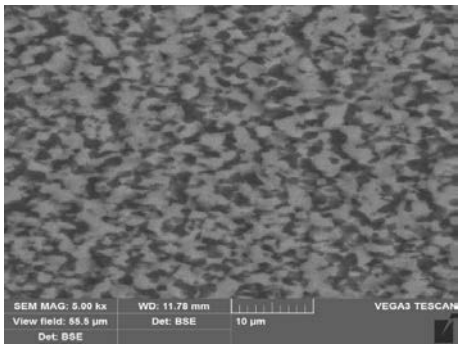

(c)

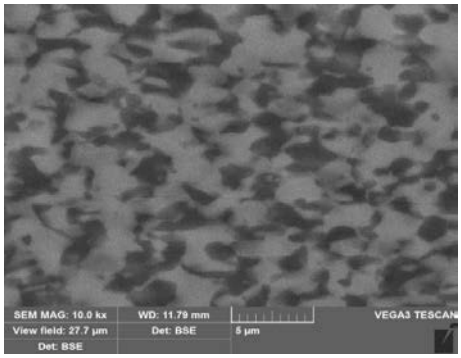

(d)

Figure 5. Microstructural images of the alloys after superplastic deformation at 725°C with a strain rate of $2\cdot10^{-3}$ s^{-1}: (a, b) – correspond to the 0Zr alloy, (c, d) – correspond to the 0.5Zr alloy,

Figure 6 shows the microstructure of alloys with different zirconium contents after superplastic deformation at 725°C and a strain rate of 2×10^{-3} s^{-1}. The alloy exhibits a fine-grained structure, characteristic of superplastic deformation, confirming the active development of dynamic recrystallization. The equiaxed grain shape indicates uniform strain distribution.

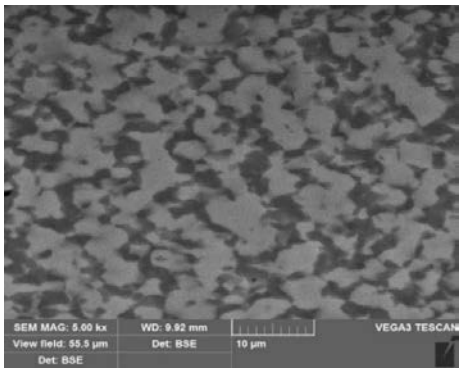

(a)

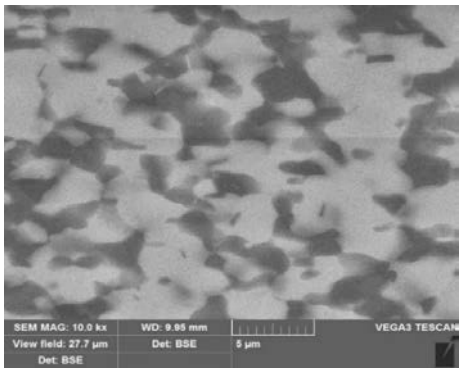

(b)

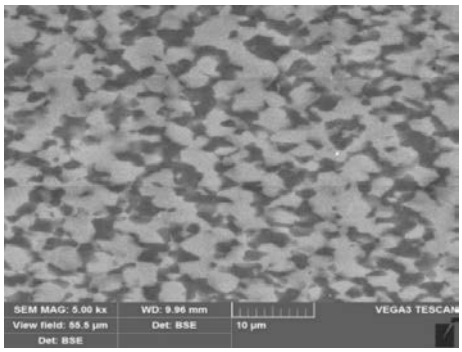

(c)

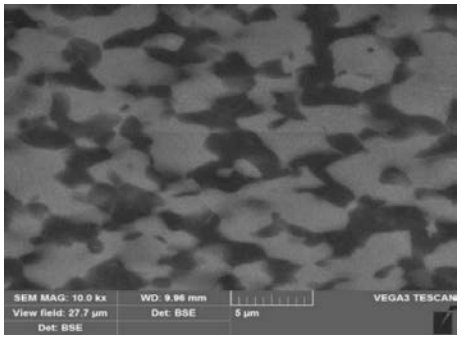

(d)

Figure 6. Microstructure images of the alloy after superplastic deformation at 725°C with a strain rate of 5×10^{-4} s^{-1}: (a, b) – correspond to the 1Zr; (c, d) – correspond to the 1.5Zr

In zirconium-free alloys (0Zr), a homogeneous two-phase structure is observed, whereas the addition of 0.5% Zr leads to further grain refinement due to the slowing down of grain boundary diffusion.

In general, the structure of the alloys after superplastic deformation consists of a dispersed mixture of equiaxed grains of the α- and β-phases, indicating the development of dynamic recrystallization. Compared to the deformed state and annealing at similar temperatures, an increase in grain growth is observed due to the influence of high temperatures and prolonged plastic deformation. At the same time, the fine-grained structure is preserved due to the inhibition of grain growth by alloying elements such as zirconium. The presence of this structure positively affects the mechanical properties of the alloy, ensuring high plasticity and resistance to fracture. Thus, superplastic deformation has a significant impact on the microstructural characteristics of the alloy, determining its operational properties.

4. Conclusions

The conducted studies have established the effect of zirconium content on the superplastic behavior of titanium alloys under various temperature-strain rate conditions. Analysis of the obtained data showed that zirconium significantly influences the strain rate sensitivity coefficient (m), mechanical stability, and plasticity of the alloys, as well as the microstructural changes occurring during deformation.

It was found that at a temperature of 700°C, alloys containing zirconium exhibit a stable m coefficient value within a certain strain rate range (up to $2\cdot10^{-3}$ s^{-1}), after which a sharp decline is observed. In alloys without zirconium, the m coefficient decreases monotonously as the strain rate increases. At 725°C, the m coefficient exceeds 0.3 in all investigated alloys over a wide range of strain rates, indicating favorable conditions for superplastic flow. With a further increase in temperature to 750°C, the maximum m value (~0.35) is reached at a strain rate of $2\cdot10^{-3}$ s^{-1}; however, this is accompanied by grain coarsening, which negatively affects plasticity.

The optimal temperature-strain rate regimes for superplastic deformation were determined as follows:

– for alloys with 0% and 0.5% zirconium, the preferred temperature is 725°C, and the strain rate is in the range of 2–$5\cdot10^{-3}$ s^{-1};

– for alloys with 1% and 1.5% zirconium, the optimal conditions include the same temperature (725°C) but a lower strain rate (~$5\cdot10^{-4}$ s^{-1}).

All studied alloys demonstrated elongation of more than 200%; however, as the zirconium content increases above 0.5% and the temperature drops below 725°C, a decrease in plasticity and non-uniform deformation flow is observed, which may limit their application in superplastic processing. Additionally, an increase in zirconium content contributes to higher flow stress, which improves strength characteristics but reduces the material's ability to undergo uniform elongation. Meanwhile, increasing the temperature to 750°C reduces flow stress but is accompanied by grain coarsening, which deteriorates mechanical properties.

Microstructural analysis using scanning electron microscopy showed that after superplastic deformation, all alloys form a dispersed mixture of equiaxed grains of the α- and β-phases. An increase in the average grain size compared to the initial state is observed, indicating processes of dynamic

recovery and recrystallization. Alloys with higher zirconium content tend to form larger grains, which may reduce their technological plasticity during subsequent processing.

Thus, the research results confirm the feasibility of using the studied titanium alloys in superplastic forming processes under specific temperature-strain rate conditions. The identified patterns allow for the optimization of thermomechanical processing parameters aimed at achieving high plasticity and mechanical stability, which is essential for industrial applications, particularly in aerospace, space, and medical engineering. Further research may focus on studying the effects of additional alloying elements and pre-treatment conditions on the mechanical properties and microstructure of titanium alloys, which will expand their application in high-tech industries.

Author contributions

Conceptualization: A.M.A.; Data curation: A.M.A., A.Zh.T.; Formal analysis: A.M.A., R.A.Sh., G.M.K.; Funding acquisition: G.K.M., A.A.M.; Investigation: A.M.A., A.A.M.; Methodology: B.T.S., A.A.M.; Project administration: A.M.A., A.Zh.T.; Resources: A.A.M., B.T.S.; Software: B.T.S., A.A.M.; Supervision: G.M.K., G.K.M.; Validation: A.A.M., G.M.K.; Visualization: B.T.S., G.K.M.; Writing – original draft: A.M.A., G.M.K.; Writing – review & editing: A.M.A., A.A.M. All authors have read and agreed to the published version of the manuscript.

Funding

This research received no external funding.

Acknowledgements

The authors would like to express their sincere gratitude to the editor and the two anonymous reviewers for their constructive comments and valuable suggestions, which significantly contributed to the improvement of the manuscript.

Conflicts of interest

The authors declare no conflict of interest.

Data availability statement

The original contributions presented in this study are included in the article. Further inquiries can be directed to the corresponding author.

References

[1] Meyers, M.A., Mishra, A. & Benson, D.J. (2006). Mechanical properties of nanocrystalline materials. *Progress in Materials Science, 51*, 427-556. https://doi.org/10.1016/j.pmatsci.2005.08.003

[2] Valiev, R.Z., Estrin, Y. & Horita, Z. (2015). Fundamentals of superior properties in bulk Nano SPD materials. *Materials Research Letters, 4*, 1-21. https://doi.org/10.1080/21663831.2015.1060543

[3] Valiev, R.Z., Estrin, Y. & Horita, Z. (2006). Producing bulk ultrafine-grained materials by severe plastic deformation. *JOM, 58*, 33-39. https://doi.org/10.1007/s11837-006-0213-7

[4] Valiev, R.Z., Langdon, T.G. (2010). The art and science of tailoring materials by nanostructuring for advanced properties using SPD techniques. *Advanced Engineering Materials, 12*, 677-691. https://doi.org/10.1002/adem.201000019

[5] Sergueeva, A.V., Stolyarov, V.V., Valiev, R.Z. & Mukherjee, A.K. (2001). Advanced mechanical properties of pure titanium with ultrafine-grained structure. *Scripta Materialia, 45*, 747-752. https://doi.org/10.1016/S1359-6462(01)01089-2

[6] Valiev, R.Z. (1995). Approach to nanostructured solids through the studies of submicron grained polycrystals. *Nanostructured Materials, 6*, 73. https://doi.org/10.1016/0965-9773(95)00031-3

[7] Salishchev, G.A., Galeyev, R.M. & Valiahmetov, O.R. (1994). Dynamic recrystallization of titanium. *Izvestiya Akademii Nauk SSSR, Metally, (1)*, 125-129

[8] Salishchev, G.A., Valiahmetov, O.R., Galeyev, R.M. & Malysheva, S.P. (1996). Formation of submicrocrystalline structure in titanium during plastic deformation and its effect on mechanical properties. *Metally, (4)*, 86

[9] Zherebtsov, S.V., Salishchev, G.A. & Galeyev, R.M. (2002). Formation of submicrocrystalline structure in titanium and its alloy under severe plastic deformation. *Defect and Diffusion Forum, 208-209*, 237-240. https://doi.org/10.4028/www.scientific.net/DDF.208-209.237

[10] Zherebtsov, S.V., Galeyev, R.M. & Valiahmetov, O.R. (1999). Formation of submicrocrystalline structure in titanium alloys by severe plastic deformation. *Kuznechno-Shtampovochnoe Proizvodstvo, (7)*, 17-22.

[11] Stolyarov, V.V., Zhu, Y.T., Alexandrov, I.V., Lowe, T.C. & Valiev, R.Z. (2001). Influence of ECAP routes on the microstructure and properties of pure Ti. *Materials Science and Engineering A, 299*, 59. https://doi.org/10.1016/S0921-5093(00)01411-8

[12] Raab, G.I., Soshnikova, E.P. & Valiev, R.Z. (2004). Influence of temperature and hydrostatic pressure during equal channel angular pressing on the microstructures of commercial-purity Ti. *Materials Science and Engineering A, 387-389*, 674-677. https://doi.org/10.1016/j.msea.2004.01.137

[13] Stolyarov, V.V., Zhu, Y.T., Lowe, T.C. & Valiev, R.Z. (2001). Microstructure and properties of pure Ti processed by ECAP and cold extrusion. *Materials Science and Engineering A, 303*, 82-89. https://doi.org/10.1016/S0921-5093(00)01884-0

[14] Valiev, R.Z., & Alexandrov, I.V. (2000). Nanostructured materials obtained by severe plastic deformation. *Logos.* https://doi.org/10.1016/S0079-6425(99)00007-9

[15] Stolyarov, V.V., Zhu, Y.T., Alexandrov, I.V., Lowe, T.C. & Valiev, R. Z. (2003). Grain refinement and properties of pure Ti processed by warm ECAP and cold rolling. *Materials Science and Engineering A, 343*, 43. https://doi.org/10.1016/S0921-5093(02)00366-0

[16] Raab, G.I., Valiev, R.Z. (2008). Equal-channel angular pressing by the 'Conform' scheme for long-length nanostructured titanium semi-finished products. *Kuznechno-Shtampovochnoe Proizvodstvo. Obrabotka Metallov Davleniem, (1), 21-27*

[17] Segal, V.M., Reznikov, V.I. & Kopylov, V.I. (1994). Plastic structure formation processes in metals. *Nauka i Tekhnika*

[18] Pippan, R., Hohenwarter, A. (2016). The importance of fracture toughness in ultrafine and nanocrystalline bulk materials. *Materials Research Letters, 4*, 127-136. https://doi.org/10.1080/21663831.2016.1166403

[19] Hohenwarter, A., Pippan, R. (2015). Fracture and fracture toughness of nanopolycrystalline metals produced by severe plastic deformation. *Philosophical Transactions of the Royal Society A, 373*, 20140366. https://doi.org/10.1098/rsta.2014.0366

[20] Hohenwarter, A., Pippan, R. (2011). An overview on the fracture behavior of metals processed by high-pressure torsion. *Materials Science Forum, 667-669*, 671-676. https://doi.org/10.4028/www.scientific.net/MSF.667-669.671

[21] Boyer, R., Welsch, G. & Collings, E.W. (1998). Materials properties handbook: Titanium alloys. *ASM International*

[22] Ritchie, R.O. (2011). The conflicts between strength and toughness. *Nature Materials, 10(11)*, 817-822. https://doi.org/10.1038/nmat3115

[23] Fan, J.K., Kou, H.C. & Lai, M.J. (2013). Relationship between fracture toughness and microstructure of a new near-β titanium alloy. *Proceedings of the 8th Pacific Rim International Congress*

on Advanced Materials and Processing, 4, 3371-3378. https://doi.org/10.1007/978-3-319-48764-9_417
[24] Skvortsova, S., Grushin, I., Umarova, O. & Speranskiy, K. (2017). Effect of rare-earth element addition on structure of heat-resistant Ti–6.5Al–4Zr–2.5Sn–2.4V–1Nb–0.5Mo–0.2Si titanium alloy. *MATEC Web of Conferences, 114*, 02008. https://doi.org/10.1051/matecconf/201711402008
[25] Kaibyshev, O.A. (1984). Superplasticity of industrial alloys. *Metallurgiya.*
[26] Valiev, R.Z. & Alexandrov, I. V. (2007). Bulk nanostructured metallic materials: Production, structure, and properties. *Academkniga.*
[27] Lutfullin, R.Ya., Kruglov, A.A., Mukhametrakhimov, M.Mh. & Rudenko, O.A. (2015). Superplasticity of metallic materials. *Letters on Materials, 5(2)*, 185. https://doi.org/10.22226/2410-3535-2015-2-185-188
[28] Grabski, M.V. (1975). Structural superplasticity of metals, 272 p. *Metallurgiya.*
[29] Smirnov, O.M. (1979). Pressure treatment of metals in the state of superplasticity, 184 p. *Mashinostroenie*
[30] Padmanabhan, K.A., Davies, J.J. (1980). Superplasticity, 314 p.. *Springer-Verlag*. https://doi.org/10.1007/978-3-642-81456-3
[31] Novikov, I.I., Portnoi, V.K. (1981). Superplasticity of alloys with ultrafine grain, 168 p. *Metallurgiya.*
[32] Kaibyshev, O.A. (1984). Superplasticity of industrial alloys (264 pp.). *Metallurgiya.*
[33] Segal, V.M., Reznikov, V.I., Kopylov, V.I. & Pavlik, D.A. (1994). Plastic structure formation in metals. *Nauka i Tekhnika.*
[34] Nieh, T.G., Wadsworth, J., Sherby, O.D. (1997). Superplasticity in metals and ceramics, 287 p. *Cambridge University Press*. https://doi.org/10.1017/CBO9780511525230
[35] Vasin, R.A., Enikeev, F.U. (1998). Introduction to the superplasticity mechanics. *Gilem.*
[36] Padmanabhan, K.A., Vasin, R.A. & Enikeev, F.U. (2001). Superplastic flow: Phenomenology and mechanics. *Springer-Verlag*. https://doi.org/10.1007/978-3-662-04367-7
[37] Chumachenko, E.N., Smirnov, O.M. & Tsepin, M.A. (2005). Superplasticity: Materials, theory, technology. *KomKniga.*
[38] Segal, V.M., Beyerlein, I.J. & Tomé, C.N. (2010). Fundamentals and engineering of severe plastic deformation. *Nova Science Publishers.*
[39] Langdon, T.G. (2016). Forty-five years of superplastic research: Recent developments and future prospects. *Materials Science Forum, 838-839*, 3-12. https://doi.org/10.4028/www.scientific.net/MSF.838-839.3
[40] Sharifullina, E.R., Shveikin, A.I. & Trusov, P.V. (2018). Review of experimental studies on structural superplasticity: Internal structure evolution of material and deformation mechanisms. *PNRPU Mechanics Bulletin, 3*, 103-127. https://doi.org/10.15593/perm.mech/2018.3.11
[41] Mikhaylovskaya, A.V., Mosleh, A.O. & Kotov, A.D. (2017). Superplastic deformation behavior and microstructure evolution of near-α Ti-Al-Mn alloy. *Materials Science and Engineering A, 708*, 469-477. https://doi.org/10.1016/j.msea.2017.10.017
[42] Mosleh, A.O., Mikhaylovskaya, A.V. & Kotov, A.D. (2018). Experimental investigation of the effect of temperature and strain rate on the superplastic deformation behavior of Ti-based alloys in the (α + β) temperature field. *Metals, 8(10)*, 819. https://doi.org/10.3390/met8100819
[43] Segal, V.M., Reznikov, V.I., Dobryshevshiy, A.E. & Kopylov, V.I. (1981). Plastic working of metals by simple shear. Russian *Metallurgy (Metally), 1(1)*, 99-105
[44] Gromov, N.P. (1967). Theory of metal forming. *Metallurgiya.*
[45] Kaibyshev, O.A., Utyashev, F.Z. (2002). Superplasticity, structure refinement, and processing of hard-to-deform alloys. *Nauka.*
[46] Cheng, Y.Q., Zhang, H., Chen, Z.H. & Xian, K.F. (2008). Flow stress equation of AZ31 magnesium alloy sheet during warm tensile deformation. *Journal of Materials Processing Technology, 208(1-3)*, 29-34. https://doi.org/10.1016/j.jmatprotec.2007.12.095
[47] Vasin, R.A., Enikeev, F.U., Kruglov, A.A. & Safiullin, R.V. (2003). On the identification of constitutive relations by the results of technological experiments. *Mechanics of Solids, 38(2)*, 90-100
[48] Lee, S.W., Yeh, J.W. (2007). Superplasticity of 5083 alloys with Zr and Mn additions produced by reciprocating extrusion. *Materials Science and Engineering A, 460-461*, 409-419. https://doi.org/10.1016/j.msea.2007.01.121

Цирконийдің титан қорытпаларының құрылымы мен қасиеттерінің қалыптасуына әсері және оның аса пластикалық деформация кезіндегі рөлі

А.М. Алимжанова[1*], А.Ж. Терликбаева[1], Б.Т. Сахова[1,2], Р.А. Шаяхметова[1], Г.М. Қойшина[2], А.А. Мухаметжанова[1], Г.К. Малдыбаев[3]

[1]*Қазақстан Республикасының минералдық шикізатты кешенді қайта өңдеу жөніндегі ұлттық орталығы, Алматы, Қазақстан*
[2]*Satbayev University, Алматы, Қазақстан*
[3]*Қазақстан-Британ техникалық университеті, Алматы, Қазақстан*

**Корреспонденция үшін автор: aliyuchca@mail.ru*

Аңдатпа. Бұл жұмыста әртүрлі температуралар мен деформация жылдамдықтарында цирконийдің титан қорытпаларының аса пластикалық қасиеттеріне әсері зерттелді. Цирконийдің деформация жылдамдығына сезімталдық коэффициентіне (m), механикалық тұрақтылыққа және пластикалылыққа едәуір ықпал ететіні анықталды. Жоғары температура жағдайында цирконий бар қорытпалар белгілі бір деформация жылдамдықтарында m коэффициентінің тұрақты деңгейін көрсетеді, кейін ол күрт төмендейді. Ал цирконийсіз қорытпаларда деформация жылдамдығы артқан сайын бұл коэффициент біртіндеп азаяды. Аса пластикалық деформацияның оңтайлы температуралық және жылдамдықтық параметрлері цирконий мөлшеріне байланысты болады. Цирконийдің төмен концентрациясы бар қорытпалар орташа температура мен деформация жылдамдығында жоғары пластикалылықпен сипатталады, ал цирконийдің жоғары мөлшері бар қорытпалар біркелкі деформацияны қамтамасыз ету үшін төмен жылдамдықты талап етеді. Белгілі бір деңгейден асқан цирконий мөлшері пластикалылықтың төмендеуіне және деформацияның локализациясына әкеледі. Сонымен қатар цирконий аққыштық кернеуді арттырады, ал температураның көтерілуі бұл кернеуді азайта-

ды, бірақ дәннің іріленуіне алып келеді, бұл механикалық қасиеттерге теріс әсер етеді. Сканерлейтін электрондық микроскопия әдісімен жүргізілген микроструктуралық талдау аса пластикалық деформациядан кейін барлық зерттелген қорытпаларда эквиаксы α- және β-дәндерден тұратын ұсақ дәнді құрылым қалыптасатынын көрсетті. Орташа дән өлшемі бастапқы күймен салыстырғанда артатыны анықталды, бұл динамикалық қалпына келу мен рекристаллизация процестерінің жүргенін білдіреді. Алынған нәтижелер зерттелген титан қорытпаларын аса пластикалық қалыптау технологияларында қолдануға болатынын дәлелдейді. Айқындалған заңдылықтар бұл материалдардың өнеркәсіптік қолданылуы үшін жоғары пластикалылық пен механикалық тұрақтылықты қамтамасыз ететін оңтайлы термомеханикалық өңдеу параметрлерін анықтауға мүмкіндік береді.

Негізгі сөздер: *ультра ұсақ дәнділік, қарқынды пластикалық деформация, құрылым, наноөлшемдер, аса пластикалылық, цирконий.*

Роль циркония в формировании структуры и свойств титановых сплавов при сверхпластической деформации

А.М. Алимжанова[1*], А.Ж. Терликбаева[1], Б.Т. Сахова[1,2], Р.А. Шаяхметова[1], Г.М. Қойшина[2], А.А. Мухаметжанова[1], Г.К. Малдыбаев[3]

[1]*Национальный центр по комплексной переработке минерального сырья Республики Казахстан, Алматы, Казахстан*
[2]*Satbayev University, Алматы, Казахстан*
[3]*Казахстанско-Британский технический университет, Алматы, Казахстан*

**Автор для корреспонденции: aliyuchca@mail.ru*

Аннотация. В работе исследовано влияние циркония на сверхпластические свойства титановых сплавов при различных температурах и скоростях деформации. Установлено, что цирконий оказывает значительное влияние на коэффициент чувствительности к скорости деформации (m), механическую стабильность и пластичность. В условиях повышенных температур сплавы, содержащие цирконий, демонстрируют устойчивый уровень коэффициента m в определённом диапазоне скоростей деформации, после чего происходит его резкое снижение. В сплавах без циркония наблюдается постепенное уменьшение коэффициента m с увеличением скорости деформации. Оптимальные температурно-скоростные параметры сверхпластической деформации зависят от содержания циркония. Сплавы с его низкой концентрацией характеризуются высокой пластичностью при умеренных температурах и средних скоростях деформации, тогда как сплавы с более высоким содержанием циркония требуют пониженных скоростей для обеспечения равномерности деформации. Увеличение содержания циркония выше определённого уровня приводит к снижению пластичности и локализации деформации. В то же время цирконий повышает напряжение течения, тогда как увеличение температуры способствует его снижению, но сопровождается укрупнением зерна, что отрицательно влияет на механические свойства. Микроструктурный анализ методом сканирующей электронной микроскопии показал, что после сверхпластической деформации все исследуемые сплавы формируют мелкозернистую структуру, состоящую из равноосных α- и β-зёрен. Установлено, что средний размер зерна увеличивается по сравнению с исходным состоянием, что свидетельствует о процессах динамического восстановления и рекристаллизации. Полученные результаты подтверждают возможность применения исследуемых титановых сплавов в технологиях сверхпластической формовки. Выявленные закономерности позволяют определить оптимальные параметры термомеханической обработки, обеспечивающие сочетание высокой пластичности и механической стабильности, что важно для промышленного использования данных материалов.

Ключевые слова: *ультрамелкозернистость, интенсивная пластическая деформация, структура, наноразмеры, сверхпластичность, цирконий.*

Publisher's note

All claims expressed in this manuscript are solely those of the authors and do not necessarily represent those of their affiliated organizations, or those of the publisher, the editors and the reviewers.

SATBAYEV UNIVERSITY

Engineering Journal of Satbayev University

Volume 147 (2025), Issue 2, 10-16

https://doi.org/10.51301/ejsu.2025.i2.02

Prospects for the processing of spent automotive catalysts with the extraction of precious, rare and rare-earth metals in Kazakhstan

K.T. Yeskalina[1], S.S. Konyratbekova[1], S.B. Yulussov[1,2], A.T. Khabiyev[1,2*]

[1]*Satbayev University, Almaty, Kazakhstan*

[2]*U.A. Joldasbekov Institute of Mechanics and Engineering, Almaty, Kazakhstan*

**Corresponding author: alibek1324@mail.ru*

Abstract. Used automotive catalysts are a valuable source of rare and precious metals, which plays a key role in modern industry. These raw materials contain rare rare earths and precious metals, which makes their processing highly efficient and economically profitable. To develop a comprehensive processing technology, catalysts were studied using various analysis methods, such as chemical, X-ray, X-ray spectral, and electron microscopic analysis. The results of the phase analysis indicate that rare rare earths and noble metals are in various phase states, in the form of oxides embedded in the aluminosilicate matrix of the catalyst. These data are of critical importance for the creation of effective methods of metal extraction. The key approaches for processing these raw materials are pyrometallurgical and hydrometallurgical technologies, each of which has its own advantages and unique performance criteria. This article focuses on the physico-chemical studies of spent catalysts and the proposed method of their opening, which makes it possible to efficiently extract rare, rare-earth and precious metals. The research results can be used to optimize existing and develop new technological schemes for processing secondary raw materials.

Keywords: *spent automotive catalysts, rare metals, precious metals, rare earth elements, platinum metals, hydrometallurgical technologies, pyrometallurgical technologies, selective precipitation, secondary raw materials.*

Received: 19 January 2025
Accepted: 15 April 2025
Available online: 30 April 2025

1. Introduction

Over the past three decades, a significant number of used cars have accumulated in Kazakhstan, and the country's vehicle fleet continues to grow at a rapid pace [1]. This has led to the formation of a vast volume of secondary technogenic raw materials, such as automotive catalysts. These catalysts, which contain valuable metals, are often dismantled and exported abroad for the extraction of precious, rare, and rare earth metals [2]. However, this approach not only deprives Kazakhstan of potential economic benefits but also creates environmental risks associated with the transportation and processing of waste abroad [3].

At the enterprise of JSC «Tau-Ken Altyn», located in the industrial park of Astana, work has begun in the field of recycling used catalysts to extract precious metals such as platinum, palladium, and rhodium [4]. However, the extraction of rare and rare earth metals (REM), whose global market demand is rapidly growing, has not been foreseen [5]. This limits the potential for comprehensive use of secondary raw materials and reduces the economic efficiency of recycling [6].

The relevance of comprehensive secondary raw material utilization is becoming increasingly evident for Kazakhstan, especially in light of the growing volumes of secondary waste [7]. Recycling used automotive catalysts is mainly aimed at extracting precious metals, while other important elements, such as rare and rare earth metals, remain undervalued [8]. This is because existing technologies focus on extracting precious metals, even though catalysts also contain significant amounts of rare and REMs, which can be economically profitable [9].

Existing recycling technologies, such as pyrometallurgy, ensure high yields of precious metal recovery but require substantial energy costs and specialized equipment [10]. This leads to increased capital and operational expenses, as well as the formation of waste, such as volatile substances and slag [11]. The main issue lies in the high cost of continuous furnace operation, which requires the use of secondary resources and increases the impurity content in the final product [12].

Modern pyrometallurgical methods, such as plasma smelting, allow for the minimization of emissions and improved recycling efficiency [13]. However, a key challenge remains addressing issues related to sulfur dioxide and chromium and other impurities [14]. Chlorination and fluorination methods are still relevant, although they are associated with the formation of toxic emissions, which requires efforts to reduce environmental impact [15].

Figure 1 presents the technological diagram of the pyrometallurgical method for recycling automotive catalysts. This process involves multiple sequential steps to recover platinum group metals (PGMs) from spent catalysts while minimizing waste generation.

kuralai_eskalina@mail.ru; salta_7504@mail.ru; s1981b@mail.ru; alibek1324@mail.ru
Engineering Journal of Satbayev University. eISSN 2959-2348. Published by Satbayev University

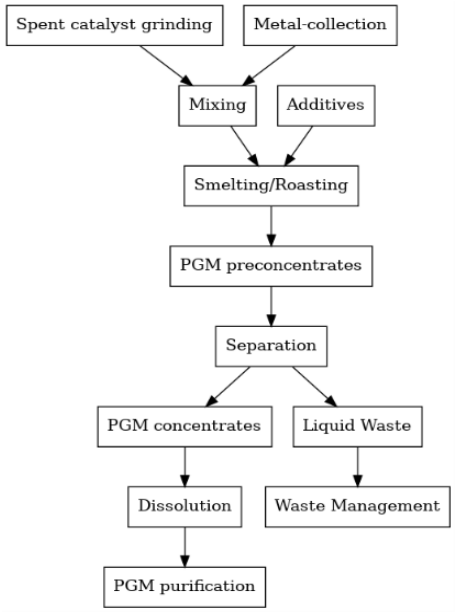

Figure 1. Pyrometallurgical and hydrometallurgical processes for PGM recovery

The process involves crushing, grinding, and smelting catalysts at temperatures above 2000°C with the addition of fluxes and collector metals [16]. After this, the precious metals are extracted from the resulting concentrate for further processing. However, components of the catalysts, such as rare metals and aluminum oxide, have significant economic value, and their joint extraction is complicated by the slag melting process [17].

Modern recycling methods aim to increase the efficiency of extracting all valuable components [18]. The development of technologies that minimize the losses of rare metals and their combinations is becoming increasingly relevant [19]. In addition, environmental and safety considerations during high-temperature processes must be addressed [20].

Improving catalyst recycling technologies could lead to better resource utilization and a reduction in the negative impact on the environment [21]. This, in turn, contributes to the sustainable development of the economy and the preservation of natural resources [22]. Investing in scientific research in this field promises new solutions and improvements in methods for extracting valuable metals [23].

In recent years, alternative hydrometallurgical procedures have been developed to improve extraction rates and the purity of the final product [24]. Despite these efforts, the efficiency of new methods has not yet reached the level of pyrometallurgical technologies, which continue to dominate the industry [25]. To improve the effectiveness of hydrometallurgical processes, new reagents and technologies need to be explored [26]. An important direction is the use of biodiversity and alternative energy sources, which helps reduce the negative environmental impact [27]. Therefore, further innovations in this area could significantly improve the sustainability and economic feasibility of metal recycling processes [28].

In light of the above, recycling used automotive catalysts in Kazakhstan represents an important direction for economic development and environmental improvement [29]. A comprehensive approach to the extraction of precious, rare, and rare earth metals could become a key factor in achieving sustainable development and reducing dependence on the import of valuable resources [30].

2. Materials and methods

2.1. Objects of research

The objects of the study were a representative sample of used automotive catalysts, selected to account for their morphological and chemical diversity. Before the experiments, the sample underwent mechanical treatment, including crushing, grinding to a fraction smaller than 100 μm, and homogenization to ensure uniform distribution of components. For the analysis of the elemental composition, X-ray fluorescence spectrometry (XRF) and scanning electron microscopy with energy-dispersive analysis (SEM-EDS) were used [1].

2.2 Analytical methods

During the physicochemical studies, chemical, X-ray phase, X-ray spectral, and electron probe methods of analysis were used. The sample preparation for ore was carried out according to the standard methodology [1].

The concentrations of precious, rare, and rare earth metals were determined using an inductively coupled plasma atomic emission spectrometer (ICP-AES), model 8300 DV (PerkinElmer Inc., USA). The instrument provided measurements in the spectral range of 165–782 nm with a resolution no lower than 0.006 nm (at a wavelength of ~200 nm) and a root mean square deviation of random error of 2.0%. Calibration curves, constructed from standard solutions with known concentrations of target elements, were used for quantitative analysis.

The efficiency of metal extraction (η, %) was calculated using the formula: $\eta = C \cdot V / m_0 \cdot w \times 100\%$, $\eta = m_0 \cdot w / C \cdot V \times 100\%$, where C is the metal concentration in the solution (mg/l), V is the solution volume (l), m_0 is the sample mass (g), and w is the metal mass fraction in the catalyst.

X-ray phase analysis was performed on a D8 Advance diffractometer (Bruker) using Cu Kα radiation (40 kV, 40 mA). The diffraction patterns were processed, including the calculation of interplanar distances, using the EVA software. Phase identification and matching were carried out using the Search/Match program and the PDF-2 powder diffraction database.

2.3 Statistical processing

Each experiment was repeated three times. The data were processed using OriginPro 2023 software, calculating the mean values and standard deviations.

3. Results and discussion

3.1. Physico-chemical characteristics of man-made waste

Chemical Composition and Mineralogical Analysis

Table 1 presents the results of the chemical analysis of the initial sample, including the mass fractions of various elements. The data reveal a significant content of aluminum (22.57%) and zirconium (14.53%), along with the presence of rare-earth elements (La, Ce) and platinum group metals (Pt, Pd, Rh).

Table 1. Chemical composition of spent automotive catalysts

Name of the product	The content of the elements, %						
	Ca	Mg	Al	Si	Fe	Zn	Zr
The initial sample	0.76	2.83	22.57	8.31	1.28	0.44	14.53
	Ba	La	Ce	C	Pt	Pd	Rh
	1.48	2.67	6.21	0.036	0.0632	0.1510	0.0235

The X-ray diffraction (XRD) pattern presented in Figure 2 illustrates the results of the phase analysis of the initial sample, revealing a complex mineral composition. The primary identified phases include indialite ($Mg_2Al_4Si_5O_{18}$) – 62.4%, zirconium oxide (ZrO_2) – 14.3%, zirconium-ceria oxide ($ZrCeO_4$) – 9.6%, lanthanum-zirconium oxide ($La_2Zr_2O_7$) – 9.5%, and aluminum-lanthanum-magnesium compound ($Al_2La_2Mg_3$) – 5.4%. These findings indicate the presence of aluminum, zirconium, magnesium, and rare-earth element compounds, suggesting a possible crystalline structure with high thermal and chemical stability. The diffraction peaks correlate well with PDF database references, confirming the reliability of the phase analysis.

For accurate identification and confirmation of the presence of noble, rare, rare-earth, and associated metals, as well as for elemental mapping of mineral grains, electron probe scanning was performed using a scanning electron microscope (SEM) at high magnifications (Figure 3).

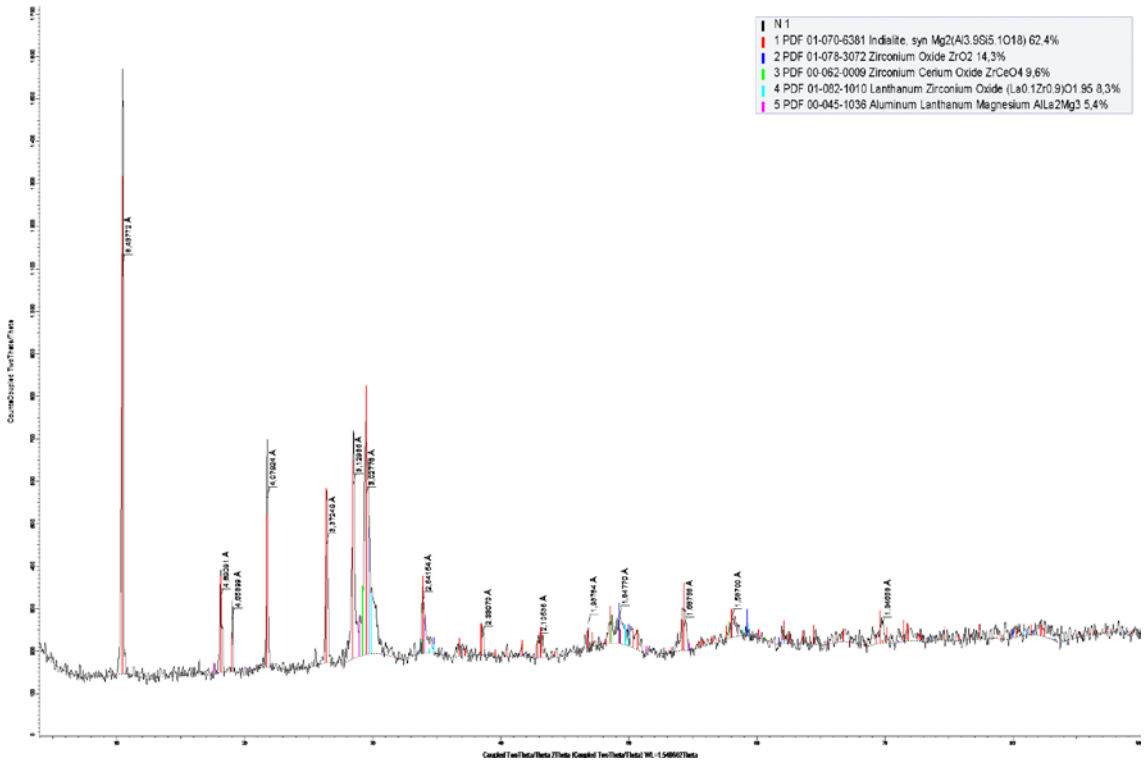

Figure 2. X-ray diffraction pattern of spent catalysts

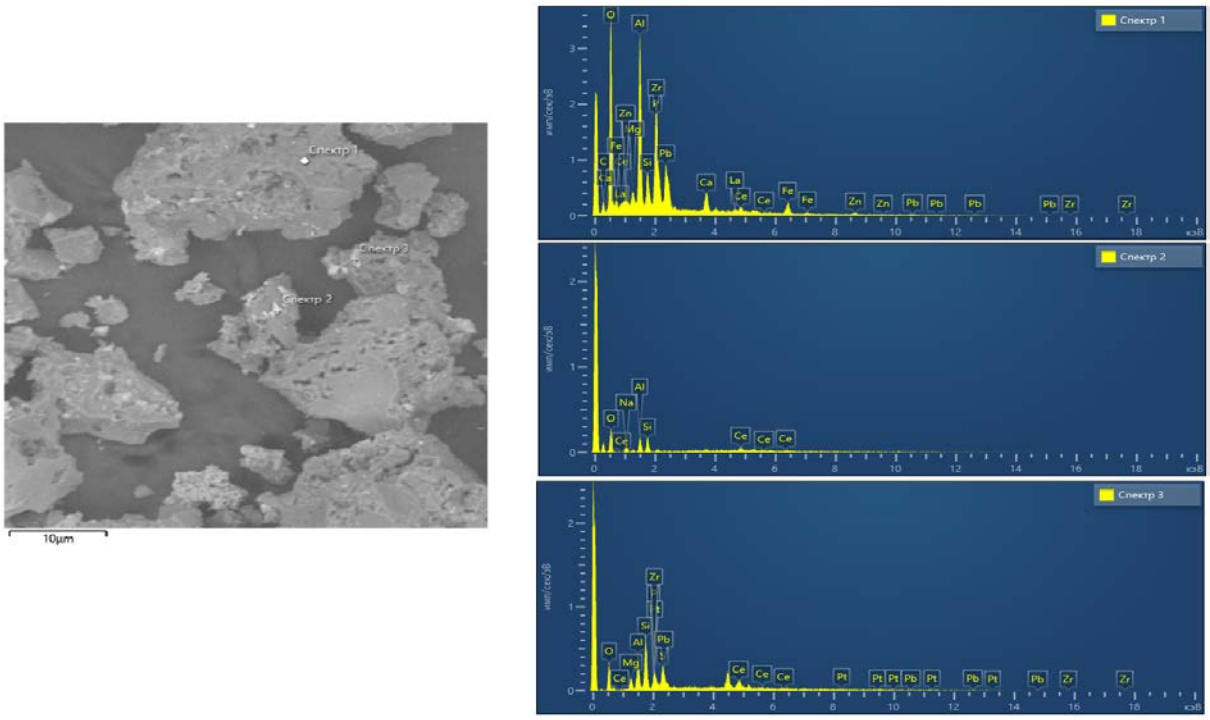

Figure 3. Micrograph and point spectral analysis of particles in the initial sample

The results of qualitative and quantitative elemental analysis, conducted in a randomly selected microscopic region, are presented in correlation with the surface topography obtained through scanning electron microscopy and a specialized electron probe microanalyzer. The acquired data are visualized in Figure 3, and the corresponding elemental composition spectrum is provided in Table 2.

Table 2. Results of electron probe spectral analysis of catalyst particles

Element	Spectrum 1	Spectrum 2	Spectrum 3
	%	%	%
C	7.98	-	-
O	36.71	-	24.67
Mg	0.95	-	3.90
Al	11.14	41.70	10.57
Si	2.25	58.30	15.71
P	4.69	-	3.67
Ca	2.65	-	-
Fe	4.76	-	-
Zn	3.25	-	-
Zr	8.67	-	8.4
La	1.74	-	-
Ce	2.97	-	14.53
Pb	12.24	-	9.05
S	-	-	7.94
Pt	-	-	1.57
Итоги	100	100	100

The presented micrograph, obtained using scanning electron microscopy (SEM), visualizes the particles of the initial sample with characteristic morphology. The image reveals a heterogeneous material structure containing both large aggregates and fine-dispersed inclusions. The scale bar of 10 μm indicates the micron-sized nature of the particles, while the marked regions (Spectrum 1, Spectrum 2, Spectrum 3) represent zones of localized spectral analysis.

The results of energy-dispersive X-ray spectroscopy (EDS) for these points demonstrate a complex elemental composition, including aluminum (Al), silicon (Si), magnesium (Mg), zirconium (Zr), iron (Fe), lead (Pb), rare-earth elements (La, Ce), and platinum (Pt). Variations in elemental concentrations across different spectra indicate the heterogeneous composition of the samples.

The spectral analysis data confirm the presence of noble and rare-earth elements, highlighting the potential value of material recycling. The obtained results are visualized in the spectrograms on the right, displaying the intensities of characteristic X-ray lines corresponding to the marked areas in the micrograph.

Table 2 presents the results of electron probe spectral analysis of catalyst particles in three different regions of investigation (Spectrum 1, Spectrum 2, Spectrum 3). The data reflect the mass fractions (in %) of the chemical elements detected in localized areas of the sample.

The analysis reveals significant variations in elemental composition across different spectral zones. In Spectrum 1, oxygen (36.71%), aluminum (11.14%), zirconium (8.67%), and lead (12.24%) are predominant, indicating the presence of oxide compounds and metallic elements. Spectrum 2 is dominated by aluminum (41.70%) and silicon (58.30%), suggesting the presence of aluminosilicate phases. Spectrum 3 exhibits high concentrations of silicon (15.71%), oxygen (24.67%), cerium (14.53%), and sulfur (7.94%), along with platinum (1.57%), confirming the presence of rare-earth and noble metals.

The overall element distribution highlights the complex and heterogeneous composition of catalyst particles, including oxides, aluminosilicates, rare-earth elements, and noble metals, which is crucial for further research into their catalytic properties and recycling potential.

Elemental mapping of catalyst particles from spent automotive catalysts, performed using energy-dispersive spectroscopy (EDS) at 750× magnification, is presented in the image. The multilayer element distribution map (left) visualizes the heterogeneous structure of the material with varying concentrations of key elements.

The mapping results (Figure 4) confirm the complex composition and inhomogeneous element distribution within the material, emphasizing the need to consider these factors when developing efficient extraction methods for valuable components.

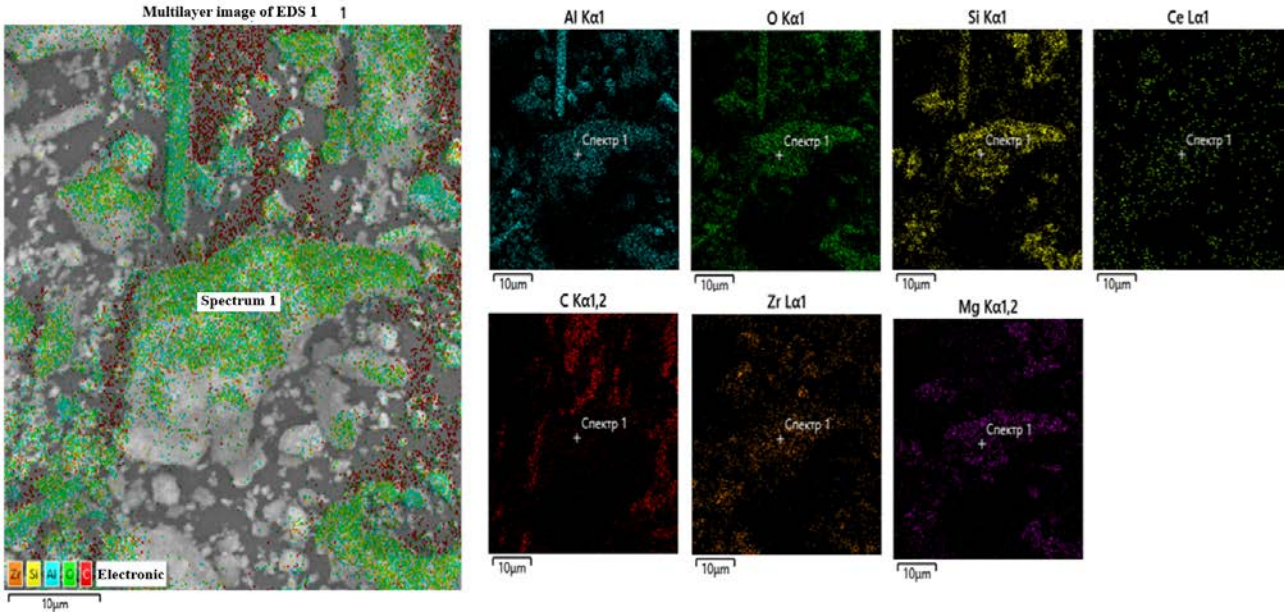

Figure 4. Elemental mapping of grains and particles of automotive catalysts

Elemental mapping of catalyst particle grains revealed a non-uniform element distribution in spent catalysts. The primary components localized in specific regions are aluminum (Al) and silicon (Si), indicating an aluminosilicate matrix of the catalyst. Oxygen (O) is relatively evenly distributed, suggesting the presence of oxide phases. Carbon (C) is detected in limited areas, likely associated with carbon-containing residues or decomposition products of organic compounds. Cerium (Ce) and zirconium (Zr) identified in localized regions point to the presence of rare-earth oxide phases, characteristic of automotive catalysts. Magnesium (Mg) is also present in the catalyst structure, though its distribution is highly uneven. However, noble metals were not detected in the analyzed areas, confirming their heterogeneous distribution within the material.

The obtained results indicate that spent catalysts contain not only noble metals but also rare and rare-earth elements, making them a promising target for recycling. Consequently, studies on the extraction of valuable components, particularly rare and rare-earth metals, were conducted using thermal treatment with concentrated sulfuric acid at the initial stage of the research.

4. Conclusions

Recycling of spent automotive catalysts is a crucial task for both the economy and the environment of Kazakhstan. The conducted studies have confirmed the presence of significant amounts of noble metals (Pt, Pd, Rh), rare and rare-earth elements (La, Ce), as well as aluminum and zirconium oxides, making these catalysts a valuable secondary raw material.

An analysis of existing recycling technologies has shown that traditional pyrometallurgical methods demonstrate high efficiency in extracting noble metals but are associated with high energy consumption and environmental risks. The results of X-ray phase analysis and energy-dispersive spectral analysis have confirmed the complex composition of catalysts, highlighting the need for further improvement in comprehensive recycling technologies.

Thus, the development and implementation of new technological solutions aimed at maximizing the recovery of all valuable components will significantly enhance the economic efficiency of recycling, reduce dependence on imported rare metals, and minimize environmental impact. Investing in scientific research and modernizing recycling facilities is a key step toward the sustainable development of Kazakhstan's metallurgical industry.

Author contributions

Conceptualization: S.S.K.; Data curation: A.T.K.; Formal analysis: S.S.K.; Funding acquisition: S.B.Y.; Investigation: S.B.Y.; Methodology: K.T.Y.; Project administration: S.B.Y.; Resources: S.B.Y.; Software: S.S.K., K.T.Y.; Supervision: S.S.K., K.T.Y.; Validation: S.B.Y.; Visualization: A.T.K., S.B.Y.; Writing – original draft: A.T.K., S.B.Y.; Writing – review & editing: S.B.Y. All authors have read and agreed to the published version of the manuscript.

Funding

This research funded by the Science Committee of the Ministry of Science and Higher Education of the Republic of Kazakhstan, grant number AP19676107.

Acknowledgements

The authors would like to express their sincere gratitude to the editor and the two anonymous reviewers for their constructive comments and valuable suggestions, which significantly contributed to the improvement of the manuscript.

Conflicts of interest

The authors declare no conflict of interest.

Data availability statement

The original contributions presented in this study are included in the article. Further inquiries can be directed to the corresponding author.

References

[1] Noya, I., Inglezakis, V., González-García, S., Katsou, E., Feijoo, G. & Moreira, M.T. (2018). Comparative environmental assessment of alternative waste management strategies in developing regions: A case study in Kazakhstan. *Waste Management & Research, 36*(8), 689-697. https://doi.org/10.1177/0734242X18786388

[2] Kovalčík, J., Straka, M., Kačmáry, P. & Pavlík, T. (2021). Catalyst processing and recycling. *Acta Tecnologia, 7*(3), 99-104. https://doi.org/10.22306/atec.v7i3.118

[3] Parajuly, K. & Fitzpatrick, C. (2020). Understanding the impacts of transboundary waste shipment policies: The case of plastic and electronic waste. *Sustainability, 12*(6), 2412. https://doi.org/10.3390/su12062412

[4] Kipkeeva, A., Ermetova, I., Matyakubov, U. & Palvanbayev, U. (2024). Modern methods for efficiency assessment of special economic and small industrial zones' ecosystems. *BIO Web of Conferences, (130)*, 08011. https://doi.org/10.1051/bioconf/202413008011

[5] Gaustad, G., Williams, E. & Leader, A. (2021). Rare earth metals from secondary sources: Review of potential supply from waste and byproducts. *Resources, Conservation and Recycling, 167*, 105213. https://doi.org/10.1016/j.resconrec.2020.105213

[6] Hagelüken, C. (2014). Recycling of (critical) metals. *Critical metals handbook, 41-69.*

[7] Tleuken, A., Tokazhanov, G., Jemal, K. M., Shaimakhanov, R., Sovetbek, M. & Karaca, F. (2022). Legislative, institutional, industrial and governmental involvement in circular economy in Central Asia: A systematic review. *Sustainability, 14*(13), 8064. https://doi.org/10.3390/su14138064

[8] Padamata, S. K., Yasinskiy, A. S., Polyakov, P. V., Pavlov, E. A. & Varyukhin, D. Y. (2020). Recovery of noble metals from spent catalysts: a review. *Metallurgical and materials transactions B, 51*, 2413-2435. https://doi.org/10.1007/s11663-020-01913-w

[9] Saguru, C., Ndlovu, S. & Moropeng, D. (2018). A review of recent studies into hydrometallurgical methods for recovering PGMs from used catalytic converters. *Hydrometallurgy, 182*, 44-56. https://doi.org/10.1016/j.hydromet.2018.10.012

[10] Harvey, J. P., Khalil, M. & Chaouki, J. (2022). Pyrometallurgical processes for recycling waste electrical and electronic equipment. *Electronic Waste: Recycling and Reprocessing for a Sustainable Future*, 135-164. https://doi.org/10.1002/9783527816392.ch7

[11] Liddell, K., Newton, T., Adams, M. & Muller, B. (2011). Energy consumption for Kell hydrometallurgical refining versus conventional pyrometallurgical smelting and refining of PGM concentrates. *Journal of the Southern African Institute of Mining and Metallurgy, 111*(2), 127-132.

[12] Reck, B.K. & Graedel, T.E. (2012). Challenges in metal recycling. *Science, 337*(6095), 690-695. https://doi.org/10.1126/science.1217501

[13] Peng, Z., Li, Z., Lin, X., Tang, H., Ye, L., Ma, Y., & Jiang, T. (2017). Pyrometallurgical recovery of platinum group metals

from spent catalysts. *JOM, 69*, 1553-1562. https://doi.org/10.1007/s11837-017-2450-3
[14] Golwalkar, K. (2025). Typical Features of Metallurgical Industries. In Industrial Work Cultures: Impact on Productivity. *Cham: Springer Nature Switzerland*
[15] Gustin, J.L. (2005). Safety of chlorine production and chlorination processes. *Chemical Health & Safety*, *12*(1), 5-16. https://doi.org/10.1016/j.chs.2004.08.002
[16] Stegemann, L. & Gutsch, M. (2025). Environmental Impacts of Pyro-and Hydrometallurgical Recycling for Lithium-Ion Batteries-A Review. *Journal of Business Chemistry*, *22*(1), 62-76. https://doi.org/10.17879/43998523309
[17] Zheng, H., Ding, Y., Wen, Q., Zhao, S., He, X., Zhang, S. & Dong, C. (2022). Slag design and iron capture mechanism for recovering low-grade Pt, Pd, and Rh from leaching residue of spent auto-exhaust catalysts. *Science of The Total Environment, 802, 149830*. https://doi.org/10.1016/j.scitotenv.2021.149830
[18] Vidyadhar, A. (2016). A review of technology of metal recovery from electronic waste. *InTech*. https://doi.org/10.5772/61569
[19] Ramprasad, C., Gwenzi, W., Chaukura, N., Azelee, N.I.W., Rajapaksha, A.U., Naushad, M. & Rangabhashiyam, S. (2022). Strategies and options for the sustainable recovery of rare earth elements from electrical and electronic waste. *Chemical Engineering Journal, 442, 135992*. https://doi.org/10.1016/j.cej.2022.135992
[20] Machado, T.S.S., da Costa Leal, P.H.A., Cardoso, T.A.S., da Silva Borges, L., de Melo Santos, C.J. & Sant'Anna, A.M.O. (2023). Risk and safety assessment in the foundry process in the metallurgical industry. *Revista Produção Online, 23*(3), 5104-5104. https://doi.org/10.14488/1676-1901.v23i3.5104
[21] Zabelina, A.V. & Sergienko, O.I. (2021). Applying of the Best Available Techniques in the Municipal Solid Waste Recycling. *IOP Conference Series: Earth and Environmental Science, 720*(1), 012073. https://doi.org/10.1088/1755-1315/720/1/012073
[22] Sverdrup, H.U. (2019). Sustainable resource management. *Sustainability*, *11*(10), 2874. https://doi.org/10.3390/su11102874
[23] Costa-Campi, M.T., García-Quevedo, J. & Martínez-Ros, E. (2017). What are the determinants of investment in environmental R&D?. *Energy Policy, 104*, 455-465. https://doi.org/10.1016/j.enpol.2017.01.024
[24] Pathak, A., Al-Sheeha, H., Navvamani, R., Kothari, R., Marafi, M. & Rana, M. S. (2022). Recycling of platinum group metals from exhausted petroleum and automobile catalysts using bioleaching approach: a critical review on potential, challenges, and outlook. *Reviews in Environmental Science and Bio/Technology, 21*(4), 1035-1059. https://doi.org/10.1007/s11157-022-09636-x
[25] Kumari, R. & Samadder, S. R. (2022). A critical review of the pre-processing and metals recovery methods from e-wastes. *Journal of Environmental Management, 320*, 115887. https://doi.org/10.1016/j.jenvman.2022.115887
[26] Birloaga, I. & Vegliò, F. (2022). An innovative hybrid hydrometallurgical approach for precious metals recovery from secondary resources. *Journal of Environmental Management, 307*, 114567. https://doi.org/10.1016/j.jenvman.2022.114567
[27] Jadhao, P.R., Mishra, S., Pandey, A., Pant, K.K. & Nigam, K.D.P. (2021). Biohydrometallurgy: A sustainable approach for urban mining of metals and metal refining. *Catalysis for Clean Energy and Environmental Sustainability: Biomass Conversion and Green Chemistry, (1)*, 865-892. https://doi.org/10.1007/978-3-030-65017-9_27
[28] Atlee, J.R. (2005). Operational sustainability metrics: a case of electronics recycling (doctoral dissertation). *Massachusetts Institute of Technology*
[29] Nukusheva, A., Rustembekova, D., Abdizhami, A., Au, T. & Kozhantayeva, Z. (2023). Regulatory obstacles in municipal solid waste management in Kazakhstan in comparison with the EU. *Sustainability*, *15*(2), 1034. https://doi.org/10.3390/su15021034
[30] De Sa, P. & Korinek, J. (2021). Resource efficiency, the circular economy, sustainable materials management and trade in metals and minerals. *OECD Publishing*. https://doi.org/10.1787/69abc1bd-en

Қазақстанда асыл, сирек және сирек жер металдарын шығарумен пайдаланылған автомобиль катализаторларын қайта өңдеу перспективалары

К.Т. Ескалина[1], С.С. Коныратбекова[1], С.В. Юлусов[1,2], А.Т. Хабиев[1,2*]

[1]*Satbayev University, Алматы, Қазақстан*
[2]*Ө.А. Жолдасбеков атындағы Механика және машинатану институты, Алматы, Қазақстан*

**Корреспонденция үшін автор: alibek1324@mail.ru*

Аңдатпа. Пайдаланылған автомобиль катализаторлары қазіргі заманғы өнеркәсіпте шешуші рөл атқаратын сирек кездесетін және асыл металдардың құнды көзі болып табылады. Бұл шикізатта сирек кездесетін сирек кездесетін және асыл металдар бар, бұл оларды өңдеуді жоғары тиімді және үнемді етеді. Кешенді қайта өңдеу технологиясын әзірлеу үшін химиялық, рентгендік фазалық, рентгендік спектрлік және электронды микроскопиялық талдау сияқты әртүрлі талдау әдістерін қолданатын катализаторлар зерттелді. Фазалық талдау нәтижелері сирек кездесетін сирек кездесетін және асыл металдардың әртүрлі фазалық күйлерде, оксидтер түрінде, катализатордың алюминий Силикат матрицасындағы кіріктірілген қоспалар түрінде болатындығын көрсетеді. Бұл деректер металдарды алудың тиімді әдістерін жасау үшін маңызды мән береді. Бұл шикізатты өңдеудің негізгі тәсілдері пирометаллургиялық және гидрометаллургиялық технологиялар болып табылады, олардың әрқайсысының өзіндік артықшылықтары мен бірегей тиімділік критерийлері бар. Бұл мақалада пайдаланылған катализаторларды физика-химиялық зерттеулерге және оларды ашудың ұсынылған әдісіне назар аударылады, бұл сирек кездесетін, сирек кездесетін және асыл металдарды тиімді алуға мүмкіндік береді. Зерттеу нәтижелерін қолданыстағы шикізатты қайта өңдеудің жаңа технологиялық схемаларын оңтайландыру және әзірлеу үшін пайдалануға болады.

Негізгі сөздер: *пайдаланылған автомобиль катализаторлары, сирек металдар, асыл металдар, сирек жер элементтері, платина металдары, гидрометаллургиялық технологиялар, пирометаллургиялық технологиялар, селективті тұндыру, қайталама шикізат.*

Перспективы переработки отработанных автомобильных катализаторов с извлечением благородных, редких и редкоземельных металлов в Казахстане

К.Т. Ескалина[1], С.С. Коныратбекова[1], С.В. Юлусов[1,2], А.Т. Хабиев[1,2*]

[1]*Satbayev University, Алматы, Казахстан*

[2]*Институт механики и машиноведения имени академика У.А. Джолдасбекова, Алматы, Казахстан*

**Автор для корреспонденции: alibek1324@mail.ru*

Аннотация. Отработанные автомобильные катализаторы представляют собой ценный источник редких и благородных металлов, который играет ключевую роль в современной промышленности. Данное сырье содержит редкие редкоземельные и благородные металлы, что делает их переработку высокоэффективной и экономически выгодной. Для разработки комплексной технологии переработки исследовались катализаторы с использованием различных методов анализа, такие как химический, рентгенофазовый, рентгеноспектральный и электронно-микроскопический анализ. Результаты фазового анализа указывают на то, что редкие редкоземельные и благородные металлы находятся в различных фазовых состояниях, в виде оксидов, встроенных включений в алюмосиликатной матрице катализатора. Эти данные дают критическое значение для создания эффективных методов извлечения металлов. Ключевыми подходами для переработки данного сырья являются пирометаллургические и гидрометаллургические технологии, каждая из которых обладает своими преимуществами и уникальными критериями эффективности. В этой статье акцентируется внимание на физико-химических исследованиях отработанных катализаторов и предложенном способе их вскрытия, что позволяет эффективно извлекать редкие, редкоземельные и благородные металлы. Результаты исследований могут быть использованы для оптимизации существующих и разработки новых технологических схем переработки вторичного сырья.

Ключевые слова: *отработанные автомобильные катализаторы, редкие металлы, благородные металлы, редкоземельные элементы, платиновые металлы, гидрометаллургические технологии, пирометаллургические технологии, селективное осаждение, вторичное сырье.*

SATBAYEV UNIVERSITY

Engineering Journal of Satbayev University

Volume 147 (2025), Issue 2, 17-23

https://doi.org/10.51301/ejsu.2025.i2.03

Technology for producing pure lead-free zinc oxide from electric arc furnace (EAF) dust

G. Koishina[1], N. Dosmukhamedov[1], V. Kaplan[2], I. Nursainov[1], Ye. Zholdasbay[3*]

[1]*Satbayev University, Almaty, Kazakhstan*
[2]*Weizmann Institute of Science, Rehovot, Israel*
[3]*Zhezkazgan University named after O.A. Baikonurov, Zhezkazgan, Kazakhstan*

**Corresponding author: zhte@mail.ru*

Abstract. An economical and environmentally advantageous two stages method with efficient recovery of pure lead-free zinc oxide from electric arc furnace dust in parallel with clinker containing iron and carbon production for easy return to the iron smelting furnace was described. At the first stage, the electric arc furnace dust was mixed with a mixture of chloride salts and sintered at various temperatures to lead removing. In the second stage, the clinker after the first sintering stage was mixed with carbonaceous agent and sintered again to obtain pure lead-free zinc oxide. The clinker after the second sintering stage, containing iron and carbon, can be sent to the main iron production. Laboratory-scale measurements with electric arc furnace dust from one of the Kazakhstan metallurgical ferrous plants show that process allows receive lead-free zinc oxide with the total impurity content is 0.06–0.07 mass%, and the lead content is 0.001 mass%. Based on the laboratory studies carried out, a technological scheme for the two-stage processing of electric arc dust was developed to produce marketable products. The environmental benefit of the method is to reduce emissions of harmful substances into the environment associated with the recycling of electric arc furnace dust. In addition, the process allows to recycle production waste and reduce the consumption of natural resources.

Keywords: *electric arc furnace dust, sintering, zinc oxide lead-free, calcium chloride, carbonaceous agent.*

Received: 24 December 2024
Accepted: 15 April 2025
Available online: 30 April 2025

1. Introduction

The steady increase in zinc consumption and the long-term development of the global mining and metallurgical complex based on the model of extensive subsoil use inevitably contributed to the depletion of reserves of rich deposits being developed and the formation of significant volumes of technogenic waste. In this regard, the issues of complex processing of man-made raw materials containing zinc, as well as the development of innovative and environmentally friendly technologies for extracting this valuable metal from poor and difficult-to-enrich ores are of particular relevance.

Processing of mining and metallurgical waste, such as slag, gas cleaning dust and leaching cakes, is a promising area that allows not only to involve valuable components in economic circulation, but also to reduce the negative impact on the environment.

Modern methods of extracting zinc from difficult-to-enrich ores include the use of hydrometallurgical processes such as heap leaching, bioleaching and electrowinning, which allow for the efficient extraction of zinc even from ores with a low metal content.

The development and implementation of new technologies aimed at the complex extraction of zinc and other valuable components from various types of raw materials is an important task that requires the consolidation of the efforts of scientists, engineers and industry representatives. Solving this problem will ensure sustainable development of the global zinc industry and minimize its negative impact on the environment.

Ferrous metallurgy processes are characterized by the generation of large amounts of waste. On average, for 1 ton of steel produced in AC furnaces, about 15-25 kg of Electric Arc Furnace dust (EAF dust) is generated [1]. Considering the high productivity of steel plants, the world's dust reserves amount to about 5.6 billion tons. In 2023, Kazakhstan’s steel enterprises increased steel production by 16.4% compared to 2022, to 3.92 million tons [2], and the volume of EAF dust generated is approximately 9-11 thousand tons. EAF dust contains both valuable and hazardous metals, including, for example, Fe, Zn, Pb, Cr, Mn, V, Ca, Ti and others. Air pollution and dust accumulation have a negative impact on the environment and the population. Effective disposal of EAF dust is a major challenge in the steel industry: the steel industry generates several million tons of dust each year, which has negative impacts on the environment and human health. The average zinc content in them is about 35-40%, that is, 3-4 thousand tons of zinc are lost in the form of dust. This dust also contains up to 2% lead, >10-20% iron and other heavy

gulzada.koishina@mail.ru; nurdos@bk.ru; valery.kaplan@weizmann.ac.il; ilyasnursainov@gmail.com; zhte@mail.ru
Engineering Journal of Satbayev University. eISSN 2959-2348. Published by Satbayev University

non-ferrous metals. This amount of valuable raw materials can partially cover the need for raw materials of ferrous and non-ferrous metallurgy enterprises. Of the total volume of material loaded into the furnace, almost 100% zinc, about 10% of manganese, and 40% of lead are transferred into EAF dust [3]. The chemical and phase composition of EAF dust from the steelmaking industry differs depending on the technology used during which it is formed, process temperature, and on the composition of the feedstock.

The main components of EAF dust are iron oxides (mainly magnetite Fe_3O_4), zinc oxide (ZnO), lead oxide (PbO), and franklinite ($ZnFe_2O_4$, $ZnMnFeO_4$) [3]. When galvanized steel is treated, the zinc content in the dust can reach 30% or more [3]. Most of the elements are associated with oxygen in the form of oxides; in addition, chlorides, fluorides, sulfates, and sulfides may also be present.

Currently, various EAF dust pyrometallurgical and hydrometallurgical treatment processes have been proposed and tested. However, more than 95% of EAF dust is processed by pyrometallurgical methods. The most common are Waelz rotary kiln [4, 5, 6], rotary hearth furnace, plasma furnace [7, 8], shaft (OxyCup) furnace [9], [10], microwave heating furnaces [11, 12] and other reducing processes [13-15]. Waelz rotary kilns process 80% of all EAF dust [16].

Unfortunately, in all these processes, only the extraction of zinc and iron was controlled and studied. It is obvious that in the processes of collecting electric arc furnace dust at high temperatures, almost all the lead sublimates together with zinc and contaminates the resulting zinc oxide, which makes it impossible to use.

At the same time, the composition and behavior of other valuable and potentially hazardous elements, such as cadmium, copper, nickel, chromium, remain largely unstudied. This creates serious problems in developing effective strategies for processing and recycling electric arc furnace dust, since without a complete understanding of the behavior of these elements, it is impossible to predict their distribution in different fractions and, therefore, to develop optimal technological solutions.

The need for a comprehensive study of the behavior of the entire spectrum of elements in the processes of collecting electric arc furnace dust is dictated not only by economic considerations related to the possible extraction of valuable components, but also by environmental requirements. Environmental pollution with heavy metals poses a serious threat to human health and ecosystems.

In this regard, it is an urgent task to conduct detailed studies aimed at determining the phase composition and distribution of all significant elements in electric arc furnace dust, as well as studying their behavior at different temperatures and processing conditions. The data obtained will allow developing effective methods for the selective extraction of valuable components and neutralization of hazardous substances, which will contribute to the creation of environmentally friendly and cost-effective technologies for processing electric arc furnace dust.

Such studies should include both experimental works using modern analytical equipment and mathematical modeling of the processes occurring in the electric arc furnace and dust collection system. An integrated approach will provide the most complete understanding of the processes occurring with various elements and develop optimal strategies for managing these processes.

In this paper, an economical and environmentally friendly method is proposed to effectively capture pure lead-free zinc oxide from electric arc furnace dust in parallel with the production of iron-carbon containing clinker for easy return to iron smelting furnace with a detailed study of the behavior of heavy non-ferrous metals.

2. Materials and methods

2.1. Analytical methods

Material composition, prior to and following treatment, was characterized by X-ray fluorescence (XRF) spectroscopy (Niton handheld XRF Analyzers, R.B.M. Control & Mechanization Ltd, Israel). Quantitation and material balance were provided by inductively coupled plasma mass spectroscopy ICP-MS (Agilent 7700s ICP-MS System Technologies) measurements following 24-h dissolution of the EAF dust and clinker powders in aqua regia at room temperature with continuous stirring. Powder X-ray diffraction (XRD) was performed on an Ultima III diffractometer (Rigaku Corporation, USA). Phase identification and quantitative phase analysis were accomplished using Jade Pro (MDI, Cal.) software and the Inorganic Crystal Structure Database (ICSD).

2.2. Materials

The initial samples of Electric Arc Furnace dust (EAF dust) were received from one of the Kazakhstan metallurgical plants. Chemical composition of the initial samples of the EAF dust by ICP-MS measurements are present in Table 1.

Table 1. Chemical composition of the initial material (EAF dust)

Chemical composition (mass%)									
Fe	Zn	Cu	Pb	Cd	As	Sb	Sn	Au	Ag
8.48	37.69	0.2	1.36	0.054	0.004	0.017	0.031	0.008	0.004

Prior to each of the sintering procedures, XRF spectroscopy (Figure 1) and Powder X-ray diffraction (XRD) (Figure 2), were used to determine the contents of basic components in the EAF dust.

Sintering procedures

The experiments were carried out in two stages (Figure 3). At the first stage, the EAF dust was mixed with a mixture of chloride salts and sintered at various temperatures to remove lead as $PbCl_2$. At the second stage, the clinker after the first sintering stage was mixed with carbonaceous agent and sintered again to obtain pure lead-free zinc oxide. The clinker after the second sintering stage, containing iron and carbon, can be sent to the main iron production.

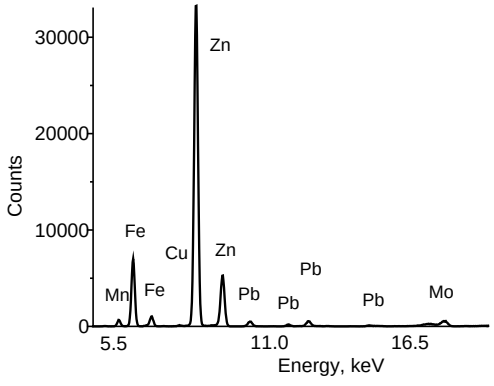

Figure 1. XRF spectra of the EAF dust

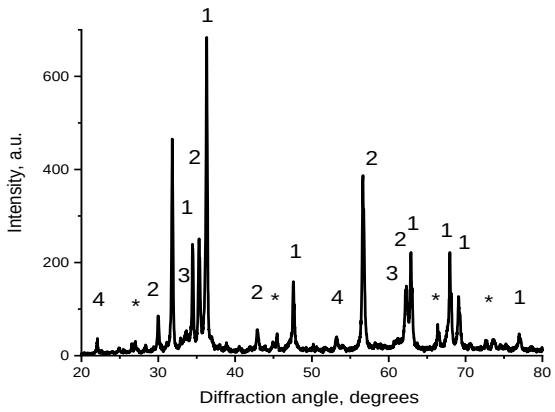

Figure 2. X-ray diffraction (XRD) pattern of the EAF dust: 1 – Zincite, ZnO; 2 – Franklinite, $ZnFe_2O_4$; 3 – Lead, Pb; 4 – Zinc Chloride Hydroxide Hydrate, $Zn_5Cl_2*(OH)_8*H_2O$, * – unidentified peaks

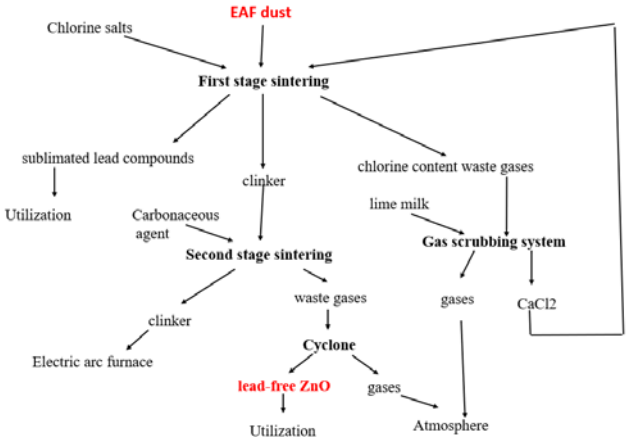

Figure 3. EAF dust treatment process

Reactor furnace

A custom-built, quartz tube reactor placed inside a temperature-controlled laboratory furnace was used for sintering. The accessible temperature range was 973-1373 K. A diagram of the reactor furnace, including placement of the powdered EAF dust initial sample is shown in Figure 4.

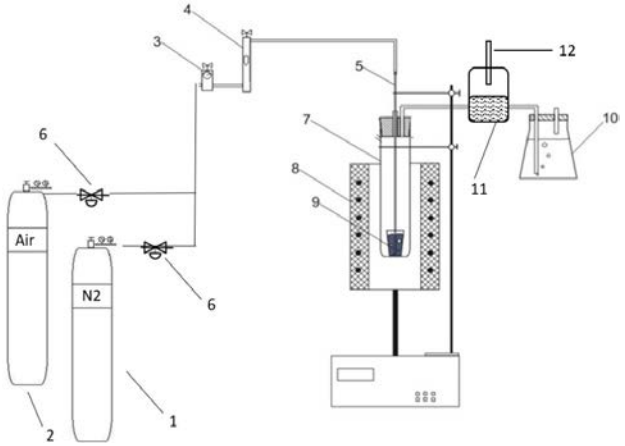

Figure 4. Laboratory reactor: (1) – nitrogen cylinder; (2) – air cylinder; (3) – gas stop; (4) – flowmeter; (5) – tube for gas; (6) – valve; (7) – quartz reactor; (8) – furnace with temperature controller; (9) – alumina crucible with sample; (10) – gas cleaning bottle, (11) – zinc oxide filter and collector; (12) – place for air addition

Mixture of the EAF dust and chloride salts or clinker after the first sintering stage and carbonaceous agent were placed in the furnace in an alumina crucible (total weight approximately 40-50 g).

Prior to heating, the quartz reactor with the mixtures powder was cleaned with a 100 ml/min flow of dry nitrogen gas for 15 min. The furnace was then heated at a uniform rate from room temperature to test temperatures (973-1373K) during 60 min, again in the presence of 100 ml/min nitrogen flow. After the furnace had reached the designated temperature, air was fed into the reactor for 1 h for the first stage sintering. The second stage sintering was carried out in the presence of 100 ml/min nitrogen flow without air flow.

Thermodynamic calculations for chemical reactions of metal oxides with chloride salts and carbon

Calculations were performed using software developed in the framework of Microsoft Excel and based on standard values of enthalpy of compound decomposition (ΔH) and entropy (ΔS) for the pure substances [17] as well as on values from the NIST-JANAF database [18].

3. Results and discussion

3.1 Thermodynamic analysis of the chemical reactions of metal oxides with chloride salts and carbon

The Gibbs energy values for chlorination and reduction reactions within the temperature range 673-1473 K are shown in Table 2.

Group 1 includes chlorination reactions between EAF dust components and calcium chloride. Under sintering conditions, the Gibbs energy of all reactions in Group 1 is strongly negative (–250-450 kJ/mole): thermodynamic calculations predict that the reaction of non-ferrous metals oxides and iron (III) oxide from EAF dust with $CaCl_2$ can result in the formation of metals chloride within a wide temperature range, including the range of interest 1073-1273 K.

Group 2 includes chlorination reactions between EAF dust components and ammonium chloride. The thermodynamic likelihood of reactions in the Group 2 is ensured over the entire temperature range of interest, with the most negative value being for reactions:

Fe_2O_3 (s) + $6NH_4Cl$ (s) = $2FeCl_3$ (g) + $6NH_3$ (g) + $3H_2O$ (g)
and PbO (s)+ $2NH_4Cl$ (s) = $PbCl_2$ (g) + $2NH_3$ (g) + H_2O (g).

The third group of reactions in Table 2 includes the reaction between EAF dust components and calcium chloride in the presence of SiO_2. The Gibbs energy of reactions in the Group 3 under sintering conditions is strongly negative (≈–300-500 kJ/mole).

Group 4 includes reduction reactions between clinker components and carbon. Thermodynamic calculations of the Group 4 reaction predict that that the reaction of non-ferrous metals oxides from second sintering stage clinker with carbon can result in the formation of metals within a wide temperature range, including the range of interest 1273-1473 K. The Gibbs energy of reactions in the Group 4 under sintering conditions is negative (≈–30-100 kJ/mole). This means that if lead and cadmium are not completely removed from the EAF dust in the first sintering stage, then the zinc oxide obtained in the second sintering stage will be contaminated with lead and cadmium.

Table 2. Gibbs energy (ΔG) calculated for chemical reactions of metal oxides with $CaCl_2*2H_2O$ (Group 1), NH_4Cl (Group 2), mixture $CaCl_2*2H_2O+SiO_2$ (Group 3) and for metal oxides with carbon (Group 4) in the temperature region of interest

Reaction	Gibbs Energy, kJ/mole				
	673 K	873 K	1073 K	1273 K	1473 K
Group 1					
$PbO_{(s)} + CaCl_2*2H_2O_{(s)} = PbCl_{2(g)} + CaO_{(s)} + 2H_2O_{(g)}$	-12	-128	-250	-375	-502
$ZnO_{(s)} + CaCl_2*2H_2O_{(s)} = ZnCl_{2(g)} + CaO_{(s)} + 2H_2O_{(g)}$	36	-79	-200	-327	-458
$CuO_{(s)} + CaCl_2*2H_2O_{(s)} = CuCl_{2(g)} + CaO_{(s)} + 2H_2O_{(g)}$	66	-52	-176	-306	-440
$CdO_{(s)} + CaCl_2*2H_2O_{(s)} = CdCl_{2(g)} + CaO_{(s)} + 2H_2O_{(g)}$	20	-94	-215	-341	-472
$ZnFe_2O_{4(s)} + CaCl_2*2H_2O_{(s)} = ZnCl_{2(g)} + Fe_2O_{3(s)} + CaO_{(s)} + 2H_2O_{(g)}$	56	-55	-174	-299	-428
$Fe_2O_{3(s)} + 3CaCl_2*2H_2O_{(s)} = 2FeCl_{3(g)} + 3CaO_{(s)} + 6H_2O_{(g)}$	251	-72	-413	-770	-1141
Group 2					
$PbO_{(s)} + 2NH_4Cl_{(s)} = PbCl_{2(g)} + 2NH_{3(g)} + H_2O_{(g)}$	-71	-179	-283	-378	-465
$ZnO_{(s)} + 2NH_4Cl_{(s)} = ZnCl_{2(g)} + 2NH_{3(g)} + H_2O_{(g)}$	-23	-130	-232	-329	-421
$CuO_{(s)} + 2NH_4Cl_{(s)} = CuCl_{2(g)} + 2NH_{3(g)} + H_2O_{(g)}$	7	-104	-209	-308	-402
$CdO_{(s)} + 2NH_4Cl_{(s)} = CdCl_{2(g)} + 2NH_{3(g)} + H_2O_{(g)}$	-39	-146	-247	-344	-434
$ZnFe_2O_{4(s)} + 2NH_4Cl_{(s)} = ZnCl_{2(g)} + Fe_2O_{3(s)} + 2NH_{3(g)} + H_2O_{(g)}$	-3	-107	-206	-301	-392
$Fe_2O_{3(s)} + 6NH_4Cl_{(s)} = 2FeCl_{3(g)} + 6NH_{3(g)} + 3H_2O_{(g)}$	73	-227	-511	-778	-1030
Group 3					
$PbO_{(s)} + CaCl_2*2H_2O_{(s)} + SiO_{2(s)} = PbCl_{2(g)} + CaSiO_{3(s)} + 2H_2O_{(g)}$	-102	-219	-341	-466	-593
$ZnO_{(s)} + CaCl_2*2H_2O_{(s)} + SiO_{2(s)} = ZnCl_{2(g)} + CaSiO_{3(s)} + 2H_2O_{(g)}$	-54	-169	-291	-417	-549
$CuO_{(s)} + CaCl_2*2H_2O_{(s)} + SiO_{2(s)} = CuCl_{2(g)} + CaSiO_{3(s)} + 2H_2O_{(g)}$	-25	-143	-267	-396	-530
$CdO_{(s)} + CaCl_2*2H_2O_{(s)} + SiO_{2(s)} = CdCl_{2(g)} + CaSiO_{3(s)} + 2H_2O_{(g)}$	-71	-185	-306	-432	-562
$ZnFe_2O_{4(s)} + CaCl_2*2H_2O_{(s)} + SiO_{2(s)} = ZnCl_{2(g)} + Fe_2O_{3(s)} + CaSiO_{3(s)} + 2H_2O_{(g)}$	-34	-146	-265	-389	-518
$Fe_2O_{3(s)} + 3CaCl_2*2H_2O_{(s)} + 3SiO_{2(s)} = 2FeCl_{3(g)} + 3CaSiO_{3(s)} + 6H_2O_{(g)}$	-21	-345	-686	-1042	-1413
Group 4					
$ZnO_{(s)} + 0.5\ C_{(s)} = 0.5\ CO_{2(g)} + Zn_{(g)}$	136	94	52	11	-30
$ZnFe_2O_{4(s)} + C_{(s)} = CO_{2(g)} + Zn_{(g)} + 2FeO_{(s)}$	160	96	33	-30	-91
$PbO_{(s)} + 0.5\ C_{(s)} = 0.5\ CO_{2(g)} + Pb_{(g)}$	77	38	-1	-36	-69
$CdO_{(s)} + 0.5\ C_{(s)} = 0.5\ CO_{2(g)} + Cd_{(g)}$	30	-11	-52	-91	-131
s – solid phase, g – gas phase.					

Thermodynamic calculations predict that the reaction of non-ferrous metals oxides and iron (III) oxide from EAF dust with $CaCl_2$ and NH_4Cl can result in the formation of metal chlorides within a wide temperature range, including the range of interest 1073-1273 K. The addition of silica to the initial mixture leads to a decrease in the Gibbs energy of chlorination reactions and an increase in the thermodynamic probability of these reactions.

3.2 First stage sintering of the EAF dust

Almost all lead at the first stage of sintering with the addition of chloride salts turns into lead chloride, which is removed from the clinker. The effect of sintering temperature on the residual lead content in the clinker and on the degree of its extraction into sublimates is shown in Figure 5.

The addition of ammonium chloride to the chlorinating mixture did not have a significant effect on the degree of lead sublimation. But silica addition increases the degree of lead sublimation by 15-20% and decrease the lead content in the first stage clinker.

The behavior of cadmium during chlorination is similar to that of lead (Figure 6).

All iron, zinc, and a large amount of copper (more than 60-70%) remain almost completely in the clinker. Apparently, this is due to kinetic difficulties during chlorination due to the formation of oxide films on the surface of particles of these metals, which complicate the chlorination process. It is known [19], that ammonium chloride dissolves oxide films on the surface of zinc particles, which promotes the process of zinc chlorination and its sublimation.

It was received that during sintering with the addition of a small amount of ammonium chloride (2% of the weight of the EAF dust), a slight sublimation of zinc to 4-5% was observed.

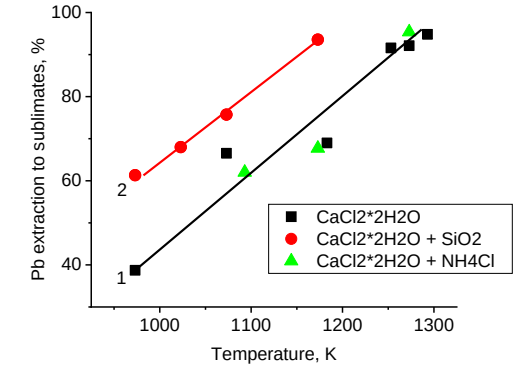

(a)

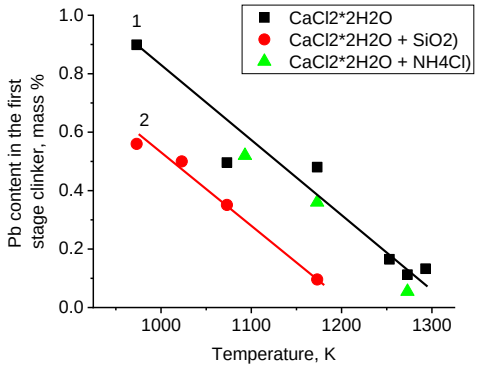

(b)

Figure 5. The effect of sintering temperature on the residual lead content in the clinker (a) and on the degree of its extraction into sublimates (b): 1 – EAF dust with $CaCl_2*2H_2O$ and with mixture ($CaCl_2*2H_2O$ + NH_4Cl); 2 – EAF dust with mixture ($CaCl_2*2H_2O$ + SiO_2)

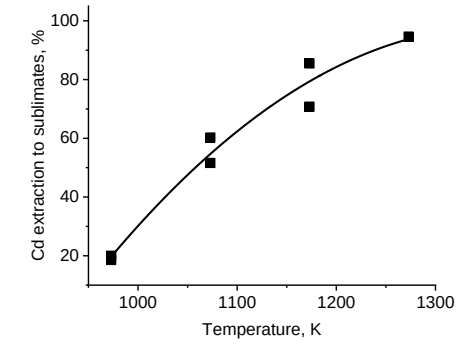

(a)

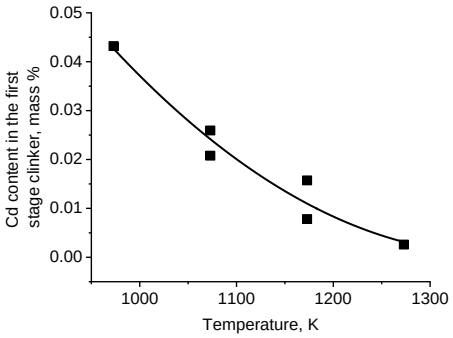

(b)

Figure 6. The effect of sintering temperature on the degree of cadmium extraction into sublimates (a) and on the residual cadmium content in the clinker (b)

Arsenic, antimony, and tin are also practically not removed from the EAF dust and remain in the clinker, but since their content in the dust is very small (less than 0.02-0.03%), this does not affect the dust processing process. Gold and silver are chlorinated with calcium chloride and their chlorides sublimate at high temperatures by 10-15%, but with their content in the EAF dust are 0.004-0.008%, this also does not have a significant effect on the EAF dust treatment process.

3.3 Second stage sintering of the EAF dust

After lead and cadmium removing through the first stage sintering process, the resulting clinker was sintered again with the addition of a carbonaceous agent to produce pure zinc oxide. Table 3 shows the chemical analysis of the resulting zinc oxide. The total impurity content was 0.06-0.07 mass%, and the lead content was 0.001 mass% when charcoal was used as a reducing agent. In the case of using graphite, the total impurity content was 0.1-0.3 mass%, and the lead content was 0.0015-0.006 mass%. Apparently, this is due to the greater chemical activity of power charcoal compared to compact crystalline graphite.

Table 3. Chemical composition of the Zn oxide after reducing sintering at 1373 K

Reducing agent	Chemical composition				
	Fe	Cu	Zn	Pb	Cd
	mass%	mass%	mass%	mass%	ppm
charcoal	0.06	0.01	80.58	0.0011	0.24
charcoal	0.05	0.01	79.95	0.0012	0.23
graphite	0.09	0.02	72.26	0.0014	0.32
graphite	0.17	0.22	85.81	0.0020	0.38
graphite	0.17	0.08	76.11	0.0057	0.62

Clinker after the second stage of sintering practically does not contain non-ferrous metals (Table 4) and can be used in ferrous metallurgy.

Table 4. Chemical composition of the clinker after reducing sintering at 1373 K

Sample number	Chemical composition				
	Fe	Cu	Zn	Pb	Cd
	mass%	mass%	mass%	mass%	ppm
Sample 1	18.18	0.25	0.65	0.0045	0.96
Sample 2	21.41	0.31	0.31	0.0023	0.58

4. Conclusions

Economical and environmentally advantageous two stages method with efficient recovery of pure lead-free zinc oxide from EAF dust in parallel with clinker containing iron and carbon production for easy return to the iron smelting furnace was proposed. Laboratory-scale measurements with EAF dust from one of the Kazakhstan metallurgical ferrous plants show that process allows receive lead-free zinc oxide with the total impurity content is 0.06-0.07 mass%, and the lead content is 0.001 mass%. The clinker after the second sintering stage, containing iron and carbon and with total content of the non-ferrous metals < 1%, can be sent to the main iron production.

The economic benefit of the method is to reduce the costs of recycling electric arc furnace dust, as well as to obtain a valuable product – pure zinc oxide, which can be used in various industries. In addition, the return of clinker containing iron and carbon to the cast iron smelting furnace allows to reduce the consumption of primary raw materials and material costs for electricity.

The environmental benefit of the method is to reduce emissions of harmful substances into the environment associated with the recycling of electric arc furnace dust. In addition, the process allows to recycle production waste and reduce the consumption of natural resources.

Author contributions

Conceptualization: N.D.; Data curation: N.D., Ye.Zh; Formal analysis: G.K., N.D., V.K.; Funding acquisition: G.K.; Investigation: N.D., I.N.; Methodology: N.D., V.K.; Project administration: Ye.Zh., I.N.; Resources: I.N., V.K.; Software: I.N., V.K.; Supervision: N.D., G.K.; Validation: Ye.Zh., V.K.; Visualization: G.K., Ye.Zh.; Writing – original draft: G.K., N.D.; Writing – review & editing: N.D., V.K. All authors have read and agreed to the published version of the manuscript.

Funding

This research was carried out within the framework of grant funding from the Science Committee of the Ministry of Science and Higher Education of the Republic of Kazakhstan for 2023-2025 in the priority area «Rational use of water resources, flora and fauna, ecology» of the project AR19679572 «Development of a new technology for recycling zinc dust from steelmaking production with the production of marketable products».

Acknowledgements

The authors would like to express their sincere gratitude to the editor and the two anonymous reviewers for their constructive comments and valuable suggestions, which significantly contributed to the improvement of the manuscript.

Conflicts of interest

The authors declare no conflict of interest.

Data availability statement

The original contributions presented in this study are included in the article. Further inquiries can be directed to the corresponding author.

References

[1] Kania, H. & Saternus, M. (2023). Evaluation and Current State of Primary and Secondary Zinc Production – A Review. *Applied Sciences, 13(3), 2003*. https://doi.org/10.3390/app13032003

[2] Kolisnichenko, V. (2023). Kazakhstan increased steel production by 16.4% y/y in 2023. During the year, the country's steel enterprises produced 3.92 million tons of steel (Global market, Kazakhstan). *Retrieved from:* https://gmk.center/en/news/kazakhstan-increased-steel-production-by-16-4-y-y-in-2023/

[3] Toporkova, Y.I., Bludova, D., Mamyachenkov, S.V. & Anisimova, O.S. (2021). A review of processing methods for electric arc furnace dust. *iPolytech Journal, 25(5), 643-680.* https://doi.org/10.21285/1814-3520-2021-5-643-680

[4] Simonyan, L.M., Alpatova, A.A. & Demidova, N.V. (2019). The EAF dust chemical and phase composition research techniques. *Journal of Materials Research and Technology, 8(2), 1601-1607*. https://doi.org/10.1016/j.jmrt.2018.11.005

[5] Wang, J. (2023). A Study on the Recovery of Zinc and Pig Iron from Byproducts after Steelmaking Dust Treatment. *Archives of Metallurgy and Materials, 68(1), 205-208*. https://doi.org/10.24425/amm.2023.141495

[6] Grudinsky, P., Zinoveev, D., Kondratiev, A., Delitsyn, L., Kulumbegov, R., Lysenkov, A., Kozlov, P. & Dyubanov, V. (2023). Reduction Smelting of the Waelz Slag from Electric Arc Furnace Dust Processing: An Experimental Study. *Crystals, 13(2), 318*. https://doi.org/10.3390/cryst13020318

[7] Xiaolong, L., Zhiwei, P., Jiaxing, Y., Zhizhong, L., Jiann-Yang, H., Yuanbo, Z., Guanghui, L. & Tao, J. (2017). Pyrometallurgical recycling of electric arc furnace dust. *Journal of Cleaner Production, (149), 1079-1100*. https://doi.org/10.1016/j.jclepro.2017.02.128

[8] Chapman, C.D. & Cowx, P.M. (1991). Treatment of EAF dust by the tetronics plasma process. *Steel Times, (219), 301-304*

[9] Holtzer, M., Kmita, A. & Roczniak, A. (2015). The Recycling of Materials Containing Iron and Zinc in the OxyCup Process. *Archives of foundry engineering, 15(1), 126-130*

[10] Brožová, S., Pustějovská, P., Zbránková, M. & Havránek, J. (2018). Processes of Waste Recycling and Utilization in the Shaft Furnaces. *Hutnické listy, (LXXI), 89-93*

[11] Xiong, Y., Wang, K., Qiu, D., Omran, M., Huang, R., Li, Y., Wei, S., Khan, I.U., Zhang, D., Ahmed, A. & Yu, Y. (2023). Recent Developments on the Removal of Zinc from Electric Arc Furnace Dust by Using Microwave Heating. *Preprint from Research Square, 23*. https://doi.org/10.21203/rs.3.rs-2795609/v1

[12] Omran, M., Fabritius, T. & Heikkinen, E. (2019). Selective Zinc Removal from Electric Arc Furnace (EAF) Dust by Using Microwave Heating. *Journal of Sustainable Metallurgy, (5), 331-340*. https://doi.org/10.1007/s40831-019-00222-0

[13] Reiter, W., Rieger, J., Raupenstrauch, H., Cattini, L., Maystrenko, N., Kovalev, D. & Mitrofanov, A.A. (2023). Recovery of Valuable Materials with the RecoDust Process. *Metals, 13*(7), *1191*. https://doi.org/10.3390/met13071191

[14] Małecki, S., Gargul, K., Warzecha, M., Stradomski, G., Hutny, A., Madej, M., Dobrzynski, M., Prajsnar, R. & Krawiec, G. (2021). High-Performance Method of Recovery of Metals from EAF Dust – Processing without Solid Waste. *Materials, 14(20), 6061*. https://doi.org/10.3390/ma14206061

[15] Wegscheider, S., Steinlechner, S., Pichler, C., Rösler, G. & Antrekowitsch, J. (2015). The 2sDR process – Innovative treatment of Electric Arc Furnace Dust. *WASTES 2015 – Solutions, Treatments and Opportunities, 355-360*. https://doi.org/10.1201/b18853-59

[16] Popovici, V. (2009). By-Products from EAF Dust Recycling and Their Valorisation. *5th Global Slag Conference, Brussels*

[17] Turkdogan, E.T. (1980). Physical Chemistry of High Temperature Technology. *New-York: Academic Press*

[18] Chase, M.W. (1998). NIST-JANAF thermochemical tables. *American Chemical Society, New York*

[19] Zaitsev, V.Ia. & Margulis, E.V. (1985). Metallurgy of the lead and zinc. *Moscow, Metallurgy*

Электр доғалы пештердің (ЭДП) шаңынан қорғасынсыз таза мырыш оксидін алу технологиясы

Г. Койшина[1], Н. Досмухамедов[1], В. Каплан[2], И. Нурсаинов[1], Е. Жолдасбай[3*]

[1]*Satbayev University, Алматы, Қазақстан*
[2]*Вейцман ғылыми институты, Реховот, Израиль*
[3]*О.А. Байқоңыров атындағы Жезқазған университеті, Жезқазған, Қазақстан*

**Корреспонденция үшін автор: zhte@mail.ru*

Аңдатпа. Шойын балқыту пешіне қайта оңай оралатын құрамында темір мен көміртегі бар клинкерді алатын, электр доғалы пеш шаңынан таза қорғасынсыз мырыш оксидін тиімді алу арқылы үнемді және экологиялық тиімді екі сатылы әдіс сипатталған. Бірінші кезеңде электр доғалы пештердің шаңы хлорид тұздарының қоспасымен араластырылып, қорғасынды бөліп алу үшін әртүрлі температурада күйдіріледі. Екінші кезеңде күйдірудің бірінші кезеңінен өткен клинкер құрамында көміртегі бар реагентпен араластырылып, қорғасынсыз таза мырыш оксидін алу үшін қайтадан күйдіріледі. Құрамында темір мен көміртегі бар күйдірудің екінші кезеңінен кейінгі клинкер шойынның негізгі өндірісіне бағытталуы мүмкін. Қазақстанның қара металлургия зауыттарының бірінен электр доғалы пештердің шаңын пайдалана отырып жүргізілген зертханалық нәтижелер құрамында 0.06-0.07 мас.% қоспалары бар қорғасынсыз мырыш оксидін алуға мүмкіндік беретінін көрсетті және қорғасын мөлшері 0.001 мас.% құрады. Жүргізілген зертханалық зерттеулер негізінде тауарлық өнімді ала отырып, электр доғаларының шаңын екі сатылы өңдеудің технологиялық схемасы жасалды. Әдістің экологиялық пайдасы электр доғалы пештердің шаңын

жоюға байланысты қоршаған ортаға зиянды заттардың шығарындыларын азайту болып табылады. Сонымен қатар, процесс өндіріс қалдықтарын қайта өңдеуге және табиғи ресурстарды тұтынуды азайтуға мүмкіндік береді.

Негізгі сөздер: *электр доғалы пештердің шаңы, күйдіру, қорғасынсыз мырыш оксиді, кальций хлориді, көміртегі бар реагент.*

Технология получения чистого оксида цинка, не содержащего свинца, из пыли электродуговых печей (ЭДП)

Г. Койшина[1], Н. Досмухамедов[1], В. Каплан[2], И. Нурсаинов[1], Е. Жолдасбай[3*]

[1]*Satbayev University, Алматы, Казахстан*
[2]*Научный институт Вейцмана, Реховот, Израиль*
[3]*Жезказганский университет имени О.А. Байконурова, Алматы, Казахстан*

**Автор для корреспонденции: zhte@mail.ru*

Аннотация. Описан экономичный и экологически выгодный двухэтапный метод с эффективным извлечением чистого оксида цинка, не содержащего свинца, из пыли электродуговых печей параллельно с получением клинкера, содержащего железо и углерод, для легкого возврата в чугуноплавильную печь. На первом этапе - пыль электродуговых печей смешивали со смесью хлоридных солей и спекали при различных температурах для удаления свинца. На втором этапе клинкер, прошедший первую стадию спекания, смешивали с углеродсодержащим веществом и снова спекали для получения чистого оксида цинка, не содержащего свинца. Клинкер после второй стадии спекания, содержащий железо и углерод, может быть направлен на основное производство чугуна. Лабораторные результаты с использованием – пыли электродуговых печей с одного из казахстанских металлургических заводов черной металлургии показали, что процесс позволяет получать оксид цинка, не содержащий свинец, с общим содержанием примесей 0.06-0.07 мас.% и содержанием свинца 0.001 мас.%. На основе проведённых лабораторных исследований была разработана технологическая схема двухэтапной переработки пыли электродуговых с получением товарной продукции. Экологическая выгода метода заключается в снижении выбросов вредных веществ в окружающую среду, связанных с утилизацией пыли электродуговых печей. Кроме того, процесс позволяет перерабатывать отходы производства и сокращать потребление природных ресурсов.

Ключевые слова: *пыль электродуговых печей, спекание, не содержащий свинца оксид цинка, хлорид кальция, углеродсодержащий реагент.*

Publisher's note

All claims expressed in this manuscript are solely those of the authors and do not necessarily represent those of their affiliated organizations, or those of the publisher, the editors and the reviewers.

SATBAYEV UNIVERSITY

Engineering Journal of Satbayev University

Volume 147 (2025), Issue 2, 24-30

https://doi.org/10.51301/ejsu.2025.i2.04

Development of the coagulant obtaining technology from substandard bauxite of Kazakhstan for wastewater treatment

U. Mussina[1], L. Kurbanova[1], B. Tussupova[1*], G. Bizhanova[1], S. Sarsenbayev[2]

[1]*Al-Farabi Kazakh National University, Almaty, Kazakhstan*
[2]*Satbayev University, Almaty, Kazakhstan*

**Corresponding author: tussupova@yandex.ru*

Abstract. One of the important environmental problems of Kazakhstan is the insufficient quality of natural and wastewater treatment, the reason for which is the lack of the main, mandatory reagent in water purification technology – coagulant. Aluminum-containing natural and man-made raw materials can be comprehensively processed in order to obtain modified mixed reagents-coagulants. One of the promising types of raw materials on the territory of Kazakhstan for the production of coagulants are substandard bauxites of the Krasnooktyabrsky deposit. This article presents a fundamentally new approach to the development of a technology for producing an effective coagulant with high coagulating properties in a wide pH range – a mixed sulfate aluminum-iron-silica coagulant (MSAISC) – when decomposing Red October bauxite with sulfuric acid with maximum extraction of aluminum, iron and silicon into a paste-like phase. Such a composition of the coagulant, called by us MSAISC (mixed sulfate aluminum-iron-silica coagulant) allows you to expand the range of action both in temperature and pH of the medium. In this sense, silicon coagulant, as well as modern aluminum polyoxychlorides, can be used without flocculant. The simultaneous presence of aluminum, iron and silicon salts in the composition of the coagulant makes it possible to combine the properties of «three in one».

Keywords: *bauxite, technology, coagulant, flocculant, water treatment, particle size distribution.*

Received: 15 January 2025
Accepted: 15 April 2025
Available online: 30 April 2025

1. Introduction

The basis for sustainable development of the Republic of Kazakhstan is to ensure and realization of the right of the Republic of Kazakhstan to protect national interests in matters of development, use of its natural resources, as well as to reduce the impact on the environment, which can be achieved by solving socio-economic and environmental problems. One of the modern tasks of our time is the protection of water resources, which consists in the creation of drainless water supply systems, effective wastewater treatment, etc [1].

Among the methods of wastewater treatment, special attention should be paid to physical and chemical methods using coagulants. They are used to remove fine colloidal particles, petroleum products, radioactive substances, metal cations, and the disposal of valuable components. Natural compounds of aluminum and iron, their oxides or hydroxides, as well as waste from a number of industries containing salts of these metals are used as raw materials for the production of coagulants. Along with the public utilities, the main consumers of coagulants are the production of pigments, synthetic fibers, the pulp and paper, leather, textile, oil-producing industries and other industries [2-9].

Currently, the production of coagulants in Kazakhstan is practically absent, in the nearest neighboring states it is limited, and the deficit is replenished by importing Russian coagulants of an insufficiently wide range [10].

New types of coagulants obtained by Russian and Ukrainian scientists are known, which are difficult to introduce into production as a result of departmental barriers: mixed coagulant AWR (Al_2O_3 – 3.5%; Fe_2O_3 – 0.3%); ALG – aluminum sulfate without iron; aluminum oxychloride; aluminum polyoxychloride (POXA); «SIZOL» (OJSC «Aurat», Moscow; Institute of Bioorganic Chemistry and Petrochemistry of the National Academy of Sciences of Ukraine: coagulant-flocculant SIZOL-1 – for domestic wastewater and disinfection of sediments and industrial waters; SIZOL-2500 – for drinking water treatment; aluminum sulfate JSC «Aluminum of Kazakhstan» is supplied to Russia, displacing Ukraine, Finland, Sweden and China [11].

The main consumers of coagulants are: public utilities; pulp and paper industry; production of synthetic fibers; production of pigments; leather, textile, oil producing, mechanical engineering, energy, metallurgy and other industries [1-6].

The coagulant traditionally used to purify colored and turbid waters with a pH of 5-7.5. Aluminum sulfate is quite expensive and ineffective at a water temperature of +11ºC and during floods. In addition, there is another negative factor in the use of aluminum sulfate a change in the salt composition of the treated water, as a result of which the alkalini-

07061960@mail.ru; laura.kurbanova@kaznu.edu.kz; tussupova@yandex.ru; g.bizhanova@gmail.com; fyrcan@mail.ru
Engineering Journal of Satbayev University. eISSN 2959-2348. Published by Satbayev University

ty and hydrogen index decrease and the sulfate content increases. This increases the corrosive activity of water, which reduces the service life of networks and water pipes and reduces their throughput. One of the main disadvantages of the coagulant – aluminum sulfate is significant amounts of residual aluminum in purified water [12].

Known methods of using mechanical mixtures of aluminum and iron salts as coagulants, many technologies have been developed for obtaining standard aluminum sulfate from various types of natural raw materials and production waste, but all technologies include limits for cleaning aluminum coagulant from iron impurities, the properties and behavior of mixed aluminum-iron coagulants in (AIC) have been poorly studied [11].

Currently, the production of coagulants in Kazakhstan is practically non-existent, and their deficit is covered by importing Russian coagulants of a poor assortment. The need is satisfied only by 50-60% by aluminum sulfate of the enterprise JSC «Aluminum of Kazakhstan», obtained from pure aluminum hydrate [12].

The development of technologies for obtaining and using new coagulants for treatment of natural and wastewater from substandard natural and man-made raw materials will allow obtaining the necessary products for all regions of Kazakhstan. It will effectively treat wastewater from natural and industrial complexes to the required standards and obtain high-quality drinking water, since the issues of effective treatment of drinking and wastewater in Kazakhstan are particularly acute and concern all its regions.

The methods for obtaining coagulants – purified and unrefined aluminum sulfates – include all methods of processing aluminum-containing raw materials using sulfuric acid.

Aluminum sulfate are the most important sorbents for purifying drinking water and fixatives in dyeing fabrics. The most common method for obtaining aluminum sulfate is the decomposition of pure chemical compounds with sulfuric acid, for example, aluminum hydrate – a semi-finished product of alumina production. Such aluminum sulfate complies with state standards, but the cost of it is high.

When obtaining a coagulant from natural raw materials, stages of purification of the aluminum sulfate solution from iron were required, which increased the cost of the production technology [12].

Currently, many methods for obtaining coagulants have been developed - mixed, unrefined from iron. In this case, the main raw material for obtaining coagulants can be any aluminum-containing raw material: bauxites, nepheline syenites, clay, kaolin; alumina-containing materials: thermal power plant ash and overburden clay rocks [1-11].

In terms of obtaining alumina acid methods are economically feasible for processing high-silicon aluminum-containing raw materials, allowing the removal of silica from the technological process at the head of the process flow chart [12]. If we consider these methods for obtaining a coagulant, then the process flow chart would be simplified by ignoring all subsequent stages of obtaining alumina after acid decomposition.

2. Materials and methods

Currently, Kazakhstan has a large reserve of aluminum-containing ores, including [13-14]:

– bauxites (kaolinite-gibbsite deposits);

– nepheline syenites (Kubasadyr and Ishim deposits);

– clays (Kostanay region);

– kaolin (Kostanay region);

– alumina-containing materials: thermal power plant ash and overburden clay rocks.

One of the promising types of raw materials for the production of coagulants is substandard bauxite, unsuitable for the production of alumina, having a high content of iron in the form of siderite and silicon.

Bauxite is a rock consisting mainly of aluminum and iron hydroxides with an admixture of aluminosilicates, titanium and calcium minerals and other impurities (magnesium, chromium, vanadium, etc.) in small quantities [14].

To obtain modified mixed coagulant-reagents, complex processing of natural, technogenic raw materials containing aluminum is possible. In Kazakhstan, there are large reserves of raw materials in the form of bauxite, the quality of which is determined by the silica content (bauxite with a silica content of 5-10% is low-quality) – Torgai, Krasnooktyabrskoye, Belinskoye deposits, Amangeldy group, Altai and others. One of the promising types of raw materials for the production of coagulants is substandard bauxite from the Krasnooktyabrsk Ore Mining Administration [15].

The main minerals of the Krasnooktyabrskoye bauxites are gibbsite, hydro hematite, hematite, kaolinite, recurrent siderite, calcite, and in small quantities magnetite, rhodochrosite, anatase, rutile, hydro goethite, hematogel, quartz, limonite, lepidocrocite, gypsum, zircon, ankerite, ferrous chromite, corundum, boehmite, leucoxene, magnesite, arsenopyrite, pyrite, and marcasite [15]. They differ from the widely known Torgay bauxites in their physical properties, structure, chemical, and material composition and are stony, loose, and clayey. The content of aluminum oxide (Al_2O_3) fluctuates from 39.5 to 55.3%, silicon dioxide (SiO_2) – from 3.2 to 13.6%, siderite iron (Fe_2O_3) – from 5.6 to 24.6%. The modulus of siliceous bauxite varies from 2.99 to 15.1% [16]. Such impurities complicate the processing of bauxite into alumina using the traditional alkaline method.

Bauxites are processed at the Pavlodar Aluminum Plant using a sequential Bayer-sintering scheme. Production is based on the processing of low-grade, high-siliceous Krasnooktyabrskoye bauxites (97%) with a relatively low content of harmful impurities, the reserves of which are gradually depleted [16]. Deterioration of the quality of bauxites leads to an increase in the cost of raw materials, auxiliary materials, energy resources, their transportation, as well as to the formation of a large amount of waste - sludge and emissions into the atmosphere. One of the problems in solving this problem, as well as the rational use of natural resources and waste reduction, is the development of a technology for the production and use of coagulants for the purification of natural and wastewater from natural and man-made raw materials.

The most applicable is aluminum sulfate out of the traditionally used coagulants.

Kazakhstan has large reserves of high-silica and high-iron bauxites, the use of which by the aluminum industry is very difficult due to the high content of harmful impurities [13]. In this regard, the possibility of using them to obtain coagulants for treatment of waste and drinking water is of particular interest. The average chemical composition of bauxites in northern Kazakhstan is as follows, %: Al_2O_3 – 42-44; Fe_2O_3 – 5-7; SiO_2 – 20-25; CaO – 1.5-2.5; MgO – 0.5-1.0.

The new technology for obtaining mixed coagulants is developed: sulfate aluminum-iron, sulfate-chloride aluminum-iron, sulfate coagulant-flocculant from bauxite, etc., which have a number of advantages traditionally used in industry: a wide pH range, high treatment efficiency, low cost of the coagulant, additional flocculant properties of the coagulant. These properties of coagulants arise due to the diversity and physicochemical properties of the hydrolysis products. The effect of water treatment with a mixed coagulant at 20ºC is close to the effect of coagulation with iron sulfate at 50°C and aluminum sulfate at 80°C.

In laboratory research and testing, bauxite and sulfuric acid were utilized. The chemical composition of bauxite, %: Al_2O_3: – 40.8; Fe_2O_3 – 3-27.0; SiO_2 – 8.7; CaO – 0.75; Na_2O + K_2O – 0.5; loss on ignition (LOI) – 0.7. The sulfuric acid used was technical-grade contact acid of the 1st or 2nd grade, conforming to state standard, and is produced at several enterprises in Kazakhstan.

Figure 1 illustrates a laboratory setup for sulfuric acid leaching of bauxite. This setup consists of specialized vessels made of thermo- and chemically resistant glass, interconnected with a thermostat, and equipped with reflux condensers and stirrers.

Figure 1. Laboratory Setup for Acid Decomposition of Krasnooktyabr Bauxite

Technology for producing the coagulant includes the following process steps: 1 – raw material preparation; 2 – leaching with sulfuric acid; 3 – crystallization (Figure 2).

Bauxites up to 300 mm in size are crushed to 25 mm and grounded to 0.15 mm. The crushed ore is fed to a ball crusher with a water ratio of S:L=1:1. The pulp in the vessel (2) with a S:L ratio of 1:1 is pumped for decomposition into the reactor (4) through the discharge tank (2) (Figure 2).

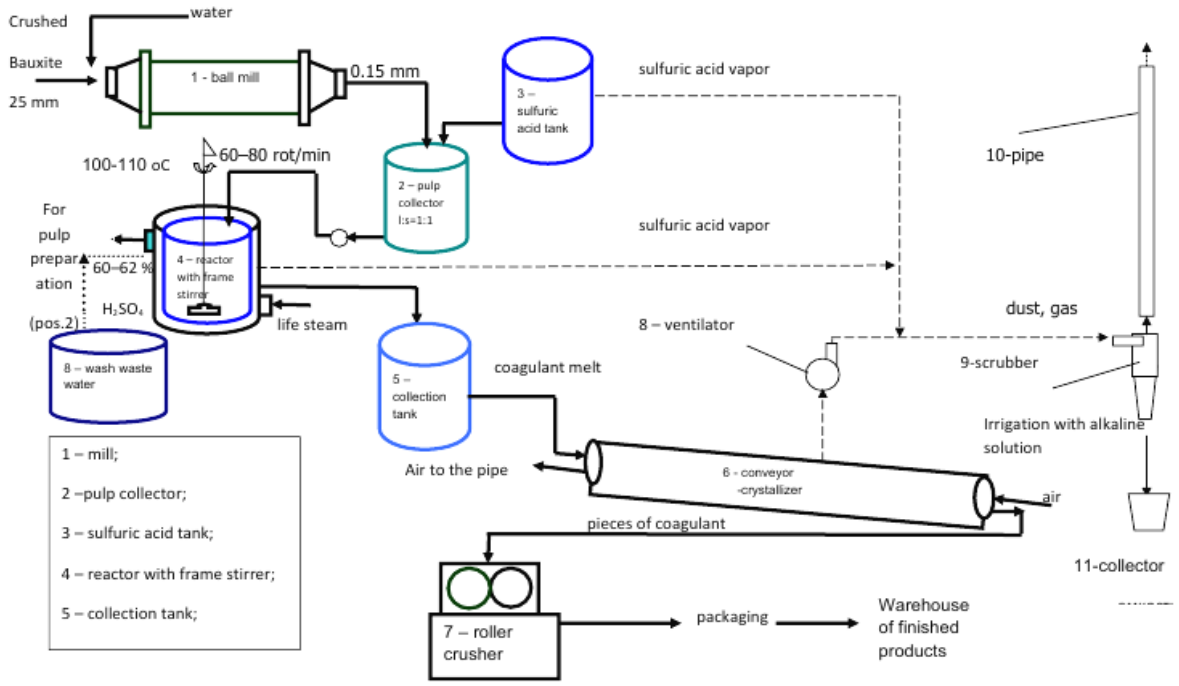

Figure 2. Basic technological scheme of obtaining the MSAISC

Concentrated (92%) sulfuric acid is fed into the same reactor from the pressure vessel (3) to achieve an acid concentration in the reaction mass of 60-62%. The decomposition of sulfuric acid is carried out at a temperature of 100-110°C for 40-60 minutes. Heating occurs by feeding the heat of reaction and blind steam into the reactor body. After leaching is complete, the melt is fed to the belt crystallizer (6). The thickness of the through layer of the belt is 10-20 mm. The surface of the melt is cooled by blown air at a rate of 800–1200 m³ per ton of finished product. The crystallizer belt is equipped with a casing. The process of curing and removing the product is improved by wetting the tape with water. The melt solidifies on the belt in the form of plates with a thickness of 12-18 mm and linear dimensions up to 150 mm.

Air is supplied to the crystallizer body by a fan and sucked in by an air blower in order to accelerate the process of hardening the finished coagulant. The speed of movement is 1.5-2 m/min, the time of passage through the belt is 30 min.

Wastewater from washing the decomposition reactor and condensate is collected in a tank (8), where it enters the container (2) of the decomposition reactor for preparation of the initial pulp. Filling the reactor with the decomposed mass is carried out to 1/2 of the volume associated with foaming. To suppress foaming, the mixing speed of frame mixers should be 60-80 rpm. The list of main process equipment is presented in Table 1.

Table 1. List of main process equipment

Name of equipment	Process parameters			Materials	Characteristics of the product
	Temperature	Duration	Pressure		
Fresh water pressure tank	20-25	Periodical	-	Steel 63	Technical water
Belt conveyor	90-100	Continous	-	Thermostatic tape type P	bauxite
Wet grinding rod or ball mill	25-40	Continous	-	Steel 3	bauxite, water
Screw feeder	20-25	Continous	-	Steel 3	pulp
Pulp tank	70-80	Continous	-	Steel	pulp
Reactor	100-110ºC	Continous	-	Steel 06XH28MDT frame, stirrer	melt
Dosing pump	20-25	Periodical	-	Chromium cast iron	acid 90%
Acid collection tank	20-25	Periodical	atm.	Steel 3	oil of vitriol 90% H_2SO_4
Pressure water tank	-	-	-	Steel 3	technical water
Acid pressure tank	-	-	-	Steel 08X22H28MDT	acid
Centrifugal pump	95-100	-	-	Steel 06XH28MDT	
Belt conveyor crystallizer				Rubberized fabric tape, type P, heat-resistant	melt
- Melt for crystallization	100-110	Continous	atm.		
- Air for cooling	20 ±10	Continous	0.08		
Ventilator	40-60	Continous	-	Carbon steel	air

To avoid the emission of sulfuric acid vapors into the atmosphere, the vapors and gases leaving the decomposition reactor, as well as the entire volume of air sucked from the crystallizer body, from the sulfuric acid pressure tank are sent to gas cleaning (9, 10). In this case, sulfuric acid vapors are absorbed by a weakly alkaline solution of pH 8-8.5.

When the solution is saturated with sulfuric acid till pH value of 7.5, it is being sent to prepare a pulp for the decomposition of sulfuric acid and a new portion of the alkaline solution is prepared for gas treatment.

The finished coagulant MSAISC is delivered to a cold closed rail warehouse or directly to the wagon. If necessary, the coagulant can be crushed into pieces of the required size and placed in paper bags or other containers permitted by technical specifications.

3. Results and discussion

It should be noted that most of the work on this topic is aimed at obtaining purified aluminum sulfate, which increases the cost of the resulting product. The use of methods for obtaining mixed coagulants simplifies the process, since there is no need to carry out operations such as separation of liquid and solid phases, degreasing, evaporation and etc (Figure 3).

The obtained coagulant was analyzed for the content of aluminum, iron, free acid and insoluble residue. Evaluating the test results, the most optimal parameters for obtaining modified MSAISC were selected: H_2SO_4 concentration – 60%, stoichiometric dosage; the amount of sulfuric acid is 90–98% of the stoichiometrically required; temperature – 110°C; process duration – 90 minutes; Al_2O_3 production – 94%; Fe_2O_3 production – 93%. Chemical composition of the solid coagulant, %: Al_2O_3 – 11.18; Fe_2O_3 – 4.66; sulfates – 42.0; hydrated water – 32.3; free acid – none.

The technology for obtaining a coagulant includes the following process operations: raw material preparation (grinding), sulfuric acid leaching, crystallization, and crushing of finished products. The basic hardware diagram includes a mill, a pulp collector, a sulfuric acid tank, a reactor with a frame mixer, a conveyor-crystallizer, and a roller crusher.

Using this method for obtaining a mixed coagulant simplifies the process of processing bauxites since it eliminates the precipitation of sulfuric pulp, the operation of evaporation and dehydration of sulfuric acid solutions and crushing of the product, which is a weakness of the acid technology.

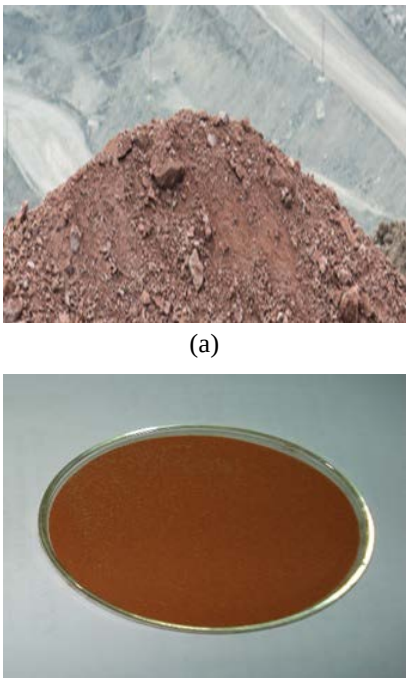

(a)

(b)

Figure 3. Coagulant from substandard bauxite: (a) – substandard bauxite; (b) – coagulant SSAZhKK

Obtaining a coagulant in granular form facilitates its loading and transportation. The main disadvantages include an increased content of insoluble impurities. Since the method did not include an operation for separating liquid and solid phases, bauxites with a low content of silica and aluminum silicates were processed in accordance with the proposed technology to reduce the amount of insoluble sediment in the product. In the case of recycling bauxite with a large amount of these impurities and if necessary, after separation with sulfuric acid to obtain purified coagulant. Additional operations should be carried out to dilute the pulp, separate the liquid and solid phases and wash the latter, which would significantly increase the cost of the process.

The proposed technologies for obtaining combined aluminum iron coagulants of various modifications allow processing aluminum raw materials with a high iron content and with a high silicon content.

To produce 1 ton of the coagulant MSAISC containing 11% Al_2O_3, the following materials and energy costs are required: Krasnooktyabrsky bauxite – 0.33 tons (based on processing ore of the following composition, %: Al_2O_3 – 42.76; Fe_2O_3 (total) – 19.05; SiO_2 – 14.77; CaO – 3.5; CO_2 – 2.89), industrial water – 0.24 m^3, the amount of 92% sulfuric acid – 0.43 tons, electricity – 19.8 kW/h, air for cooling – 1.15 thousand m^3, thermal energy to maintain the reaction – 0.1 Gcal.

An environmental assessment was conducted for the MSAISC coagulant production technology, focusing on the following aspects:

1). Presence of toxic ompurities. Evaluation of toxicological impurities generated during production, as well as by-products formed during usage, their transformation, decomposition, or interaction with the environment.

2). Distribution and spread conditions. Assessment of how toxic impurities and by-products disperse and persist in application regions, considering factors like mobility, migration, stability, and lifespan.

3). Transformation and decomposition. Analysis of the conditions under which by-products transform or decompose in the natural environment and the duration of these processes.

4). Monitoring and detection. Evaluation of current methods and proposed measures for controlling and detecting toxic impurities in the product and its by-products.

5). Environmental impact. Assessment of negative ecological consequences resulting from the release of toxic impurities and by-products into the environment, including their effects on food, housing, and industrial premises.

The acid decomposition process of substandard bauxite in this technology results in:

1). Emissions of pollutants. Sulfuric acid decomposition of bauxite emits pollutants such as sulfuric acid vapors (1–3 mg/nm³), necessitating purification before atmospheric release, and inorganic dust. Emissions from raw material preparation and acid reactors are neutralized using aspiration systems. Vapors and gases extracted from decomposition reactors, crystallizer casings, and pressure tanks are directed to gas purification systems for neutralization. Acid vapors are absorbed using a mildly alkaline solution (pH 8-8.5), ensuring that pollutant emissions remain below permissible limits, thereby preventing air pollution.

2). Wastewater. The technological scheme produces two types of wastewaters:

3). Conditionally clean (warm) wastewater. This is cooled and reused for reactor cooling.

4). Industrial wastewater. Generated from floor washing, equipment cleaning, etc. at the stage of condensation of water vapor in the dust and gas emissions treatment system Combined wastewater is used to dilute bauxite suspension after wet grinding.

5). Production waste. The insoluble residue (sludge) amounts to 1174.7 kg (with 30% moisture) per 1000 kg of mixed aluminum-iron-silicate coagulant. Depending on consumer preference, this residue can be separated on-site, becoming a by-product, or sent in solid form without separation, effectively used in treating industrial and low-turbidity wastewater. Alternatively, it can be stored for future processing into cement or extraction of valuable components. Thus, the insoluble residue is better regarded as a valuable technogenic raw material.

No toxic impurities were detected during coagulant production. In regions where the coagulant is produced and used for natural water purification, no toxic by-products are formed. Negative environmental impacts from by-products entering the environment, food, housing, or industrial premises are not anticipated, as residual concentrations of pollutants and introduced impurities (aluminum, iron, silicon oxides) during water purification with the coagulant comply with various permissible limits depending on water use categories.

4. Conclusions

Therefore, based on the conducted studies it was established that the mixed sulfate alumina-iron coagulant MSAIC in its coagulation properties and efficiency is close to commercial aluminum sulfate.

The technology for obtaining the coagulant includes the following process operations: raw material preparation (grinding); sulfuric acid leaching; crystallization; crushing of final products.

The main equipment and process flow chart for obtaining the coagulant includes a mill, a pulp collector, a sulfuric acid tank, a reactor with a frame mixer, a conveyor-crystallizer and a roller crusher.

The optimal process parameters were established: pulp L:S ratio = 1:1.5; sulfuric acid concentration 60% ration = 2:1, process temperature 110-130°C, exposure time 30-50 min; extraction of Al_2O_3 – 97%; Fe_2O_3 – 93%., SiO_2 = 83%. Chemical composition of MSAISC, %: Al_2O_3 – 11.18; Fe_2O_3 (total) – 6.66; SiO_2 – 7.7; sulfuric acid – 0.8; insoluble residue – 6.5.

During the coagulant production process, the following wastes are generated:

– wastewater from washing the decomposition reactor and condensate, which are returned to the bauxite decomposition process and to the preparation of the initial pulp;

– sulfuric acid vapors leaving the decomposition reactor and the crystallizer casing and sulfuric acid pressure tank, which will be sent for gas treatment by absorption with a weak alkaline solution and sent to the preparation of pulp for sulfuric acid decomposition;

– solid production waste – insoluble residue (sludge).

The main disadvantage of mixed unrefined coagulants is the increased content of insoluble residue, but when treating slightly turbid waters, this disadvantage becomes an advantage since insoluble impurities act as opacifiers, improving the coagulation process.

In order to reduce the number of insoluble residues in the product it is recommended to process bauxites with a low content of silica and aluminum silicates. The operation of separating the liquid and solid phases is necessary to separate the insoluble residue. When processing bauxites with a high content of these impurities if it is necessary to obtain a purified coagulant, then it is required to introduce additional operations to dilute the pulp after separation with sulfuric acid, separate the liquid and solid phases and wash the latter.

The new generation MSAISC coagulant has coagulation capacity, works in clarification of wastewater, significantly accelerates the treatment process and is not inferior in quality of purification to commercial coagulants (aluminum sulfate, iron chloride). The coagulant is able to soften water, reduce carbonate hardness, sodium-potassium salinity, chemically purify water from heavy and harmful elements.

Obtaining the proposed coagulant and its application not only increases the effect of natural and wastewater treatment but also improves the ecological state of the bauxite mining area, reduces the area of placement and storage of substandard raw materials on the territory of the natural-industrial complex, as well as its deficit. In addition, it allows preventing damage to the environment during treatment as a result of coagulation of natural and wastewater containing suspended substances, heavy metal cations, oil products, radioactive substances, as well as for the disposal of precious alloyed metals.

The use of this method for obtaining a mixed coagulant simplifies the process of bauxite processing since it eliminates the operation of settling sulfuric pulps, evaporation and dehydration of sulfuric solutions, as well as crushing the product, which are the disadvantages of acid technologies. Obtaining a coagulant in a granular form facilitates its loading and transportation. The main disadvantages include an increased content of insoluble impurities. Since the method does not include an operation for separating the liquid and solid phases, in order to reduce the content of insoluble sediment in the product it is recommended that bauxites with a low content of silica and aluminosilicates be processed using the proposed technology. In the case of processing bauxites with an increased content of these impurities and if it is necessary to obtain a purified coagulant, additional operations should be introduced to dilute the pulp after sulfuric acid opening, separate the liquid and solid phases and wash the latter, which significantly increases the cost of the process.

The proposed technologies for obtaining mixed alumina-iron coagulants of various modifications will allow processing both high-iron and high-silicon aluminum types of raw materials.

Author contributions

Conceptualization: U.N., L.K., B.T.; Data curation: L.K., B.T.; Formal analysis: U.N., L.K., B.T.; Funding acquisition: U.N.; Investigation: U.N., L.K., B.T., G.B.; Methodology: U.N., L.K., B.T.; Project administration: U.N., L.K., B.T.; Resources: L.K., B.T., G.B., S.S.; Software: G.B., S.S.; Supervision: U.N., L.K.; Validation: U.N., L.K., B.T.; Visualization: G.B., S.S.; Writing – original draft: U.N., L.K., B.T.; Writing – review & editing: L.K., B.T. All authors have read and agreed to the published version of the manuscript.

Funding

This research received no external funding.

Acknowledgements

The authors would like to express their sincere gratitude to the editor and the two anonymous reviewers for their constructive comments and valuable suggestions, which significantly contributed to the improvement of the manuscript.

Conflicts of interest

The authors declare no conflict of interest.

Data availability statement

The original contributions presented in this study are included in the article. Further inquiries can be directed to the corresponding author.

References

[1] Teh, C.Y., Budiman, P.M., Shak, K.P.Y. & Wu, T.Y. (2016). Recent advancement of coagulation-flocculation and its application in wastewater treatment. *Industrial & Engineering Chemistry Research, 55(16), 4363-4389.* https://doi.org/10.1021/ACS.IECR.5B04703

[2] Kingsley, O.I. (2019). Prospects and Challenges of Using Coagulation-Flocculation Method in the Treatment of Effluents, *Advanced Journal of Chemistry, section A, 2(2), 105-127.* https://doi.org/10.29088/SAMI/AJCA.2019.2.105127

[3] Zubkova, O.S., Alekseev, A.I. & Zalilova. M.M. (2020). Research of Combined Use of Carbon and Aluminum Compounds for Wastewater Treatment. *Izvestiya Vysshikh Uchebnykh Zavedenii, Seriya Khimiya i Khimicheskaya Tekhnologiya, 63(4), 86-91*. https://doi.org/10.6060/ivkkt.20206304.6131

[4] Dotto, J., Fagundes-Klen, M.R., Veit, M.T., Palácio, S.M. & Bergamasco, R. (2019). Performance of different coagulants in the coagulation/flocculation process of textile wastewater. *Journal of Cleaner Production, (208), 656-665.* https://doi.org/10.1016/j.jclepro.2018.10.112

[5] Gan, Y., Li, J., Zhang, L., Wu, B., Huang, W., Li, H. & Zhang, S. (2021). Potential of titanium coagulants for water and wastewater treatment: Current status and future perspectives. *Chemical Engineering Journal, (406), 126837.* https://doi.org/10.1016/j.cej.2020.126837

[6] Zhuang, J., Qi, Y., Yang, H., Li, H. & Shi, T. (2021). Preparation of polyaluminum zirconium silicate coagulant and its performance in water treatment. *Journal of Water Process Engineering, (41), 102023.* https://doi.org/10.1016/j.jwpe.2021.102023

[7] Matveeva, V.A., Chukaeva, M.A. & Semenova, A.I. (2024). Iron ore tailings as a raw material for Fe-Al coagulant production. *Journal of Mining Institute, (267), 433-443.* https://pmi.spmi.ru/pmi/article/view/16474

[8] Almeida, V.O., Schneider, I.A.H. (2020). Production of a ferric chloride coagulant by leaching an iron ore tailing. *Minerals Engineering, (156), (106511).* https://doi.org/10.1016/j.mineng.2020.106511

[9] Naumov, K.I., Shvedov, I.M. & Maloletnev, A.S. (2014). Application of New Technologies for Producing Coagulant (Aluminum Sulfate) from Coal Waste. *Mining Information and Analytical Bulletin, (5), 67-72*

[10] Musina, U.Sh., Nureyev, S.S. & Kurbanova, L.S. (2007). Investigation of the process of obtaining a titanium-modified mixed sulfate coagulant from Krasnoktyabrsky bauxite. *Bulletin of KazNTU named after K.I. Satpayev, (5), 137-139*

[11] Valeev, D.V. (2015). Acid technology for the production of alumina and coagulants from Russian high-silica raw materials. *II Russian Annual Conference of young researchers and postgraduates «Physico-chemistry and technology of inorganic materials»*.

[12] Musina, U.Sh., Nurkeev, C.S., Kurbanova, L.S., Zharkimbaeva, G.B. & Ahmedova, G.R. (2007). Investigation of coagulating properties of a new inorganic coagulant. *Hydrometeorology & Ecology, (1), 104-108*

[13] Mondillo, N., Herrington, R. & Boni, M. (2021). Bauxite. *Encyclopedia of Geology (Second Edition).* https://doi.org/10.1016/B978-0-08-102908-4.00046-1

[14] National Minerals Information Center. (2017). Bauxite and Alumina Statistics and Information. *Retrieved from:* https://minerals.usgs.gov/minerals/pubs/commodity/bauxite/

[15] Kenzhaliev, B.K., Kuldeev, E.I., Abdulvaleev, R.A., Pozmogov, V.A., Beisembekova, K.O., Gladyshev, S.V. & Tastanov, E.A. (2017). Prospects for the development of the aluminum industry in Kazakhstan. *News of the Academy of Sciences of the Republic of Kazakhstan. Series of Geology and Technical Sciences, 3(423), 151-160*

[16] Bekturganov, N.S., Abisheva, Z.S., Abdulvaliev, R.A., Tastanov, E.A., Ahmedov, S.N., Medvedev, V.V. & Gladyshev, S.V. (2015). Perspektivy rasshireniya syr'evoj bazy alyuminievoj promyshlennosti Kazahstana. *Resursosberegayushchie tekhnologii v obogashchenii rud i metallurgii cvetnyh metallov», Almaty*

Қазақстанның кондициялық емес бокситінен ағынды суларды тазарту үшін коагулянт алу технологиясы

У.Ш. Мусина[1], Л.С. Курбанова[1], Б.Х. Тусупова[1*], Г.З. Бижанова[1], С.О. Сарсенбаев[2]

[1]*Әл-Фараби атындағы Қазақ ұлттық университеті, Алматы, Қазақстан*
[2]*Satbayev University, Алматы, Қазақстан*

**Корреспонденция үшін автор: tussupova@yandex.ru*

Аңдатпа. Қазақстанның маңызды экологиялық проблемаларының бірі – табиғи және сарқынды сулардың дұрыс сапалы түрде тазаланбауы. Себебі суды тазарту технологиясындағы негізгі, міндетті коагулянт реагентінің тапшылығы болып табылады. Құрамында алюминий бар табиғи және техногендік шикізатты модификацияланған аралас реагенттер-коагулянттар алу мақсатында кешенді өңдеуге болады. Қазақстан аумағында коагулянттар өндірісі үшін болашағы бар шикізат түрлерінің бірі – Краснооктябрь кен орнының кондициялық емес бокситтері болып табылады. Бұл мақалада pH кең диапазонында жоғары коагуляциялық қасиеттері бар тиімді коагулянтты – аралас сульфатты алюминий-темір – кремний коагулянтын (АСАТКК) – Краснооктябрь бокситін күкірт қышқылымен ыдырату арқылы, алюминий, темір және кремнийді паста фазасына барынша шығара отырып, коагулянт алу технологиясын әзірлеу бойынша түбегейлі жаңа тәсіл ұсынылған. Біз АСАТКК (аралас сульфатты алюминий-темір-кремний коагулянты) деп аталған коагулянттың мұндай құрамы қоршаған ортаның температурасы мен pH бойынша әсер ету ауқымын кеңейтуге мүмкіндік береді. Бұл тұрғыда кремний коагулянты қазіргі алюминий полиоксихлоридтері сияқты флокулянтсыз қолдануға болады. Коагулянттың құрамында алюминий, темір және кремний тұздарының бір мезгілде болуы «үшеуі бір» қасиеттерін біріктіруге мүмкіндік береді.

Негізгі сөздер: *боксит, технология, коагулянт, флокулянт, су тазарту, дисперстік құрамы.*

Технология получения коагулянта из некондиционных бокситов Казахстана для очистки сточных вод

У.Ш. Мусина[1], Л.С. Курбанова[1], Б.Х. Тусупова[1*], Г.З. Бижанова[1], С.О. Сарсенбаев[2]

[1]*Казахский национальный университет имени аль-Фараби, Алматы, Казахстан*
[2]*Satbayev University, Алматы, Казахстан*

**Автор для корреспонденции: tussupova@yandex.ru*

Аннотация. Одна из важных экологических проблем Казахстана – недостаточно качественная очистка природных и сточных вод, причиной, которой является дефицит основного, обязательного реагента в технологии очистки воды – коагулянта. Алюминий содержащее природное и техногенное сырье можно комплексно перерабатывать в целях получения модифицированных смешанных реагентов-коагулянтов. Одним из перспективных видов сырья на территории Казахстана для производства коагулянтов являются некондиционные бокситы Краснооктябрьского месторождения. В настоящей статье представлены принципиально новый подход по разработке технологии получения эффективного коагулянта, обладающего высокими коагулирующими свойствами в широком диапазоне pH, – сульфатного смешанного алюможелезисто-кремниевого коагулянта (ССАЖКК) – при разложении краснооктябрьского боксита серной кислотой с максимальным извлечением алюминия, железа и кремния в пастообразную фазу. Такой состав коагулянта, названного нами ССАЖКК (смешанный сульфатный алюмо-железо-кремниевый коагулянт) позволяет расширить диапазон действия как по температуре, так и по pH среды. В этом смысле кремниевый коагулянт так же, как и современные полиоксихлориды алюминия можно применять без флокулянта. Одновременное присутствие в составе коагулянта солей алюминия, железа и кремния позволяет объединить свойства «три в одном».

Ключевые слова: *боксит, технология, коагулянт, флокулянт, очистка воды, дисперсный состав.*

SATBAYEV UNIVERSITY

Engineering Journal of Satbayev University

Volume 147 (2025), Issue 2, 31-39

https://doi.org/10.51301/ejsu.2025.i2.05

Geomechanical assessment of stress-strain conditions in structurally heterogeneous rock masses of Kyrgyzstan

A.R. Abdiev[1*], J. Wang[2], R.Sh. Mambetova[1], A.A. Abdiev[1], A.Sh. Abdiev[1]

[1]*Kyrgyz State Technical University named after I. Razzakov, Bishkek, Kyrgyzstan*
[2]*Northwest University, Xi'an, China*

**Corresponding author: atsanbek.abdiev@kstu.kg*

Abstract. This study focuses on assessing the stress-strain state of rock masses in structurally heterogeneous ore deposits of Kyrgyzstan. The primary objectives include identifying stress distribution patterns with depth, analyzing the impact of tectonic faults, and establishing the relationship between the elastic properties of rocks and their strength parameters. A comprehensive methodological approach is employed, including in-situ stress measurements using the overcoring technique to determine principal normal stresses at various depths, laboratory tests to evaluate elastic wave velocities, Young's and shear modulus, and statistical analysis to derive regression relationships. Furthermore, the orientation of principal stresses is reconstructed, and the influence of tectonic discontinuities on the stress field within the rock mass is evaluated. The results indicate that vertical stresses in the rock mass approximately correspond to the overburden pressure, expressed as γH. Regression models obtained for competent and moderately strong rocks confirm that the experimental data lies between the values predicted by N. Hast's relationships and those derived from hydrostatic stress distribution. The analysis of elastic properties reveals a high degree of anisotropy, where variations in P-wave velocity strongly correlate with changes in Young's and shear moduli. The practical significance of this research lies in its contribution to developing more accurate predictive models for the stress-strain behavior of ore-bearing rock masses, thereby enhancing the design of underground excavations.

Keywords: *mining, stress-strain state, elastic properties, rock mass, ore deposits.*

Received: 08 October 2024
Accepted: 15 April 2025
Available online: 30 April 2025

1. Introduction

Mining plays an important role in the economic development of the Kyrgyz Republic, serving as one of the key sources of raw materials and contributing significantly to the national budget [1-3]. The development of ore deposits not only fosters job creation and infrastructure growth but also drives technological advancement, forming the foundation for sustainable economic growth and enhancing the country's competitiveness in the global market. Furthermore, continued investment in mining innovation and rigorous safety measures ensure that the sector remains resilient and capable of meeting both domestic and international demands [4, 5].

As mining operations advance to greater depths and encounter increasingly complex geological structures, ensuring the safety and efficiency of extraction processes has become a central challenge for Kyrgyzstan's mining industry [6]. Structurally heterogeneous rock masses, characterized by complex tectonic features and numerous fault systems, exhibit unstable stress-strain behavior [7-9]. This instability is critical in hazardous dynamic events, such as rock bursts and geotectonic shocks, which pose serious risks to personnel and can lead to accidents in underground excavations [10, 11].

The challenges associated with the safe and efficient extraction of structurally complex ore deposits are largely driven by the inevitable manifestation of rock pressure at deeper mining levels [12, 13]. The geological complexity, expansion of mined-out zones, high tectonic stress levels, and heterogeneity of rock physical properties contribute to sudden structural failures in the rock mass [14-16]. Such failures often manifest as large-scale roof collapses, pillars' destruction, excavation junctions' damage, and dynamic phenomena like rock and geotectonic bursts. These events significantly impact mining productivity and may lead to the suspension of underground development projects [17-20].

Effective rock pressure management requires reliable methods for assessing and monitoring the geomechanical state of the rock mass. Contemporary methodologies advocate for an integrated approach, which considers the stress-strain state, rock properties, geodynamic processes, and the specific characteristics of deposit exploitation [21-24]. This approach forms the basis for scientifically grounded strategies to mitigate rock pressure hazards and optimize engineering decisions in the design and execution of mining operations.

This study presents the results of experimental investigations conducted at ore deposits in Kyrgyzstan using both in-situ and laboratory techniques. Special emphasis is placed on developing a methodology for assessing the stress-strain state that enables precise forecasting of the nature and extent of

atsanbek.abdiev@kstu.kg; wangjd@nwu.edu.cn; mambetova-r@mail.ru; camry009@mail.ru; abdiev.wer@mail.ru
Engineering Journal of Satbayev University. eISSN 2959-2348. Published by Satbayev University

geodynamic phenomena. Such predictive capability is essential for minimizing the risk of hazardous events and ensuring the long-term stability of underground workings in structurally complex rock environments.

1.2. Study area

The study focuses on structurally heterogeneous ore deposits in the Kyrgyz Republic, characterized by significant geological diversity and complex structural organization. The sites investigated include the Khaydarkan, Kadamjay, Mamkala, Kumtor, and Chon-Koy deposits. These collectively provide insight into geomechanical parameters at depths ranging from 800 m to prospective levels of 900-1000 m and beyond. These ore-bearing formations exhibit pronounced tectonic activity, with localized stress concentrations reaching 35-40 MPa in areas adjacent to major fault zones [25-27].

For example, at the Uluu-Too mine of the Khaydarkan Mercury Combine, deep levels are accessed via two shafts-Deep and Central-reaching depths of 685 m and 860 m, respectively, clearly indicating increased rock pressure with depth. Deposits located near major tectonic faults display elevated localized stress levels. Mining sites at Khaydarkan, Kadamjay, Mamkala, Kumtor, and Saryjaz frequently experience manifestations of rock pressure in the form of extensive roof collapses, damage to excavation junctions, and large-scale displacements of the rock mass [28-32].

Variations in the physical properties of rocks, such as elasticity, elastic wave velocities, and anisotropy coefficients, significantly influence the stress distribution within the mass [33, 34]. These differences result in pronounced spatial variability of the stress-strain state, depending on depth and proximity to tectonic discontinuities.

One notable example is the Kumtor mine, where underground workings collapsed near the fifth transfer chamber at a depth of 3821 m and at a horizontal distance of 6100620 meters from the shaft collar. This incident led to the suspension of underground construction in June 2009 and highlights the high risk posed by both gravitational and tectonic stress. The study, therefore, aimed to evaluate stress-strain conditions, identify depth-related stress patterns, analyze the influence of rock properties on stress distribution, and inspect underground excavations operating under elevated rock pressure [35-37].

Consequently, the diversity of mining conditions ranging from deep multi-shaft operations to zones adjacent to major faults necessitates a comprehensive approach for assessing the geomechanical state of ore-bearing rock masses. The adopted methodology accounts for the internal physical properties of rocks and external geodynamic influences, which are essential for predicting hazardous dynamic events and ensuring the safety of mining operations in Kyrgyzstan.

2. Materials and methods

Field and laboratory methods were applied to investigate the in-situ stress conditions within structurally heterogeneous rock masses of ore deposits in Kyrgyzstan.

Field measurements of natural stresses were conducted at several mining sites using specialized sensors installed at various depths (e.g., 930 m and 960 m). The overcoring method directly determined principal normal stresses within the rock mass, which is crucial for assessing the influence of geodynamic processes.

Rock samples were analyzed in the laboratory to determine their elastic properties, including the velocities of longitudinal and shear waves, Young's modulus, and anisotropy coefficients. These data served as a basis for analyzing the impact of internal rock heterogeneity on stress distribution.

The experimental results were subjected to statistical processing to identify dependencies of stress on depth and tectonic activity parameters. Regression models were constructed, and correlation analysis was performed to compare experimental findings with theoretical models, including Dinnik's model and the empirical relationships proposed by N. Hast [38].

Particular attention was given to assessing the influence of fault zones on stress distribution. To this end, spatial data on fault locations were compared with measurement results to evaluate how the orientation and magnitude of stresses vary with proximity to active structural discontinuities [39].

To ensure the methodological robustness of the approach, the stress-strain state analysis was grounded in fundamental physical and mechanical principles represented by the equations. The equation defines the hydrostatic vertical stress:

$$\sigma_v = \gamma \cdot H \,, \tag{1}$$

where σ_v is the vertical stress; γ is the unit weight of the rock; H is the depth. This expression provides a basic reference for evaluating vertical stress and serves as a benchmark corresponding to the overburden pressure.

Hooke's law describes elastic deformation:

$$\sigma_v = E \cdot \varepsilon \,, \tag{2}$$

where E is the Young's modulus; ε is the strain.

Hooke's law is used to interpret laboratory data, enabling the evaluation of rock elastic properties from experimentally measured wave velocities and related parameters.

The regression model for stress as a function of depth takes the form:

$$\sigma = \sigma_0 + k \cdot H \,, \tag{3}$$

where: σ_0 is the initial stress at the surface; k is a coefficient characterizing the stress gradient with depth.

This linear model (3) provides a generalized framework for assessing the gravitational contribution to the formation of the stress-strain state.

Applying the fundamental principles (1)-(3) not only facilitates the comparison of experimental results with theoretical models but also forms the basis for developing more accurate methods for evaluating the geomechanical state of ore-bearing rock masses. Integrating gravitational and tectonic stress components within a unified analytical framework ensures methodological rigor and scientific validity of the research approach.

3. Results and discussion

Statistical processing of experimental data obtained from in-situ stress measurements in structurally heterogeneous rock masses enabled the development of regression equations describing changes in the average values of principal normal stresses with depth. For competent rocks with Young's modulus ranging from $5\text{-}6 \cdot 10^4$ to $10\text{-}11 \cdot 10^4$ MPa, the following relationships were established:

$$\sigma_x = \sigma_y = 9.5 + 2.78\gamma H \,, \tag{4}$$

$$\sigma_x = 5.0 + 2.78\gamma H \,, \tag{5}$$

$$\sigma_y = 4.5 + 1.12\gamma H \,, \tag{6}$$

For moderately strong rock masses with Young's modulus of approximately 2-3·10⁴ MPa, the relationships are as follows:

$$\sigma_x + \sigma_y = 5.0 + 2.14\gamma H, \quad (7)$$

$$\sigma_x = 3.0 + 1.14\gamma H, \quad (8)$$

$$\sigma_x = 2.0 + \gamma H, \quad (9)$$

where: γ is the unit weight of the rock, equal to $2.7 \cdot 10^{-2}$ MPa/m; H is the depth from the surface in meters.

In a first approximation, vertical stresses σ_y correspond to the overburden pressure γH.

Comparison with values derived from hydrostatic theory revealed that the experimental results lie below those predicted by N. Hast's empirical relationships but above those calculated under a purely hydrostatic stress assumption.

Beyond regression modeling, experimental work enabled the identification of key patterns in stress distribution within the rock mass. At the Kadamjay mine, measurements at the 930 m level revealed that in the southern limb of the fold, the maximum principal stress reached 35.1 MPa (azimuth 156°). At the same time, at the southwestern periclinal closure, it was 40.1 MPa (azimuth 282°), reflecting changes in stress axis symmetry during fold formation.

A comparison between the 930 m and 960 m levels showed that the experimental site at 960 m (located just 240 m below the surface 90 to 140 m less than at 930 m) exhibited vertical stresses 2.2-2.6 times lower and horizontal stresses 1.6-2.0 times lower than those at the 930 m level. This difference is attributed to the predominance of tectonic stresses influenced by the distribution of faults.

Analysis showed that the magnitude of maximum principal stresses depends on the depth and the distance to active fault zones. For example, in the southern drift (930 m level), the stress measured was 35.1 MPa at a depth of 330 m, whereas near the shaft of the "Novaya" mine (460 m deep, 690 m away from the fault), it was only 18.6 MPa. The tectonic component, approximately 22 MPa was highest near the fault and decreased exponentially with distance.

At the Chon-Koy deposit, significant variation was observed between zones. In the southern ore-bearing zone (depth H = 160 m), vertical stresses were around 4.2 MPa, and horizontal stresses ranged from 7.4 to 9.6 MPa. In contrast, vertical and horizontal stresses reached 21.3 MPa and 19.2-21.7 MPa in the northern zone near the flexural bend, respectively.

Principal stress orientations were reconstructed based on geomechanical data, confirming the consistency of overcoring measurements. Statistical analysis demonstrated that vertical stresses closely aligned with theoretical values, while horizontal stresses were significantly elevated due to the pronounced influence of tectonic discontinuities.

The research also revealed a strong correlation between the propagation velocity of elastic waves and rock strength. Marbled rocks and Chatbazar limestones, which are relatively homogeneous and isotropic, showed a high correlation between strength parameters and elastic wave velocity. The strength anisotropy coefficient $K = \sigma^{\perp} / \sigma^{\parallel}$, for these rocks indicates uniform mechanical properties regardless of loading direction.

In contrast, rocks from the Uluu-Too deposit (including effusive rocks, listvenites, schists, and serpentinites) exhibited substantial heterogeneity and anisotropy in their physical properties, resulting in a lower correlation coefficient between wave velocity and strength ($\rho \approx 0.64$). This suggests that in anisotropic rocks, strength characteristics depend on the magnitude of the applied load and the orientation of elastic symmetry axes relative to the compression direction.

Notably, a rise in strength anisotropy generally accompanies an increase in the elastic anisotropy coefficient, while lower elastic anisotropy is associated with greater resistance to uniaxial compression. Therefore, considering the anisotropic nature of rocks, alongside a detailed analysis of their elastic and strength properties, enables more reliable forecasting of the stress-strain state and evaluation of geotechnical risks during mining in structurally heterogeneous environments. The relationship between elastic anisotropy and strength characteristics is presented in Table 1.

Table 1. Relationship between elastic anisotropy and strength characteristics

Rock type	Wave velocity, m/s		Elastic wave velocity anisotropy, %	Uniaxial compressive strength, kg/cm²		Strength anisotropy coefficient $K = \frac{\sigma_{\max}\sigma_{\min}}{\sigma_{\min}}$, %
	$V_{P\parallel}$	$V_{P\perp}$		$\sigma_{\max}$	$\sigma_{\min}$	
Basalt	4610	4410	4.5	1070	940	13.9
Marmarized limestone	5460	5100	6.8	865	830	4.1
Chlorite schist	7120	6400	11.3	3140	2400	30.8
Jasperoid	4760	4050	17.0	1290	850	51.9
Bedded limestone	4740	3280	44.6	805	610	32.0
Carbonaceous schist	5105	2715	87.5	1400	830	68.6
Mica-quartz schist	5100	2550	100.0	880	525	68.1

Figures 1 and 2 illustrate the relationships between elastic wave velocities and rock strength parameters, as well as the degree of anisotropy based on experimental data.

Figure 1 presents the measured values of both longitudinal and shear wave velocities for various rock types. The highest longitudinal wave velocities are observed in crystalline and marmarized rocks, consistent with their high strength and relative structural homogeneity. In contrast, schists and other rocks exhibiting pronounced fissuring or bedding demonstrate significant anisotropy, evident in the directional variability of elastic wave propagation.

The degree of anisotropy in longitudinal wave velocities is shown in Figure 2. It demonstrates a tendency toward increased anisotropy coefficients in rocks with complex internal structures and dominant planes of stratification, confirming that the orientation of structural elements has a considerable impact on wave velocity.

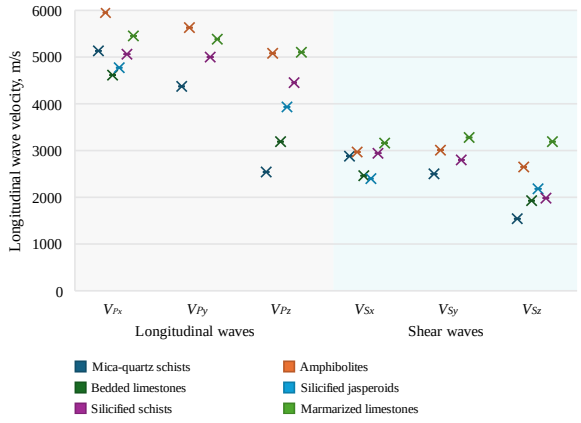

Figure 1. Variation of elastic wave velocities in the investigated rock types

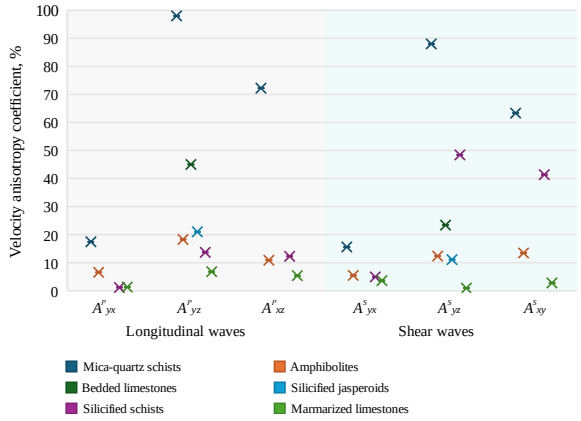

Figure 2. Variation of longitudinal wave velocity anisotropy coefficients in the investigated rock types

In addition to internal structural factors, external stress also plays a significant role. Experimental data show that when the applied load increases from zero to 50% of the rock's ultimate strength, the velocity of longitudinal waves $V\sigma^{\perp}(\rho)$, measured perpendicular to bedding or the axis of elastic symmetry, increases by 25-35%. In contrast, wave velocities measured parallel to stratification $V\sigma^{\parallel}(\rho)$ increase by only 7-15%. This effect highlights the nonlinear relationship between wave velocity and increasing compressive stress. With increasing pressure, microcracks and pores tend to close, resulting in an overall increase in wave velocity, especially in directions initially exhibiting reduced velocities due to the rock's anisotropic fabric.

For the studied rock types, elastic properties were determined using an anisotropy-based calculation scheme and equations applicable to orthotropic and transversely isotropic symmetry. Figure 3 presents the averaged values of Young's moduli (E_x, E_y, E_z), shear moduli (G_x, G_y, G_z), and Poisson's ratios (μ_{xy}, μ_{yz}, μ_{zx}) for selected anisotropic and isotropic rocks.

As shown by previous experimental data, the anisotropy of elastic wave velocities in the studied rocks can range from 5-10% in relatively isotropic marmarized limestones to 80-100% in mica-quartz schists and certain varieties of siliceous rocks. This variability is attributed to microstructural features such as bedding, fracturing, and mineral grain orientation, which create directional differences in the propagation paths of elastic waves.

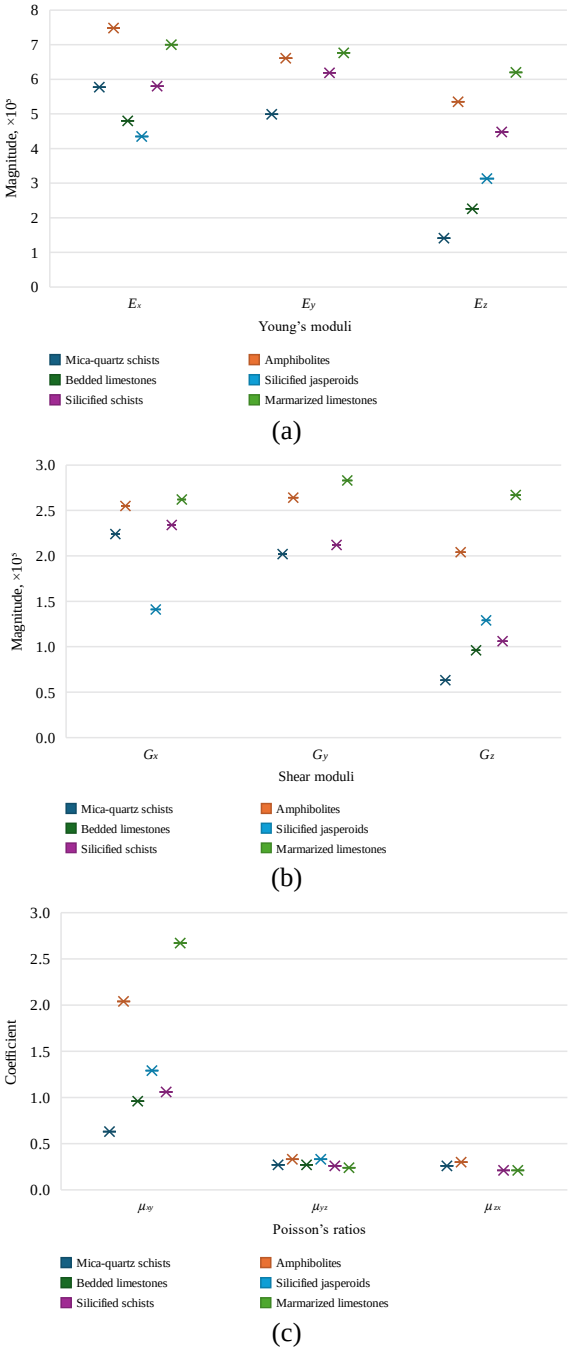

Figure 3. Comparison of elastic properties in the investigated anisotropic and isotropic rocks: (a) – distribution of Young's moduli (E_x, E_y, E_z); (b) – distribution of shear moduli (G_x, G_y, G_z); (c) – distribution of Poisson's ratios (μ_{xy}, μ_{yz}, μ_{zx})

According to the graphs in Figure 3a, the values of $E_{\parallel}$ (measured along the bedding or principal symmetry axis) often exceed those of $E_{\perp}$ (measured perpendicular to bedding). Similar patterns are observed for shear moduli ($G_{\parallel}$, $G_{\perp}$) and Poisson's ratios ($\mu_{\parallel}$, $\mu_{\perp}$), indicating higher stiffness and reduced deformability of rocks along the direction of greater structural continuity.

A comparison of the ratios $E_{\parallel} > E_{\perp}$ and $G_{\parallel} > G_{\perp}$ demonstrates that stronger elastic wave anisotropy correlates with more pronounced contrasts in elastic parameters measured in different directions. In other words, the higher the anisotropy degree of the rock, the more significant the differences in the values of E and G moduli along and across the bedding planes.

The previously observed trend of increased longitudinal wave velocity V_p several times when measured along different structural directions aligns with proportional changes in Young's and shear modulus (by a factor of n_2). Thus, the increase or decrease in wave velocity directly reflects the change in material stiffness and its capacity to resist compressive and shear deformation.

Thus, the results presented in Figure 3 confirm the pronounced anisotropy of the investigated rocks and highlight characteristic differences in their elastic properties associated with the orientation of tectonic and structural-textural elements within the rock mass. Box-and-whisker plots characterizing the elastic behavior of the studied rock types are presented in Figure 4.

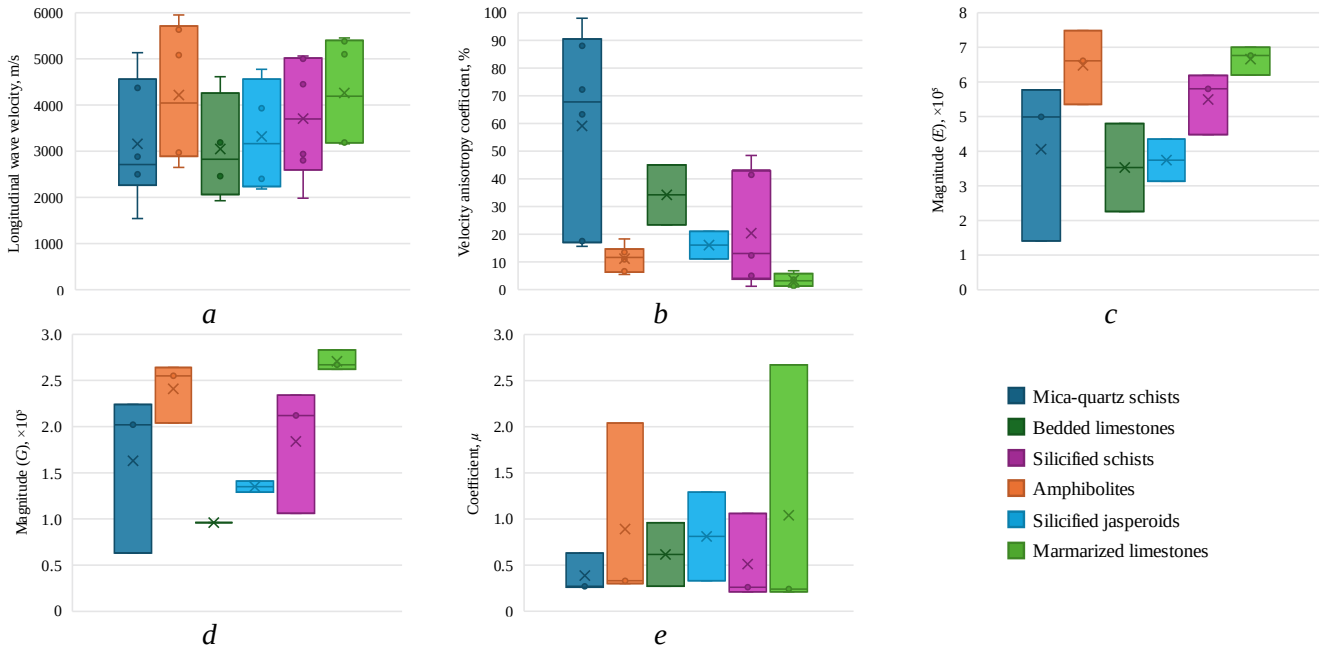

Figure 4. Box-and-whisker plots illustrating the properties of the investigated rocks: (a) – elastic wave velocities; (b) – longitudinal wave velocities; (c) – Young's moduli; (d) – shear moduli; (e) – Poisson's ratios

The range of elastic wave velocities (Figures 4a and 4b) varies significantly across rock types, indicating a high degree of anisotropy in the studied materials. Homogeneous rocks exhibit relatively narrow value intervals, while those with pronounced textural heterogeneity show a considerably wider spread.

Analysis of the box plots reveals that Young's modulus values (Figure 4c) measured parallel to bedding ($E_{||}$), are consistently higher than those measured perpendicular to bedding ($E_{\perp}$). A similar trend is observed for shear moduli, where $G_{||} > G_{\perp}$ (Figure 4d). This finding indicates stiffer mechanical behavior along the primary axis of symmetry, which is attributed to the preferential alignment of mineral grains or structural layers.

The box plot for Poisson's ratios (Figure 4e) shows a narrower spread than Young's and shear moduli but reveals noticeable differences among rock types. Poisson's ratio reflects the lateral-to-axial strain ratio and is a critical parameter in assessing the deformability of a material.

The studied rocks exhibit a high degree of anisotropy based on the analysis of all measured parameters – wave velocities, Young's moduli, shear moduli, and Poisson's ratios. Variations in longitudinal wave velocity, which proportionally reflect changes in elastic parameters (by a factor of n^2), indicate that the greater the anisotropy, the more pronounced the differences in parameters measured along and across the primary bedding direction.

Survey results, consistent with findings reported in [40-44], show that in unsupported vertical, main, and single preparatory workings, rock failures in the sidewalls are typically localized in areas where the span direction aligns with the orientation of high horizontal tectonic stresses. In horizontal excavations, failures predominantly occur in the roof and floor.

As part of the assessment of stoping chambers, the condition of over 200 active and depleted panels with varying operational lifespans was examined. The inspection included documentation of actual chamber dimensions and inter-chamber pillar widths, bedding and fracturing parameters, water saturation levels, mining depth, the collapses' area and volume, and the tectonic stresses' orientation in the examined zones. A total of 22 instances of individual roof collapses were recorded. The spans of chambers in collapse zones ranged from 6 to 50-55 meters, with depths between 20 and 300 meters. The collapsed areas covered 6 to 500 m², with volumes ranging from 0.2 to 3.0-4.0 m³. The fallen rock typically accumulated in piles along the chamber floor and rarely filled the entire excavation area. Notably, most collapses occurred after chamber stoping was completed.

Analysis of the obtained data indicates that the critical stress state in rock masses, depending on the excavation orientation, is most commonly reached on the roof and floor, where compressive stress concentrations significantly exceed those observed in undisturbed rock. When the orientation of the excavation is close to being perpendicular to the direction of the maximum tectonic stress vector, stress concentrations along the excavation boundary can exceed the ambient stress levels in the surrounding mass by a factor of 2 to 3.

The influence of tectonic stresses extends to all types of underground excavations, including main, preparatory, and stoping workings. The mechanisms of rock instability vary and range from spalling to slab detachment. Under conditions of low tectonic activity, the predominant deformation mode is spalling along planes of structural heterogeneity, resulting in the fall of discrete structural blocks, which remain relatively intact. In contrast, under high tectonic stress conditions, the blocks are crushed and destroyed, leading to the detachment of slabs parallel to the excavation contour in zones subjected to the highest compressive stresses. This progressive transition in failure mechanisms not only alters the nature and extent of damage around underground openings but also plays a crucial role in determining the design and implementation of effective support systems, excavation sequencing, and ground control strategies, particularly in deep mining conditions or regions characterized by elevated tectonic stress, where the risk of dynamic rock failure and structural collapse is substantially higher.

Thus, rock deformation around excavations under tectonic forces highly depends on the orientation of the longitudinal axis. Adjusting the alignment of an excavation relative to the direction of maximum tectonic stress makes it possible to influence stress concentrations along its boundaries and thereby control deformation and failure processes. Various engineering methods and technological solutions have been developed to minimize the adverse effects of tectonic stresses on excavation stability, considering both the magnitude and orientation of the tectonic stress vector.

4. Conclusions

Gravity and tectonic forces govern the stress-strain state of ore-bearing rock masses in Kyrgyzstan. The developed regression models for competent rocks (with Young's moduli ranging from $5\text{-}6\cdot10^4$ and $10\text{-}11\cdot10^4$ MPa) and moderately strong rocks (approximately $2\text{-}3\cdot10^4$ MPa) confirm that vertical stresses σ_y are, in the first approximation, equivalent to the overburden pressure, expressed as γH.

The experimental data fall between the values predicted by N. Hast's empirical relationships and those calculated from hydrostatic theory, indicating a substantial influence of horizontal tectonic stresses.

Field measurements at the Kadamjay mine reveal that principal stress magnitudes depend on depth and the distance to fault zones. At the 930 m level, the maximum stress reaches 35.1-40.1 MPa, and a comparison between the 930 m and 960 m levels shows a 2.2-2.6-fold and 1.6-2.0-fold decrease in vertical and horizontal stresses, respectively.

The study of elastic properties revealed significant anisotropy: rocks with pronounced heterogeneity exhibit anisotropy coefficients up to 80-100%, while marmarized limestones show 5-10% values. A corresponding rise in strength anisotropy accompanies an increase in elastic anisotropy.

The inspection of underground excavations showed that rock failures most frequently occur in areas where the span direction of the excavation aligns with the vector of high horizontal tectonic stresses. These findings underscore the necessity of incorporating tectonic stress factors into the design parameters of underground workings.

Author contributions

Conceptualization: ARA, JW; Data curation: RSM, AAA; Formal analysis: AAA, ASA; Funding acquisition: ARA, RSM; Investigation: AAA, ASA; Methodology: RSM; Project administration: ARA, JW; Resources: RSM, ASA; Supervision: ARA, JW; Validation: AAA, ASA; Visualization: AAA; Writing – original draft: ARA, JW, RSM; Writing – review & editing: ARA, RSM. All authors have read and agreed to the published version of the manuscript.

Funding

This research received no external funding.

Acknowledgements

The authors would like to express their sincere gratitude to the editor and the two anonymous reviewers for their constructive comments and valuable suggestions, which significantly contributed to the improvement of the manuscript.

Conflicts of interest

The authors declare no conflict of interest.

Data availability statement

The original contributions presented in this study are included in the article. Further inquiries can be directed to the corresponding author.

References

[1] Bogdetsky, V., Stavinskiy, V., Shukurov, E. & Suyunbaev, M. (2001). Mining industry and sustainable development in Kyrgyzstan. *Mining, Minerals and Sustainable Development, 110, 23-37*

[2] Aguirre-Unceta, R. (2024). Has Kyrgyzstan suffered from a resource curse?. *The Extractive Industries and Society, 17, 101427*. https://doi.org/10.1016/j.exis.2024.101427

[3] Calabrese, L. (2024). Diversifying Away from Extractives: The Belt and Road Initiative, Chinese Capital and Industrialisation in the Kyrgyz Republic. *The European Journal of Development Research, 36*(3), *601-638*. https://doi.org/10.1057/s41287-024-00632-1

[4] Bazaluk, O., Ashcheulova, O., Mamaikin, O., Khorolskyi, A., Lozynskyi, V. & Saik, P. (2022). Innovative activities in the sphere of mining process management. *Frontiers in Environmental Science, (10), 878977*. https://doi.org/10.3389/fenvs.2022.878977

[5] Koval, V., Kryshtal, H., Udovychenko, V., Soloviova, O., Froter, O., Kokorina, V. & Veretin, L. (2023). Review of mineral resource management in a circular economy infrastructure. *Mining of Mineral Deposits, 17*(2), *61-70*. https://doi.org/10.33271/mining17.02.061

[6] Yuldashev, F. & Sahin, B. (2016). The political economy of mineral resource use: The case of Kyrgyzstan. *Resources Policy, 49*, 266-272. https://doi.org/10.1016/j.resourpol.2016.06.007

[7] Abdiev, A.R., Mambetova, R.Sh., Abdiev, A.A., & Abdiev, Sh. A. (2020). Studying a correlation between characteristics of rock and their conditions. *Mining of Mineral Deposits, 14(3), 87-100*. https://doi.org/10.33271/mining14.03.087

[8] Gornostayev, S.S., Crocket, J.H., Mochalov, A.G. & Laajoki, K.V.O. (1999). The platinum-group minerals of the Baimka placer deposits, Aluchin horst. *Canadian Mineralogist, 37(5), 1117-1129*

[9] Sotskov, V. & Saleev, I. (2013). Investigation of the rock massif stress strain state in conditions of the drainage drift overworking.

Annual Scientific-Technical Colletion - Mining of Mineral Deposits, 197-201. https://doi.org/10.1201/b16354-35

[10] Umarov, T., Abdiev, A., Moldobekov, K., Mambetova, R. & Isaev, B. (2023). Creation of digital maps of land disturbed by mining operations. *E3S Web of Conferences, 420, 03023*. https://doi.org/10.1051/e3sconf/202342003023

[11] Bazaluk, O., Kuchyn, O., Saik, P., Soltabayeva, S., Brui, H., Lozynskyi, V. & Cherniaiev, O. (2023). Impact of ground surface subsidence caused by underground coal mining on natural gas pipeline. *Scientific Reports, (13), 19327*. https://doi.org/10.1038/s41598-023-46814-5

[12] Khomenko, O.Ye. (2012). Implementation of energy method in study of zonal disintegration of rocks. *Naukovyi Visnyk Natsionalnoho Hirnychoho Universytetu, (4), 44-54*

[13] Rysbekov, K.B., Huayang, D., Nurpeisova, M.B., Lozynskyi, V.H., Kyrgyzbayeva, G.M., Kassymkanova, K. & Abenov, A.M. (2022). Modern monitoring tools – effective way to ensure safety in subsoil use. *Engineering Journal of Satbayev University, 144(3), 34-40*. https://doi.org/10.51301/ejsu.2022.i3.06

[14] Shavarskyi, Ia., Falshtynskyi, V., Dychkovskyi, R., Akimov, O., Sala, D. & Buketov, V. (2022). Management of the longwall face advance on the stress-strain state of rock mass. *Mining of Mineral Deposits, 16(3), 78-85*. https://doi.org/10.33271/mining16.03.078

[15] Song, J.F., Lu, C.P., Zang, A., Zhang, X.F., Zhou, J., Zhan, Z. W. & Zhao, L. M. (2024). Assessment of Microseismic Events via Moment Tensor Inversion and Stress Evolution to Understand the Rupture of a Hard–Thick Rock Stratum. *Rock Mechanics and Rock Engineering, 57(11), 10009-10025*. https://doi.org/10.1007/s00603-024-04066-3

[16] Zhang, H., Guo, G., Li, H., Wang, T., Ni, J. & Meng, H. (2025). A new numerical method for calculating residual deformation in mined-out areas considering water-rock interaction and its application. *Scientific Reports, 15(1), 11207*. https://doi.org/10.1038/s41598-025-94001-5

[17] Kononenko, M. & Khomenko, O. (2010). Technology of support of workings near to extraction chambers. *New Techniques and Technologies in Mining, 193-197*. https://doi.org/10.1201/b11329-31

[18] Matayev, A.K., Lozynskyi, V.H., Musin, A., Abdrashev, R.M., Kuantay, A.S. & Kuandykova, A.N. (2021). Substantiating the optimal type of mine working fastening based on mathematical modeling of the stress condition of underground structures. *Naukovyi Visnyk Natsionalnoho Hirnychoho Universytetu, (3), 57-63*. https://doi.org/10.33271/nvngu/2021-3/057

[19] Fang, C., Yuan, Y., Chen, J., Gao, D. & Peng, J. (2024). Examination of Green Productivity in China's Mining Industry: An In-Depth Exploration of the Role and Impact of Digital Economy. *Sustainability, 16(1), 463*. https://doi.org/10.3390/su16010463

[20] Saik, P., Dychkovskyi, R., Lozynskyi, V., Falshtynskyi, V. & Ovcharenko, A. (2024). Achieving climate neutrality in coal mining regions through the underground coal gasification. *E3S Web of Conferences, 526, 01004*. https://doi.org/10.1051/e3sconf/202452601004

[21] Mussin, A., Imashev, A., Matayev, A., Abeuov, Ye., Shaike, N. & Kuttybayev, A. (2023). Reduction of ore dilution when mining low-thickness ore bodies by means of artificial maintenance of the mined-out area. *Mining of Mineral Deposits, 17(1), 35-42*. https://doi.org/10.33271/mining17.01.035

[22] An, H., & Mu, X. (2025). Contributions to Rock Fracture Induced by High Ground Stress in Deep Mining: A Review. *Rock Mechanics and Rock Engineering, 58(1), 463-511*. https://doi.org/10.1007/s00603-024-04113-z

[23] Lan, T., Liu, Y., Yuan, Y., Fang, P., Ling, X., Zhang, C. & Feng, W. (2024). Determination of mine fault activation degree and the division of tectonic stress hazard zones. *Scientific Reports, 14(1), 12419*. https://doi.org/10.1038/s41598-024-63352-w

[24] Salieiev, I., Bondarenko, V., Kovalevska, I., Malashkevych, D. & Galkov, R. (2025). Principles of mining-geological classification for maintaining mine workings in conditions of weakly metamorphosed rocks. *Mining of Mineral Deposits, 19(1), 26-36*. https://doi.org/10.33271/mining19.01.026

[25] Abdiev, A.R., Mambetova, R.Sh., Abdiev, A.A. & Abdiev, Sh.A. (2020). Development of methods assessing the mine workings stability. *E3S Web of Conferences, 201, 01040*. https://doi.org/10.1051/e3sconf/202020101040

[26] Abdiev, A.R., Mambetova, R.Sh., Abdiev, A.A. & Abdiev, Sh.A. (2020). Razvitie metodov otsenki geomekhanicheskogo sostoyaniya porodnogo massiva vokrug gornykh vyrabotok. *Nauchnye issledovaniya v Kyrgyzskoy Respublike, 1-12*

[27] Mambetov, Sh.A., Kozhogulov, K.Ch. & Abdiev, A.R. (2021). Vzaimosvyaz svoystv i sostoyaniya porod strukturno-neodnorodnykh mestorozhdeniy poleznykh iskopaemykh. *Sovremennye problemy mekhaniki, 43(1), 3-17*

[28] Abdiev, A.R., Mambetova, R.Sh. & Mambetov, Sh.A. (2017). Geomechanical assessment of Tyan-Shan's mountains structures for efficient mining and mine construction. *Gornyi Zhurnal, (4), 1-9*

[29] Mambetov, Sh.A., Abdiev, A.R. & Mambetov, A.Sh. (2002). Zonal and step-by-step evaluation of the stressed-strained state of Tyan'-Shan' rock massif. *Gornyi Zhurnal, (10), 1-12*

[30] Rahman, A., Shah, R.A., Yadava, M.G. & Kumar, S. (2024). Carbon and nitrogen biogeochemistry of a high-altitude Himalayan lake sediment: Inferences for the late Holocene climate. *Quaternary Science Advances, 14, 100199*. https://doi.org/10.1016/j.qsa.2024.100199

[31] Mambetov, Sh.A., Kozhogulov, K.Ch. & Abdiev, A.R. (2021). Kontrol svoystv i napryazhenno-deformirovannogo sostoyaniya porod strukturno-neodnorodnykh mestorozhdeniy poleznykh iskopaemykh. *Sovremennye problemy mekhaniki, 43(1), 35-49*

[32] Mambetov, Sh.A., Abdiev, A.R. & Mambetova, R.Sh. (2020). *Osnovy geomekhaniki. Klassicheskiy uchebnik. Bishkek, KRSU*

[33] Eljufout, T. & Alhomaidat, F. (2024). Utilizing waste rocks from phosphate mining in Jordan as concrete aggregates. *Results in Engineering, 22, 102350*. https://doi.org/10.1016/j.rineng.2024.102350

[34] Rezaei, M. & Mousavi, S.Z.S. (2024). Slope stability analysis of an open pit mine with considering the weathering agent: Field, laboratory and numerical studies. *Engineering Geology, 333, 107503*. https://doi.org/10.1016/j.enggeo.2024.107503

[35] Patent KR №2238. (2020). Sposob otsenki geomekhanicheskogo sostoyaniya porodnogo massiva vysokogornykh mestorozhdeniy. *Bishkek, Kyrgyzstan*

[36] Matayev, A., Abdiev, A., Kydrashov, A., Musin, A., Khvatina, N. & Kaumetova, D. (2021). Research into technology of fastening the mine workings in the conditions of unstable masses. *Mining of Mineral Deposits, 15(3), 78-86*. https://doi.org/10.33271/mining15.03.078

[37] Abdiev, A.R., Mambetova, R.Sh. & Abdiev, A.A. (2020). Izuchenie zakonomernostey izmeneniya struktury i svoystv gornykh porod v zone tektonicheskikh narusheniy. V LKhKhIII Mezhdunarodnye nauchnye chteniya. *Sbornik statey Mezhdunarodnoy nauchno-prakticheskoy konferentsii, 111-114*

[38] Khomenko, O. & Bilegsaikhan, J. (2018). Classification of theories about rock pressure. *Solid State Phenomena, 277, 157-167*. https://doi.org/10.4028/www.scientific.net/SSP.277.157

[39] Baymakhan, R.B., Muta, A.N., Tileikhan, A. & Kozhogulov, K.C. (2023). On the use of the finite element method in the study of the stress-strain state of the contour of the Annie Cave on Mount Arsia. *Engineering Journal of Satbayev University, 145(2), 31-36*. https://doi.org/10.51301/ejsu.2023.i2.05

[40] Kazatov, U., Raimbekov, B., Bekbosunov, R., Ashirbaev, B. & Orokov, A. (2023). Some results of the study of rock properties of the Sulukta deposit. *E3S Web of Conferences, 431, 03009*. https://doi.org/10.1051/e3sconf/202343103009

[41] Shakenov A., Abdiev, A.R. & Stolpovskih I. (2023). Energy potential of mining transport at mines of Kyrgyzstan located at high altitude. *IOP Conference Series: Earth and Environmental Science, 1254, 012142.* https://doi.org/10.1088/1755-1315/1254/1/012142

[42] Kozhogulov, K.Ch. & Abdiev, A.R. (2023). Napryazhenno-deformirovannoe sostoyanie neodnorodnykh strukturnykh massivov vysokogornykh rudnykh mestorozhdeniy Kyrgyzstana. *Fundamentalnye i prikladnye voprosy gornykh nauk, 10(2), 39-46.* https://doi.org/10.15372/FPVGN2023100206

[43] Zhienbayev, A., Takhanov, D., Zharaspaev, M., Kuttybayev, A., Rakhmetov, B. & Ivadilinova, D. (2025). Identifying rational locations for field mine workings in the zone influenced by mined-out space during repeated mining of pillars. *Mining of Mineral Deposits, 19(1), 1-12.* https://doi.org/10.33271/mining19.01.001

[44] Mambetova, R.Sh., Abdiev, A.A. & Abdiev, A.R. (2023). Issledovaniya gidrogeologicheskikh usloviy Sulyuktinskogo burougolnogo mestorozhdeniya dlya sozdaniya estestvennoy tsifrovoy gidrodinamicheskoy modeli. *Vestnik Kyrgyzsko-Rossiyskogo Slavyanskogo universiteta, 23(8), 150-155*

Қырғызстанның құрылымдық-гетерогенді тау жыныстарының кернеулі-деформацияланған күйін геомеханикалық бағалау

А.Р. Абдиев[1*], Ц. Ван[2], Р.Ш. Мамбетова[1], А.А. Абдиев[1], А.Ш. Абдиев[1]

[1]*И. Раззаков атындағы Қырғыз мемлекеттік техникалық университеті, Бішкек, Қырғызстан*
[2]*Солтүстік-Батыс университеті, Сиань, Қытай*

**Корреспонденция үшін автор: atsanbek.abdiev@kstu.kg*

Аңдатпа. Зерттеулер Қырғызстанның құрылымдық жағынан біртекті емес кен орындарының тау жыныстарының кернеулі-деформацияланған жай-күйін бағалауға, тектоникалық үзілістердің тереңдігі мен әсеріне байланысты кернеулердің таралу заңдылықтарын анықтауға, сондай-ақ тау жыныстарының серпімді сипаты мен олардың беріктік қасиеттері арасындағы байланысты орнатуға бағытталған. Жұмыста әртүрлі тереңдіктегі негізгі қалыпты кернеулердің мәндерін алуға мүмкіндік беретін түсіру әдісімен далалық өлшеулерді, серпімді толқындардың жылдамдығын, серпімділік модульдерін және сдысу модульдерін анықтауға арналған зертханалық сынақтарды, сондай-ақ регрессиялық тәуелділіктерді құруға арналған статистикалық талдауды қамтитын әдістер кешені пайдаланылды. Сонымен қатар, негізгі кернеулерді бағдарлауды қайта құру және тектоникалық үзілістердің масивадағы кернеулердің таралуына әсерін бағалау жүргізілді. Зерттеу нәтижелері тау жыныстарындағы тік кернеулер, бірінші жақын жерде, жоғарғы қабаттардағы γH салмағының қысымына сәйкес келетіндігін көрсетеді. Күшті тау жыныстары мен орташа беріктік массивтері үшін алынған регрессиялық модельдер эксперименттік деректер Н. Хаст тәуелділіктері бойынша есептелген мәндер мен гидростатикалық кернеудің таралуына байланысты мәндер арасында екенін растайды. Тау жыныстарының серпімді сипаттамаларын зерттеу бойлық толқын жылдамдығының өзгеруі серпімділік модульдері мен ығысу модулінің өзгеруімен тікелей байланысты болатын анизотропияның жоғары дәрежесін анықтады. Алынған нәтижелер кен массивтерінің кернеулі-деформацияланған күйін болжаудың дәлірек модельдерін жасауға және тау-кен қазбаларын жобалауды оңтайландыруға мүмкіндік береді.

Негізгі сөздер: *тау-кен ісі, кернеулі-деформацияланған күйі, серпімді сипаттамалары, тау жыныстары.*

Геомеханическая оценка напряжённо-деформированного состояния структурно-неоднородных породных массивов Кыргызстана

А.Р. Абдиев[1*], Ц. Ван[2], Р.Ш. Мамбетова[1], А.А. Абдиев[1], А.Ш. Абдиев [1]

[1]*Кыргызский Государственный Технический Университет им. И. Раззакова, Бишкек, Кыргызстан*
[2]*Северо-Западный университет, Сиань, Китай*

**Автор для корреспонденции: atsanbek.abdiev@kstu.kg*

Аннотация. Исследования направлены на оценку напряжённо-деформированного состояния породных массивов структурно неоднородных рудных месторождений Кыргызстана, выявление закономерностей распределения напряжений в зависимости от глубины и влияния тектонических разрывов, а также на установление взаимосвязи между упругими характеристиками пород и их прочностными свойствами. В работе использован комплекс методов, включающий полевые измерения методом разгрузки, позволяющие получать значения главных нормальных напряжений на различных глубинах, лабораторные испытания для определения скоростей упругих волн, модулей упругости и модулей сдвига, а также статистический анализ для построения регрессионных зависимостей. Кроме того, проведена реконструкция ориентировки главных напряжений и оценка влияния тектонических разрывов на распределение напряжений в массиве. Результаты исследования демонстрируют, что вертикальные напряжения в породном массиве, в первом приближении, соответствуют давлению веса вышележащих слоёв γH. Полученные регрессионные модели для крепких пород и массивов средней прочности подтверждают, что экспериментальные данные находятся между значениями, рассчитанными по зависимостям Н. Хаста, и значениями, обусловленными

гидростатическим распределением напряжений. Исследование упругих характеристик пород выявило высокую степень анизотропии, при которой изменение скорости продольной волны непосредственно коррелирует с изменением модулей упругости и модуля сдвига. Полученные результаты позволяют разрабатывать более точные модели прогнозирования напряжённо-деформированного состояния рудных массивов и оптимизировать проектирование горных выработок.

Ключевые слова: *горное дело, напряжённо-деформированное состояние, упругие характеристики, породный массив.*

Publisher's note

All claims expressed in this manuscript are solely those of the authors and do not necessarily represent those of their affiliated organizations, or those of the publisher, the editors and the reviewers.

SATBAYEV UNIVERSITY

Engineering Journal of Satbayev University

Volume 147 (2025), Issue 2, 40-49

https://doi.org/10.51301/ejsu.2025.i2.06

Comparative analysis of the state of desertification of the lands of West and East Kazakhstan

M.E. Amirkhanov, Y. Zhakypbek*, S.V. Tursbekov, T.B. Nurpeissova

Satbayev University, Almaty, Kazakhstan

**Corresponding author: y.zhakypbek@satbayev.university*

Abstract. The study performs an analysis and comparison of two completely different, but in some cases similar regions of West and East Kazakhstan. The influence of climate data changes, soil structure and its sensitivity on desertification in Kazakhstan over the decades of the 2000s, 2010s and from 2020 to 2024 is described using the example of West and East Kazakhstan. The author compared and detected that the soil types: Zg, XI, So, WR and KI are found both in the West and in the East of Kazakhstan exposed to degradation of soil structure. Climatic parameters, such as the temperature of the area fixed range between 3.6-4.9°C, humidity change significantly, all the time within 64% and 77%, and precipitation in different time periods changed from 416 mm to 605 mm. Using remote sensing data, the author analyzed changes in the natural environment, created visualizations and 3D modeling during the monitoring process. Thus, a set of existing research papers, statistical information and own experience were presented, since in the course of the work the results of scientific research on desertification were presented. The results of the study showed that there is an accelerated process of land desertification in Kazakhstan.

Keywords: *desertification, climate, temperature, humidity, precipitation, remote sensing, monitoring.*

Received: 06 January 2025
Accepted: 15 April 2025
Available online: 30 April 2025

1. Introduction

Desertification is the process of transforming fertile land into desert or semi-desert. This phenomenon occurs due to various factors such as climate change, improper agriculture, overgrazing, deforestation, the use of chemical fertilizers, and other human and natural impacts. As a result of desertification, soil fertility is lost, water quality deteriorates, and biodiversity decreases, which can lead to economic and social problems, especially in rural areas.

Before starting a study, it is necessary to find the differences and understand what desert and desertification mean, and in what ways they differ. Desertification and desert are two concepts that are often confused, but there are important differences between them. Desert is a natural ecosystem characterized by extreme climatic conditions (hot or cold, dry), where there is little precipitation and vegetation is limited. Deserts have a specific landscape, such as sand dunes, rocky plains, rare plants and species of flora and fauna adapted to arid conditions. Desertification is a process of land degradation, during which fertile territories lose their properties and become unsuitable for agriculture or life. This phenomenon can occur due to various factors, including climate change, land misuse, deforestation, or intensive cattle breeding. This phenomenon includes soil degradation, water loss, and deterioration of plant growth conditions. Desertification can occur in different climatic zones, not necessarily in actual deserts. Thus, a desert is a stable ecosystem, and desertification is a process that can affect even areas that were once green or fertile. The process of desertification is most often observed in arid and semi-arid areas, where the preservation of fertile soil and access to water resources are key factors in agricultural activity and population viability. The process of desertification is related to soil sensitivity and ecological vulnerability [1]. Ecological soil degradation occurs in ecologically vulnerable areas, and ecological sensitivity factors and ecological exposure factors are the basic elements for assessing ecological vulnerability [2].

The Republic of Kazakhstan is the largest landlocked country in the world that does not have direct access to the World Ocean. Most of the country's territory is desert – 44% and semi-deserts – 14%. Steppes occupy 26% of the area of Kazakhstan, forests – 5.5%. There are 8.5 thousand rivers in the country. The northeastern part of the Caspian Sea is included in the republic borders. The Aral Sea is divided between Kazakhstan and Uzbekistan. There are 48 thousand large and small lakes in Kazakhstan. The largest of them are Balkhash, Zaysan and Alakol. The remoteness from the oceans determines the sharp continental climate of the country which means ecological sensitivity is mainly reflected by desertification sensitivity [3]. The higher the desertification sensitivity is, the greater the risk of land desertification. The phenomenon of soil structural degradation and desertification has been actively expressed in Kazakhstan since the 1960s, and attention should be paid especially to the Western part of Kazakhstan, the Caspian region [4].

m.amirkhanov@satbayev.university; y.zhakypbek@satbayev.university; s.tursbekov@satbayev.university; t.nurpeissova@satbayev.university
Engineering Journal of Satbayev University. eISSN 2959-2348. Published by Satbayev University

In 1994, the United Nations Convention to Combat Desertification (UNCCD) was adopted, which is the main international legal instrument aimed at combating desertification and land degradation. The signatory countries committed to develop and implement national and regional plans to prevent desertification, restore degraded lands, and use sustainable land tenure and agriculture.

Kazakhstan became a party to the United Nations Convention to Combat Desertification (UNCCD) on December 30, 1997. On July 7, 1997, Kazakhstan took part in this process and presented its National Action Program in the form of the state program «Combating desertification in the Republic of Kazakhstan for 2005-2020» with a three-stage list of main goals and objectives [5].

The susceptibility of the soil to desertification is its tendency to degradation in conditions of lack of moisture and vegetation, which leads to loss of its productivity and transformation into desert or semi—desert areas. This process depends on a complex of factors, both natural and anthropogenic. Here are the main points that affect the susceptibility of the soil to desertification:

Climatic conditions. Low humidity: the main factor contributing to desertification is lack of precipitation. Soils in arid and semi-arid areas (such as Central and Western Kazakhstan) are susceptible to erosion and degradation, especially if precipitation does not compensate for moisture evaporation. High temperature: Intense heat also accelerates the evaporation of moisture from the soil surface, which can lead to deterioration of its structure and loss of organic matter. Republic of Kazakhstan makes up about 179.9 million ha or 60% of its territory, mostly in desert, semi desert and steppe zones. Almost all the administrative regions suffer from desertification which shown in Figure 1 [6].

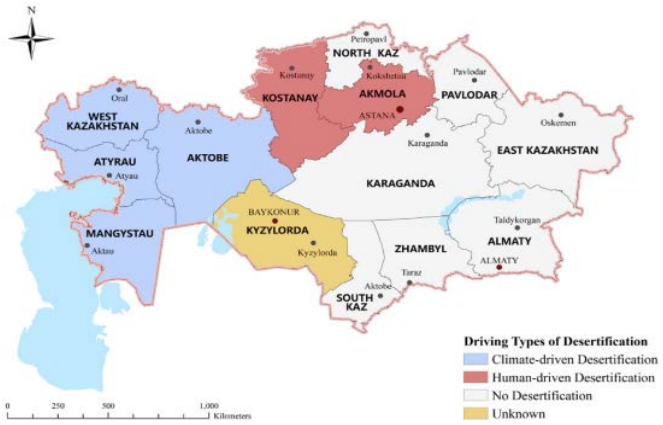

Figure 1. Driving types of desertification in Kazakhstan

Type of soil. Sandy and sandy loam soils: These soils have a low ability to retain moisture, which makes them particularly vulnerable in arid conditions. They are easily destroyed by wind (wind erosion) and water. Clay soil: Although such soils retain moisture better, they can be subject to water erosion and waterlogging if the correct water balance is not maintained. A Loamy soil: They are more stable, but if mismanaged (for example, excessive arable land or intensive grazing), they can also degrade.

The presence of vegetation: Vegetation plays a key role in protecting the soil from erosion. The presence of grass cover and shrubs helps to retain moisture and prevent the removal of the topsoil. If vegetation is destroyed (for example, because of uncontrolled grazing or agricultural activities), the soil becomes vulnerable [7].

The root system of plants helps strengthen the soil, improving its structure and ensuring water retention.

Anthropogenic factors. Excessive farming: Frequent tillage without observing crop rotation and without applying organic fertilizers can lead to a decrease in organic matter and deterioration of soil structure. This, in turn, increases the susceptibility of the soil to desertification. Pasture pressure: Overgrazing destroys vegetation cover and compacts the soil, which reduces its water retention capacity and promotes erosion. Disturbance of the water balance: Changes in the use of water resources (for example, irrigation without considering soil characteristics) can lead to soil degradation through salinization or an increase in the groundwater level [8].

Soil degradation. Erosion: Soils exposed to strong wind or rain lose their upper fertile layer. This can lead to a loss of soil structure and deterioration of its fertile qualities. Salt stress: In arid areas where there is high evaporation and lack of precipitation, salt deposits can accumulate on the soil surface, making it less suitable for plant growth. An absence of organic matter: The lack of organic matter reduces the soil's ability to retain water and nutrients, making it more vulnerable to degradation and desertification. Soils with a disturbed structure (for example, compacted or with a low content of organic matter) lose their ability to retain water and air, which contributes to their degradation and increased susceptibility to desertification.

Soil sensitivity is its ability to respond to various impacts, such as climate change, agricultural stress, or pollution. One of the main factors affecting soil sensitivity is the type and structure of the soil: Different types of soils (for example, sandy, clay, loamy) have different water retention and aeration capacities. Soils with a fine-grained structure (for example, clay soils) may be more sensitive to changes in humidity, while sandy soils may dry out faster, making them sensitive to droughts. To obtain a systematic analysis of the soil structure, it is necessary to understand in detail the soil structure of Kazakhstan [9].

The natural zones of Kazakhstan successively change from North to South: from forest-steppes to deserts, and it is shown in Figure 2.

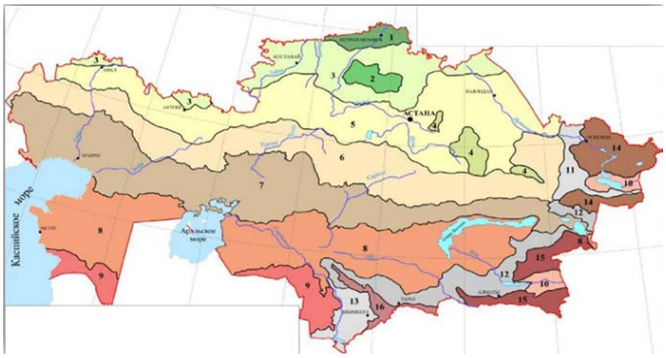

Figure 2. Map of natural zones, subzones of altitude zones of Kazakhstan in 2023

Forest steppe. A small area of the northern part of the country. This zone is characterized by a flat land surface with lowlands. This territory consists of two types: (1) – forest-steppe and mixed (Kolochnaya) steppe of plains; (2) – forest-steppe of Low Mountains.

Steppe. They occupy almost a third of the country's territory. The climate is more severe than in the forest-steppe: precipitation is much less in summer, and the average temperature in July varies from +18°C in the northern regions to +23°C in the southern regions. The steppe zone with white and green consists of: (3) – arid steppes; (4) – srid steppes and forests of low mountains.

Yellow and white-orange color territories cover semi-deserts zones. Semi-Deserts are the intermediate zone between the steppe and deserts. The climate is dry and hot in summer, cold in winter: (5) – dry steppes; (6) – desolate steppes.

Deserts. They occupy a wide strip from 500 to 700 km, stretching from the Caspian Sea to the foothills. They are: (7) – northern deserts; (8) – middle deserts; (9) – southern deserts.

In the mountainous regions of Kazakhstan, the change of natural zones is determined by the change in altitude: (10) – desert basins. Upland plains and foothills: (11) – steppe foothills; (12) – desert of the north Tianshan type; (13) – desert of the central Asian type.

Mountains: (14) – Tarbagatai-Sauro-Altai belt types; (15) – Dzungaro-North Tien Shan belt types; (16) – Karatai-Western Tien Shan belt types. High-altitude zones influence the development of nature. The change in altitude leads to alternation of natural zones and changes in vegetation and climate [10].

The study of desertification of the lands of Kazakhstan is conducted to study the causes and extent of this process, as well as to prepare measures for its prevention and management. The study process is based on data from East Kazakhstan, which is one of the regions of the country with the most affluent and rich in water resources in the region of the Republic of Kazakhstan, where desertification is beginning, and special attention is being paid to this issue [11].

Desertification is a serious problem in Kazakhstan, as most of the country is in a semi-desert and desert zone. Sources of desertification in Kazakhstan include unstable land use, irregular use of agricultural land, climate change and insufficient conservation.

The problem of desertification of lands in the Caspian region West Kazakhstan is one of the most pressing problems of Ecology and agriculture in the region. In many areas of the region, soil cover and access to plant nutrients are deteriorating due to land cover destruction and soil erosion. The Caspian region is one of the most dynamic regions on the planet. Its condition is greatly influenced by a combination of natural and anthropogenic factors.

Desertification in Atyrau and Mangystau regions is an urgent problem faced by Kazakhstan, requiring an integrated approach and long-term solutions. Effective management of water resources, the introduction of sustainable agricultural practices and the conservation of natural ecosystems will help mitigate the effects of this process and ensure the sustainable development of the region (Figure 3).

The interrelation of the desertification process in the Caspian region and East Kazakhstan is a complex ecological process that can be considered in the context of common climatic, hydrological and anthropogenic factors affecting both regions. Despite the difference in geographical location (the Caspian region is in the west of Kazakhstan, and East Kazakhstan is in the east of the country), there are several key factors of interconnection between these regions, including through climate change, water resources, and the impact of human activity.

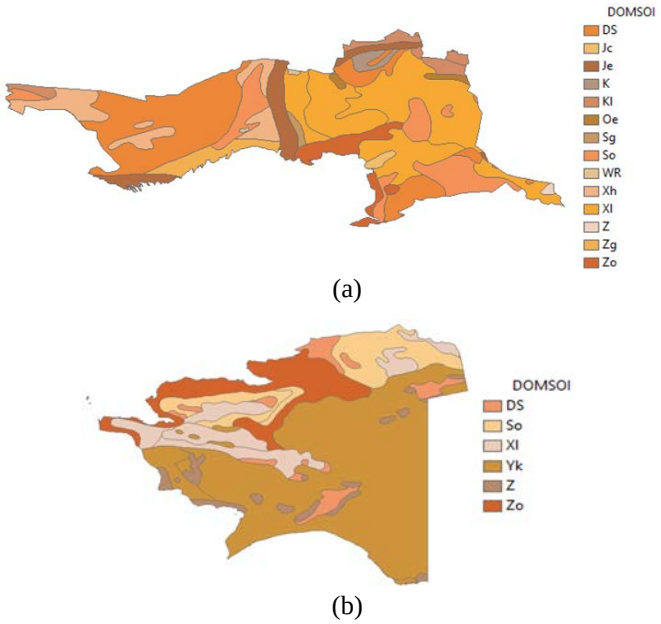

Figure 3. Soil type structure of Atyrau and Mangystau regions: (a) – tyrau region consists: Ds – Podzoluvi soils; Jc – Calcaric Fluvisols; Je – Eutric Fluvisols; K – Kastaznozems; KI – Luvic Kastanozems; Oe – Eutric Histosols; Sg – Gleyic Solonetz; So – Orthic Solonetz; WR – Planosols; Xh – Haplic Xerosols; XI – Luvic Xerosols; Z – Solonchaks; Zg – Gleyic Solonchaks; Zo – Orthic Solonchaks; Yk – Calcic Yermosols; Z – Solonchaks [12]

Although East Kazakhstan is generally less dependent on rivers, current water supply problems and declining water resources in the Caspian region (including due to changes in the Caspian Sea level) may affect overall approaches to the use of water resources in Kazakhstan. A decrease in water resources in one part of the country may increase competition for water and worsen problems in other regions.

Increased soil salinity, erosion, and deterioration of water quality are common problems both in the Caspian region and in some areas of Eastern Kazakhstan. Both regions are experiencing changes in vegetation and wildlife due to climate change and economic activity. The impact of ecosystem changes in one region may have an indirect impact on ecosystems in another region if there are natural links between them, such as animal migration routes or water flows.

The process of desertification in the Caspian region and Eastern Kazakhstan is closely linked through climate change, water resources and anthropogenic factors. Although each of these regions has its own characteristics, common problems such as land degradation, water stress, and ecosystem degradation require comprehensive solutions and coordinated efforts at the national level to mitigate them and prevent further environmental degradation [13].

2. Materials and methods

Desertification is the degradation of land in arid, semi—arid and dry sub-humid areas caused by climate change and anthropogenic activities. Remote sensing plays a key role in identifying, monitoring, and predicting this process. Monitoring of desertification by remote sensing of the Earth in the East Kazakhstan region is an important component of the management of Natural Resources and environmental protection in this region. Remote sensing is a method that uses satellite data to study and analyze changes in the Earth's surface.

In recent decades, climate change has increasingly affected ecosystems and agriculture around the world. The vulnerable ecosystem of East Kazakhstan, faced with the problem of desertification, requires special care. Global warming, changes in precipitation and other aspects of climate change have a serious impact on this region, leading to irreversible consequences for nature and humans. In this article, we will consider the impact of climate change over decades from 2000s to 2020s on the desertification of Eastern Kazakhstan and possible ways to solve this problem.

East Kazakhstan region located in the eastern part of the country. It occupies an area of 97800 sq kilometers on the soils of mountainous areas and areas with sandy and undeveloped soil. Geographical coordinates of researched region at 48°52'54.98" between 48°31'44.43" north latitude and 82°51'56.43" east longitude between 83°31 '46.61" [14].

In this research paper, special attention should be paid to the soil structure of the region under study, because the soil composition and soil structure have a significant impact on the processes of desertification. Soil degradation leads to a decrease in its productivity, deterioration of the water balance and, ultimately, to the expansion of desert areas.

The soil structure of East Kazakhstan is a way of organizing and combining soil particles (sand, silt, and clay) into aggregates of various shapes and sizes. It affects water permeability, aeration, fertility and soil resistance to erosion and it is shown in Figure 4.

Soils with a low humus content (less than 1%) are less resistant to erosion, as organic matter plays an important role in retaining moisture and nutrients. Salt marshes (Solonchaks) and saline soils: Salinization of the soil reduces its fertility and prevents vegetation growth, which accelerates the process of desertification. In arid regions, improper irrigation and evaporation lead to the accumulation of salt on the soil surface. This phenomenon can be seen under the Zg indicator (Gleylic solonchak).

Figure 4. Soil type structure of East Kazakhstan: Ch – Haplic Chernozems; Ds – Podzoluvi sols; Gl – Glaciers; Ge – Eutric Gleysols; Gm – Mollic Gleysols; I – Lithosols; Je – Eutric Fluvisols; Kh – Haplic Kastanozems; KI – Luvic Kastanozems; Oe – Eutric Histosols; Sm – Mollic Solonetz; So – Orthic Solonetz; WR – Planosols; XI – Luvic Xerosols; Y – Yermosols; Yh – Haplic Yermosols; Zg – Gleyic Solonchaks

The East Kazakhstan region has a sharply continental climate with large differences in seasonal and daily temperatures. Summers are hot and moderately dry, and winters are cold and snowy. The average temperature of the winter months, from -12°C to -15°C, in the foothills of Altai -9°C to -11°C. However, with the attack of arctic air masses, the temperature can drop to -42°C. The average maximum temperature in July is from +25°C to +30°C. The maximum summer temperature can reach the +45°C mark. The average annual level of precipitation is from 300 to 600 mm, in the mountains-about 900 mm, in some places up to 1500 mm.

The climate of the region is sharply continental, with a large daily and annual amplitude of air temperature. The average temperature in January is -17°C, July +21°C, precipitation covers 300 mm per year. The average annual wind speed is 2.3 m/s, the average annual air humidity is 66% [15].

There are two main reasons why the phenomenon of desertification occurs. They are natural and anthropogenic. As a natural factor, the indicator of seasonal drought and the amount of precipitation is less than normal. And the anthropogenic factor, that is, the reason that arose from the activities of mankind, is the misuse of land plots within the framework of economic activity agriculture. Overgrowth and improper distribution of pastures and land resources, uncontrolled use of land for growing crops, and soil contamination with toxic substances.

The methodology for studying the phenomenon of desertification of the lands of East Kazakhstan will consist of the following indicators. Indicators of climatic characteristics of Kazakhstan (Statistical information) and state of land cover of the territory of Kazakhstan (Vegetation conditions and migration of sand dunes).

The average and maximum decennial height of snow cover in winter (Tables 1, columns 1 and 2) are calculated based on daily monitoring of the height of snow cover installed in an open area within the locality. According to these data, the average decade of snow cover was determined. From them, the maximum values were selected for each winter, according to which the average values of the largest and maximum values for the control period of at least 40 years were found. The maximum daily height (Table 1, column 3) is determined as the largest of the values of the maximum height of snow cover for the year, obtained because of field surveys of snow cover, which are carried out on the last day of each decade. Snow shooting data is an average of 100 measurements on a route of one to two kilometers.

Table 1. Snow precipitation indicator, 2020s [16]

City/town/place	Snow cover, cm			Duration of the onset of stable snow cover, days
	Average for the largest decade of winter	Maximum of the largest decade	Maximum daily amount of winter on the last day of the decade	
East Kazakhstan				
Zaysan	26.2	73.0	69.0	136.0
Katon-Karagay	26.9	89.0	48.0	160.0
Ust-Kamenogorsk	57.4	104.0	-	147.0
Shemonaikha	49	83	85	151

Duration of permanent snow cover (Table 1, Column 4). Defined as the average of the annual periods of stable snow cover. The period of formation of snow cover is determined between the date of formation of permanent snow cover, when the visible area of the meteorological station is covered with more than 60% snow, and the date of disappearance of permanent cover, when the degree of environmental cover is less than 60%. In addition, snow cover is considered stable if it is maintained for at least 30 days in a row with breaks of no more than three days.

The least precipitation in East Kazakhstan falls in September. The average for this month is 29.5 mm. At the same time, most precipitation is observed in November. The level and amount of precipitation affects the vegetation of area. Visual information can be seen in Figure 5.

Figure 5. Average amount of precipitation in East Kazakhstan, 2020s

As a factor contributing to climatic indicators, we can use humidity and temperature indicators of the region between certain periods of time. Humidity is the concentration of water vapor in the air. Humidity changes depending on the temperature and pressure in the controlled system. The same amount of water vapor leads to an increase in the relative humidity of cold air compared to warm air.

Air temperature is one of the thermodynamic parameters of the state of the atmosphere. Air temperature is an indicator of a quantity that indicates the degree of its heating. Air temperature is one of the most variable indicators of the state of the atmosphere.

Remote sensing of the earth is a set of technologies that allow obtaining, processing and interpreting information about objects on the earth's surface without physical contact. The specific goals of a scientific study should include the following points: Study and analysis of the dynamics of changes in vegetation and soil cover in the East Kazakhstan region based on the analysis of remote sensing data over the past decades, assessment of the impact of natural and anthropogenic factors on the desertification process in this region, determination of optimal remote sensing parameters for effective desertification control, development of recommendations and strategies for combating desertification in this region based on the results of research and analysis of remote sensing data [17].

To study climate indicators in the region, control work can be carried out using indicators for several years free of charge through the POWER Data Access Viewer platform. In order to study climate indicators in the region, control work can be carried out using indicators for several years free of charge through the POWER Data Access Viewer platform. Power Data Access Viewer is a web—based GIS tool that allows you to see and explore various variables related to renewable energy sources anywhere around the world. The tool is provided as part of NASA's World Energy Resources Forecast (POWER) project. Using Power Data Access Viewer provides access to daily averaged data for specific date ranges and parameters for a single location, view interactive charts and data tables, download various tabular and geospatial file formats, access climate datasets for the entire globe and generate custom climatological reports and single point data [18]. The results of the research on the project are provided in the form of interactive maps, through applications and data services that describe meteorological conditions, solar radiation and other information, and show how these resources can change over time.

Spatial analysis makes it easier to answer many questions, including those related to renewable energy sources. Under GIS, NASA's solar and meteorological data can be placed on a single smart card along with socio-economic data, energy network data and other infrastructure. Thus, modern GIS software helps to bring clarity to the complex tasks of renewable energy, helping to understand the huge volumes and variety of data, showing an accurate picture of current conditions and providing users with the opportunity to model and simulate strategies [19]. Since the POWER Project was launched 20 years ago, in 2002, with the aim of making surface energy measurements available, it has seen a huge increase in the amount of data it collects and the set of answers it can offer, as well as the communities it serves.

As people around the planet explore this area more closely and invest in capturing solar and wind energy, they will study and apply Earth observation materials made by NASA from space. These NASA observations are free and accessible to everyone, they help us better understand how the complex systems of our planet work. After all, we are all astronauts on a small spaceship called Earth [20].

POWER Regional Data Access Viewer platform https://power.larc.nasa.gov/data-access-viewer/ temperature and humidity indicators in the territory of the East Kazakhstan region are monitored and analyzed. With a primary data library, you can download and edit the average air temperature and air humidity data for each month for 12 months of each year on Microsoft Excel.

According to the data downloaded through the POWER Data Access Viewer platform, average air temperature indicators were available. The lowest air temperature in the 20-year period between 2000s and 2020s is -14°C, recorded in 2000s in the Altai District of the East Kazakhstan region. The highest temperature in 2012 in Urdzhar District of East Kazakhstan region was recorded at +36°C. The area that showed the highest air humidity in East Kazakhstan region between 2000s and 2020s is Glubokovsky, in 2000s. The lowest air humidity in Ayagoz district in 2020s.

One of the methods of studying desertification through climate research is the analysis of long-term climate data, such as data on temperature, precipitation, humidity and other parameters. By analyzing such data, scientists can identify climate change trends in a particular area and determine whether desertification is occurring there. Another method of studying desertification through climate research is the modeling of climatic conditions using special computer programs. Using such models, scientists can assess the impact of various factors, such as greenhouse gas emissions, land-use changes, etc., on the desertification process. Also, special research expeditions to deserted and desolate areas are conducted to study desertification with the help of climate research. As part of such expeditions, scientists collect data on climatic conditions, soil composition, vegetation and other parameters, which help them better understand the processes of desertification and develop measures to prevent it.

Thus, methods of studying desertification through climate research allow scientists to obtain valuable data on climatic conditions in desertification areas and develop effective strategies to combat this global problem phenomenon.

3. Results and discussion

The processing of remote sensing of the Earth has recently been increasingly closely integrated with Geographic Information Systems (GIS). ArcGIS package provides a wide range of tools for working with raster data, which makes it possible to process remote sensing and use GIS analytical functions.

The Data Access Viewer platform provides access to climate data obtained through Earth remote sensing. In this research work, the necessary parameters, such as weather stations or geographical areas, were selected using the platform, and the corresponding climate indicators from 2000s, 2010s and 2020s of East Kazakhstan were obtained. The platform's interface allowed us to visualize data and export it for further analysis. To obtain climate data through Data Access Viewer, the parameters of interest were set, such as time range (2000s, 2010s and 2020s), geographical location (East Kazakhstan), and data type (Temperature, humidity). After that, the platform provided access to the relevant data sets, which can be viewed directly on the website or downloaded for further processing.

To obtain climate data through the Data Access Viewer, users need to specify parameters such as the time range, geographic location, and data type. After that, the platform provides access to the corresponding datasets, which can be viewed directly on the website or downloaded for further processing. The obtained climate data of East Kazakhstan for 2000s, 2010s and 2020s from Power NASA Data can be seen in Figure 6.

Figure 6. The obtained climatic data of East Kazakhstan for 2000, 2010 and 2020 from the Power NASA Data

According to obtained data from Power NASA Data, the average annual temperature for period 2000-2024, across East Kazakhstan was + 4.37°C, which is 1.73°C higher than the climate norm for period 1991-2000 [21]. In East Kazakhstan, temperature in three difference decades showed these numbers: the first decade from 2000 to 2009 is 4.71°C, the second decade from 2010 to 2019 is 3.56°C, and the third period from 2020 to 2024 is 4.85°C. Average temperature data for East Kazakhstan showed in Table 2.

As a digital method, thematic maps have been prepared for visual display of temperature and humidity indicators. Figure 7 below is a map showing the average air average temperature of the East Kazakhstan region for two decades 2000s, 2010s and 2020s.

Table 2. Average temperature (°C) indicator for decades 2000s, 2010s and 2020 [21]

Period	Jan	Feb	Mar	Apr	May	Jun	Jul	Aug	Sep	Oct	Nov	Dec	Ann
2000-2009	-11.8	-8.9	-7	5.7	15.3	20.6	22.6	18.8	12.2	5.1	-4.9	-11	4.71
2010-2019	-13.7	-9.8	-6.2	5.1	14.1	18.2	19.8	16.9	10.8	4.5	-5.7	-12.3	3.56
2020-2024	-14.8	-11.3	-8.5	6.3	16.1	21.2	23.4	19.5	13.6	6.2	-4.4	-9.8	4.85

Table 3. Average air temperature (°C) value indicators from 1 to 9 for decades 2000s, 2010s and 2020

Period	1	2	3	4	5	6	7	8	9
2000s	-12	-7	-4	0	+5	+10	+17	+22	+25
2010s	-10	-5	-2	0	+3	+7	+13	+19	+23
2020-2024	-12	-7	-3	0	+4	+ 9	+16	+21	+27

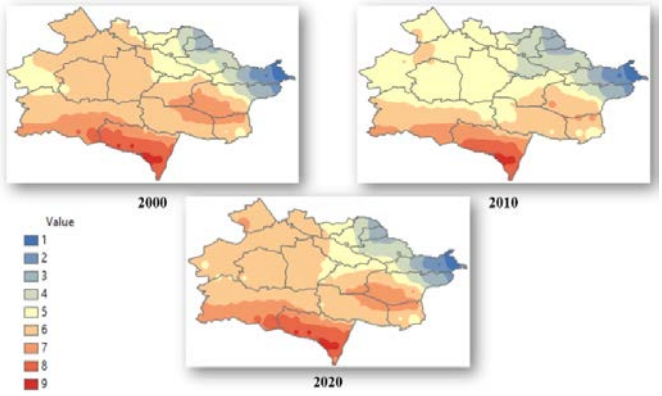

Figure 7. Map of the two-decade average temperature indicator of the East Kazakhstan

We got access to the data formed by the physical structure of the region, the terrain and the location of hydrographic objects. From the English «Value» - The Value Indicator is divided into 9 categories.

The average air temperature from 1 to 4 in the blue color is low, usually these values indicated from negative to positive Celsius (°C) and indicators from 6 to 9 characterize these regions as high and showed positive Celsius (°C). The value of 5 characterizes the relatively average value and equals to 0°C.

Figure 8 below is a Thematic Map showing the average humidity of the East Kazakhstan region for two decades 2000s, 2010s and period 2020s. Label «Value» - The Value Indicator consists of 9 categories. In this method, Blue was used as a «working color». The thickening of the blue color and their increase in values from 1 to 9 characterize an increase in the average air humidity indicator. As you move from the Altai and Saur-Tarbagatai mountains to the Balkhash-Alakol lowlands in the south-west of the region, the humidity indicator decreases.

According to thematic maps, there is a logical relationship between the average humidity and air temperature. In the territories of Gorno-Altai, Katon-Karagai and Glubokovsky, which have hydrographic resources, temperature indicators are low, and humidity is high.

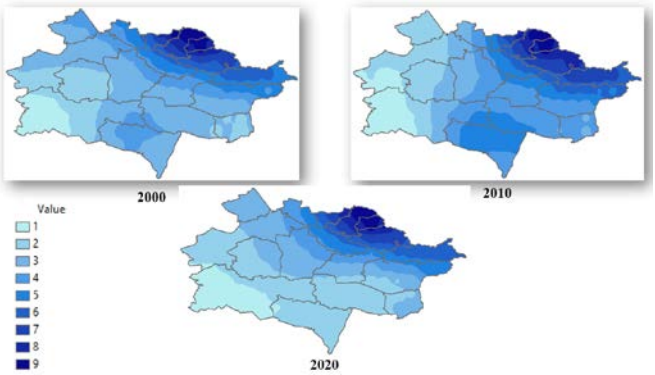

Figure 8. Map of the average humidity indicator of the East Kazakhstan for two decades

Unlike the temperature, which usually varies significantly between day and night, the dew point tends to change more slowly, so although the temperature may decrease at night, a wet day usually gives way to a wet night. The perceived humidity level in East Kazakhstan, measured as the percentage of time during which the level of humidity comfort is characterized as damp, stuffy or heavy, does not change significantly throughout the year, always remaining within 46% and 77%.

You can build a visual model of the humidity indicator using the ArcScene application of the ArcGIS software. In general, the studied goal and the 3D model on the target will help to correctly analyze the result visually. The higher the humidity index, the less likely the soil will degrade and the area will become desaturated. East Kazakhstan region according to the humidity indicator 2000s,2010s, and 2020s the 3D model is shown in Figure 9.

Figure 9. 3D model of humidity in East Kazakhstan

Depending on the operating architecture, humidity values occupy a place between categories 1 and 9. As the values increase, one can observe a change in the model. The primary data obtained during processing must undergo the process of «reclassify», that is, reclassification or reclassification.

Low levels of precipitation and high evaporation of humidity lead to water scarcity and increased desertification processes. As a result, insufficient water resources negatively affect the survival of plants on earth and the soil loses its stability by degrading and turning into sand.

According to the above data, an increase in air temperature in the summer season from +35 to +43°C leads to drought, evaporating water from the soil. The drying of the soil, in turn, leads to a decrease in fertility and the growth of desert areas.

The East Kazakhstan region is in the central part of Kazakhstan and is one of the driest and hottest regions in the country. The influence of temperature and humidity indicators plays an important role in the desertification process in this area.

High temperatures are one of the main factors affecting the desertification of the East Kazakhstan region. Summer temperatures in the area can reach 40-45 degrees Celsius, and this strongly affects the evaporation of water from the soil, contributing to dryness and drought. Desiccation of the soil, in turn, leads to a decrease in fertility and the growth of desert areas.

Humidity is another important indicator affecting desertification. The East Kazakhstan region is characterized by low humidity, especially air humidity. Low precipitation and high evaporation of moisture lead to water scarcity and increased desertification processes. As a result, in the absence of sufficient water, plants cannot survive and the soil loses its stability, becoming sandy.

The combination of high temperature and low humidity affects the formation of sand dunes (dunes), which are moved by the wind. This gives the phenomenon of desertification an additional boost because moving sand dunes makes it difficult for plants to grow and reduces soil fertility. Information about the migration or displacement of sand dunes will be described in the next chapter.

Thus, climatic indicators high temperature and low humidity are one of the main causes of desertification in the East Kazakhstan region. This causes a decrease in soil fertility, an increase in desert areas (dune) and their migration. All these points have a negative impact on the socio-economic and environmental spheres of the region, such as ecosystems and agricultural activities.

4. Conclusions

The study of desertification of the lands of the West and East Kazakhstan region by the remote sensing method is a scientific study that has significant scientific novelty and practical value.

In research case it is important to able to properly clarify difference between «Desert» and «Desertification». Desert is a stable ecosystem, especially 40% territory of Kazakhstan, and desertification is a process that can affect even areas that were once green or fertile. Process of desertification clearly identified in the West Kazakhstan. There are several reasons for occurring desertification process.

Studies have revealed that parameters such as the soil structure of the area, the level of sensitivity of the soil cover plays an important role in the process of degradation and the occurrence of desertification. The sensitivity of the soil of the studied area depends on its structure. A comparative analysis was made for two different areas of Caspian Sea region West and mountain East Kazakhstan, in individual areas there are types of soils that are susceptible to structural degradation. Soil types as: Zg (Gleyic Solonchaks), XI (Luvic Xerosols), So (Orthic Solonetz), WR (Planosols) and KI (Luvic Kastanozems) are found both in the West and in the East of Kazakhstan. According to the logical structure of the work, it can be recorded that the phenomenon of soil degradation occurred precisely in these areas.

The climatic indicators of the studied territories are another important parameter for identifying any process to logically substantiate whether there have been changes on the surface of the land cover. Climate data includes the average annual air temperature, humidity, and precipitation over the past 24 years from 2000 to 2024. By monitoring statistical data and fixing numbers using remote sensing and GIS, it will help to identify a pattern and get the desired result. It is clearly known that amount of precipitation in Western part of country is lower than in Eastern Kazakhstan. The average annual air temperature (+4.4°C) in Eastern Kazakhstan is lower than in the Western part of the country (+10.6°C). The lack of precipitation with 186 mm per year and high temperatures in Western Kazakhstan leads at best to drought, and at worst to desertification. Meanwhile, the amount of precipitation equals 416 mm per year in East Kazakhstan. Humidity can somehow offset the difference between the two regions. Humidity in the Caspian region makes the air «softer» with 64% due to hydrography. The humidity index of Eastern Kazakhstan is 77%, as well as the height of the terrain from west to east, is increasing, as can be seen in Figure 9. The absence of mountains can also indirectly affect the occurrence of desertification.

Remote sensing (remote sensing of the earth) is a method based on the use of special equipment and technologies that allow you to obtain information about the state and properties of the earth's surface by analyzing optical and infrared radiation received by satellites or aircraft. The use of the remote sensing method in the study of desertification of the lands and find differences between West and East Kazakhstan region makes it possible to observe, analyze and evaluate changes in the natural environment in large areas with high spatial resolution. This approach makes it possible to more accurately determine the boundaries and extent of desertification, as well as identify the factors and causes of this process.

The scientific novelty of this study lies in the use of modern remote sensing methods and technologies to identify areas of desertification, analyze and assess its causes and consequences. Moreover, this study can provide new data and knowledge about the factors contributing to desertification in this area, as well as suggest effective measures and strategies to prevent and eliminate desertification. The study of land desertification by the remote sensing method of the West and East Kazakhstan region can be of great practical importance for the development of environmentally sustainable land restoration strategies and plans, as well as for taking measures to protect the environment and preserve biological diversity.

Thus, the study of desertification of the lands of the West and East Kazakhstan region by the remote sensing method is a significant scientific and applied work that can be of great practical importance and contribute to the development of effective measures to prevent and eliminate desertification.

Author contributions

Conceptualization: M.E.A., Y.Z.; Data curation: M.E.A., S.V.T.; Formal analysis: M.E.A., Y.Z., T.B.N.; Funding acquisition: Y.Z., S.V.T.; Investigation: M.E.A., Y.Z.; Methodology: Y.Z., M.E.A.; Project administration: Y.Z., S.V.T.; Resources: M.E.A., Y.Z.; Software: M.E.A., T.B.N.; Supervision: Y.Z., T.B.N.; Validation: Y.Z., M.E.A.; Visualization: M.E.A., T.B.N.; Writing – original draft: M.E.A., Y.Z.; Writing – review & editing: Y.Z., S.V.T. All authors have read and agreed to the published version of the manuscript.

Funding

This research was funded by the Science Committee of the Ministry of Science and Higher Education of the Republic of Kazakhstan under the framework of the program (Grant No.BR24993218).

Acknowledgements

The authors would like to express their sincere gratitude to the editor and the two anonymous reviewers for their constructive comments and valuable suggestions, which significantly contributed to the improvement of the manuscript.

Conflicts of interest

The authors declare no conflict of interest.

Data availability statement

The original contributions presented in this study are included in the article. Further inquiries can be directed to the corresponding author.

References

[1] Jiang, L., Bao, A., Jiapaer, G., Guo, H., Zheng, G., Gafforov, K., Kurban, A. & De Maeyer, P. (2019). Monitoring land sensitivity to desertification in Central Asia: Convergence or divergence. *Science of the Total Environment, (658), 669-683.* https://doi.org/10.1016/j.scitotenv.2018.12.152

[2] Shao, H., Liu, M., Shao, Q., Sun, X., Wu, J., Xiang, Z. & Yang, W. (2014). Research on eco-environmental vulnerability evaluation of the anning River Basin in the upper reaches of the Yangtze river. *Environmental Earth Sciences, 72(5), 1555-1568.* https://doi.org/10.1007/s12665-014-3060-9

[3] Government website. (2024). About Kazakhstan. Administrative and territorial structure. *Retrieved from*: https://www.gov.kz/article/19305?lang=en

[4] Assanova, M.A. (2015). Public policy and model of sustainable development in the re-public of Kazakhstan. *Asian Social Science, 11(6), 237-243.* https://doi.org/10.5539/ass.v11n6p237

[5] Saigal Kazakhstan. (2015). Issues and approaches to Combat Desertification 2005-2015. *Retrieved from*: https://www.unccd.int/sites/default/files/naps/kazakstan-eng2005.pdf

[6] Baitulin, I.O. (2001). National Strategy and Action Plan to Combat Desertification in Kazakhstan, Sustainable Land Use in Deserts. *Springer, Berlin, Heidelberg*. https://doi.org/10.1007/978-3-642-59560-8_47

[7] Symeonakis, E., Karathanasis, N., Koukoulas, S. & Panagopoulos, G. (2016). Monitoring sensitivity to land degradation and desertification with the environmentally sensitive area index: the case of Lesvos Island. *Island Degrad. Dev., 27(6), 1562-1573.* https://doi.org/10.1002/ldr.2285

[8] Veron, S.R., Paruelo, J.M. & Oesterheld, M. (2006). Assessing desertification. *Journal of Arid Environments, 66(4), 751-763.* https://doi.org/10.1016/j.jaridenv.2006.01.021

[9] Liu, J., Wang, Y., Peng, J., Braimoh, A.K. & Yin, H. (2013). Assessing vulnerability to drought based on exposure, sensitivity and adaptive capacity: a case study in middle Inner Mongolia of China. *Chinese Geographical Science, 23 (1), 13-25.* https://doi.org/10.1007/s11769-012-0583-4

[10] Popov, M.G. (2011). Vegetation of Kazakhstan. Part 2. *Retrieved from*: https://otherreferats.allbest.ru/geography/00008737_0.html

[11] Amirkhanov, M.E. & Zhakypbek, Y. (2023). Remote sensing monitoring of desertification in the Kurchum district of east Kazakhstan region. *International journal Young Scientist, 1.1 (448.1), 13–17*

[12] Saparov, A.S. (2013). Soil Research in Kazakhstan. Annual report. *Retrieved from*: https://www.fao.org/fileadmin/user_upload/GSP/docs/eurasian_workshop/Soils_of_Russiaba.pdf
[13] Zhumabayev, E.E. (2015). Strategic measures to combat desertification in the Republic of Kazakhstan until 2025. *Retrieved from*: https://ecogosfond.kz/wp-content/uploads/2018/06/opustinivanie.pdf
[14] Mamyrkhanova, M. (2022). How the East Kazakhstan region will be divided. *Retrieved from*: https://ru.sputnik.kz/20240117/rf-i-kazakhstan-dogovorilis-ob-uvelichenii-obema-tranzita-nefti-v-knr-do-10-mln-tonn-v-god-41642222.html
[15] Oskemen Annual Weather Averages. (2017). Monthly Average High and Low Temperature. Average Precipitation and Rainfall days. *Retrieved from*: https://www.worldweatheronline.com/Oskemen-weather-averages/East-Kazakhstan/KZ.aspx
[16] Government website. (2024). Committee for construction and housing and communal services of the Ministry of investment and development of the Republic of Kazakhstan. Construction climatology of the Republic of Kazakhstan. *Retrieved from*: https://www.gov.kz/memleket/entities/kds?lang=en
[17] Robinove, C.J., Chavez, P.S., Gehring, D. & Holmgren, R. (2021). Arid land monitoring using Landsat albedo difference images. *Remote Sensing of Environment, (11), 133-156.* https://doi.org/10.1016/0034-4257(81)90014-6
[18] Sun, Q.Q., Zhang, P. Sun, D.F. Liu, A.X. & Dai, J.W. (2018). Desert vegetation-habitat complexes mapping using Gaofen-1 WFV (wide field of view) time series images in Minqin County. China. *International Journal of Applied Earth Observation and Geoinformation, (73), 522–534.* https://doi.org/10.1016/j.jag.2018.07.021
[19] Amirkhanov, M., Zhakypbek, Y., Aben, A. & Mussakhan, N. (2023). Monitoring of glaciation and melting in the east Kazakhstan region. Almaty. *Mining journal of Kazakhstan, (11),* 27-30.
[20] Ehleringer, J.R. (2021). Leaf absorptances of Mohave and Sonoran Desert plants. *Oecologia, (49), 366-370.* https://doi.org/10.1007/BF00347600
[21] Republican State Enterprise Kazhydromet. (2023). An overview of the climate features in Kazakhstan. *Retrieved from*: https://www.kazhydromet.kz/uploads/calendar/192/year_file/6646ff553af2710-05-2024_obzor-osobennostey-klimata_kazahstan-za-2023.pdf

Батыс және Шығыс Қазақстан жерлерінің шөлейттену жағдайын салыстырмалы түрде талдау

М.Е. Амирханов, Ы. Жақыпбек*, С.В. Турсбеков, Т.Б. Нурпеисова
Satbayev University, Алматы, Қазақстан
**Корреспонденция үшін автор: y.zhakypbek@satbayev.university*

Аңдатпа. Зерттеу бір-бірінен өзгеше, бірақ кейбір жағдайларда ұқсас екі Батыс және Шығыс Қазақстанның аймағына талдау және салыстыру жүргізіледі. Климаттық деректердің өзгеруінің, топырақ құрылымының және оның өзгеру сезімталдығының 2000, 2010 және 2020-2024 жылдардағы Қазақстандағы шөлейттенуге әсері Батыс және Шығыс Қазақстан мысалында сипатталған. Автор екі аймақтың топырақ құрылымында деградацияға бейімделген: Zg, XI, So, WR және KI типтері кездесетіні тіркелді. Климаттық параметрлер, оның ішінде, аймақтың температурасы 3.6-4.9°C аралығында өзгергені белгілі болды, ылғалдылық 64%-77% шегінде болды және әртүрлі уақыт кезеңдеріндегі жауын-шашын мөлшерін салыстыра келгенде 416 мм-ден 605 мм-ге дейін өзгергені анықталды. Қашықтықтан зондтау деректерін пайдалана отырып, автор табиғи ортадағы өзгерістерді талдап, бақылау процесінде визуализациялар мен 3D модельдеуді жасады. Осылайша, қолда бар ғылыми-зерттеу жұмыстарының жиынтығы, статистикалық мәліметтер және өзіндік тәжірибе ұсынылды, өйткені жұмыс барысында шөлейттену бойынша ғылыми зерттеулердің нәтижелері ұсынылды. Зерттеу нәтижелері Қазақстанда жерді шөлейттенудің жеделдетілген процесі жүріп жатқанын көрсетті.

Негізгі сөздер: *шөлейттену, климат, температура, ылғалдылық, жауын-шашын, қашықтықтан зондтау, мониторинг.*

Сравнительный анализ состояния опустынивания земель Западного и Восточного Казахстана

М.Е. Амирханов, Ы. Жақыпбек*, С.В. Турсбеков, Т.Б. Нурпеисова
Satbayev University, Алматы, Казахстан
**Автор для корреспонденции: y.zhakypbek@satbayev.university*

Аннотация. В исследовании проводится анализ и сравнение двух совершенно разных, но в некоторых случаях схожих регионов Западного и Восточного Казахстана. На примере Западного и Восточного Казахстана описано влияние изменений климатических данных, структуры почвы и ее чувствительности на процесс опустынивания в Казахстане за десятилетия 2000-х, 2010-х годов и с 2020 по 2024 год. Автор сравнил и обнаружил, что типы почв: Zg, XI, So, WR и KI встречаются как на Западе, так и на Востоке Казахстана, подверженных деградации почвенной структуры. Климатические параметры, такие как температура воздуха в данной местности, фиксированно колеблются

в пределах 3.6-4.9°C, влажность существенно меняется, все время в пределах 64%-77%, а количество осадков в разные периоды времени менялось от 416 мм до 605 мм. Используя данные дистанционного зондирования, автор проанализировал изменения в природной среде, создал визуализации и 3D-моделирование в процессе мониторинга. Таким образом, был представлен набор существующих исследовательских работ, статистическая информация и собственный опыт, поскольку в ходе работы были представлены результаты научных исследований по опустыниванию. Результаты исследования показали, что в Казахстане наблюдается ускоренный процесс опустынивания земель.

Ключевые слова: *опустынивание, климат, температура, влажность, осадки, дистанционное зондирование, мониторинг.*

Publisher's note

All claims expressed in this manuscript are solely those of the authors and do not necessarily represent those of their affiliated organizations, or those of the publisher, the editors and the reviewers.

CONTENTS

Alimzhanova A.M., Terlikbaeva A.Zh., Sakhova B.T., Shayakhmetova R.A., Koishina G.M., Mukhametzhanova A.A., Maldybaev G.K.
THE ROLE OF ZIRCONIUM IN THE FORMATION OF STRUCTURE AND PROPERTIES OF TITANIUM ALLOYS DURING SUPERPLASTIC DEFORMATION..... 1
Yeskalina K.T., Konyratbekova S.S., Yulussov S.B., Khabiyev A.T.
PROSPECTS FOR THE PROCESSING OF SPENT AUTOMOTIVE CATALYSTS WITH THE EXTRACTION OF PRECIOUS, RARE AND RARE-EARTH METALS IN KAZAKHSTAN..... 10
Koishina G., Dosmukhamedov N., Kaplan V., Nursainov I., Zholdasbay Ye.
TECHNOLOGY FOR PRODUCING PURE LEAD-FREE ZINC OXIDE FROM ELECTRIC ARC FURNACE (EAF) DUST..... 17
Mussina U., Kurbanova L., Tussupova B., Bizhanova G., Sarsenbayev S.
DEVELOPMENT OF THE COAGULANT OBTAINING TECHNOLOGY FROM SUBSTANDARD BAUXITE OF KAZAKHSTAN FOR WASTEWATER TREATMENT…….. 24
Abdiev A.R., Wang J., Mambetova R.Sh., Abdiev A.A., Abdiev A.Sh.
GEOMECHANICAL ASSESSMENT OF STRESS-STRAIN CONDITIONS IN STRUCTURALLY HETEROGENEOUS ROCK MASSES OF KYRGYZSTAN..... 31
Amirkhanov M.E., Zhakypbek Y., Tursbekov S.V., Nurpeissova T.B.
COMPARATIVE ANALYSIS OF THE STATE OF DESERTIFICATION OF THE LANDS OF WEST AND EAST KAZAKHSTAN..... 40

МАЗМҰНЫ

Алимжанова А.М., Терликбаева А.Ж., Сахова Б.Т., Шаяхметова Р.А., Қойшина Г.М., Мухаметжанова А.А., Малдыбаев Г.К.
ЦИРКОНИЙДІҢ ТИТАН ҚОРЫТПАЛАРЫНЫҢ ҚҰРЫЛЫМЫ МЕН ҚАСИЕТТЕРІНІҢ ҚАЛЫПТАСУЫНА ӘСЕРІ ЖӘНЕ ОНЫҢ АСА ПЛАСТИКАЛЫҚ ДЕФОРМАЦИЯ КЕЗІНДЕГІ РӨЛІ..... 1
Ескалина К.Т., Коныратбекова С.С., Юлусов С.В., Хабиев А.Т.
ҚАЗАҚСТАНДА АСЫЛ, СИРЕК ЖӘНЕ СИРЕК ЖЕР МЕТАЛДАРЫН ШЫҒАРУМЕН ПАЙДАЛАНЫЛҒАН АВТОМОБИЛЬ КАТАЛИЗАТОРЛАРЫН ҚАЙТА ӨҢДЕУ ПЕРСПЕКТИВАЛАРЫ..... 10
Қойшина Г., Досмухамедов Н., Каплан В., Нурсаинов И., Жолдасбай Е.
ЭЛЕКТР ДОҒАЛЫ ПЕШТЕРДІҢ (ЭДП) ШАҢЫНАН ҚОРҒАСЫНСЫЗ ТАЗА МЫРЫШ ОКСИДІН АЛУ ТЕХНОЛОГИЯСЫ..... 17
Мусина У.Ш., Курбанова Л.С., Тусупова Б.Х., Бижанова Г.З., Сарсенбаев С.О.
ҚАЗАҚСТАННЫҢ КОНДИЦИЯЛЫҚ ЕМЕС БОКСИТІНЕН АҒЫНДЫ СУЛАРДЫ ТАЗАРТУ ҮШІН КОАГУЛЯНТ АЛУ ТЕХНОЛОГИЯСЫ..... 24
Абдиев А.Р., Ван Ц., Мамбетова Р.Ш., Абдиев А.А., Абдиев А.Ш.
ҚЫРҒЫЗСТАННЫҢ ҚҰРЫЛЫМДЫҚ-ГЕТЕРОГЕНДІ ТАУ ЖЫНЫСТАРЫНЫҢ КЕРНЕУЛІ-ДЕФОРМАЦИЯЛАНҒАН КҮЙІН ГЕОМЕХАНИКАЛЫҚ БАҒАЛАУ 31
Амирханов М.Е., Жақыпбек Ы., Турсбеков С.В., Нурпеисова Т.Б.
БАТЫС ЖӘНЕ ШЫҒЫС ҚАЗАҚСТАН ЖЕРЛЕРІНІҢ ШӨЛЕЙТТЕНУ ЖАҒДАЙЫН САЛЫСТЫРМАЛЫ ТҮРДЕ ТАЛДАУ..... 40

СОДЕРЖАНИЕ

Алимжанова А.М., Терликбаева А.Ж., Сахова Б.Т., Шаяхметова Р.А., Қойшина Г.М., Мухаметжанова А.А., Малдыбаев Г.К.
РОЛЬ ЦИРКОНИЯ В ФОРМИРОВАНИИ СТРУКТУРЫ И СВОЙСТВ ТИТАНОВЫХ СПЛАВОВ ПРИ СВЕРХПЛАСТИЧЕСКОЙ ДЕФОРМАЦИИ…… 1
Ескалина К.Т., Коныратбекова С.С., Юлусов С.В., Хабиев А.Т.
ПЕРСПЕКТИВЫ ПЕРЕРАБОТКИ ОТРАБОТАННЫХ АВТОМОБИЛЬНЫХ КАТАЛИЗАТОРОВ С ИЗВЛЕЧЕНИЕМ БЛАГОРОДНЫХ, РЕДКИХ И РЕДКОЗЕМЕЛЬНЫХ МЕТАЛЛОВ В КАЗАХСТАНЕ…… 10
Койшина Г., Досмухамедов Н., Каплан В., Нурсаинов И., Жолдасбай Е.
ТЕХНОЛОГИЯ ПОЛУЧЕНИЯ ЧИСТОГО ОКСИДА ЦИНКА, НЕ СОДЕРЖАЩЕГО СВИНЦА, ИЗ ПЫЛИ ЭЛЕКТРОДУГОВЫХ ПЕЧЕЙ (ЭДП)…….. 17
Мусина У.Ш., Курбанова Л.С., Тусупова Б.Х., Бижанова Г.З., Сарсенбаев С.О.
ТЕХНОЛОГИЯ ПОЛУЧЕНИЯ КОАГУЛЯНТА ИЗ НЕКОНДИЦИОННЫХ БОКСИТОВ КАЗАХСТАНА ДЛЯ ОЧИСТКИ СТОЧНЫХ ВОД……. 24
Абдиев А.Р., Ван Ц., Мамбетова Р.Ш., Абдиев А.А., Абдиев А.Ш.
ГЕОМЕХАНИЧЕСКАЯ ОЦЕНКА НАПРЯЖЁННО-ДЕФОРМИРОВАННОГО СОСТОЯНИЯ СТРУКТУРНО-НЕОДНОРОДНЫХ ПОРОДНЫХ МАССИВОВ КЫРГЫЗСТАНА …….. 31
Амирханов М.Е., Жақыпбек Ы., Турсбеков С.В., Нурпеисова Т.Б.
СРАВНИТЕЛЬНЫЙ АНАЛИЗ СОСТОЯНИЯ ОПУСТЫНИВАНИЯ ЗЕМЕЛЬ ЗАПАДНОГО И ВОСТОЧНОГО КАЗАХСТАНА…… 40

Учредитель: Satbayev University

Регистрация:
Министерство информации и общественного развития Республики Казахстан
№ KZ19VPY00056529 от 30.09.2022

Официальный сайт: https://vestnik.satbayev.university/index.php/journal/

Основан в августе 1994 г. Выходит 6 раз в год

Адрес редакции:
г. Алматы, ул. Сатпаева,
22 тел.: 292-63-46